# MASS TRANSFER ASPECTS OF CELL CULTURE IN A BIOREACTOR

**Ph.D. THESIS**

***by***

**SOHAIL RASOOL LONE**

**DEPARTMENT OF CHEMICAL ENGINEERING**
**INDIAN INSTITUTE OF TECHNOLOGY ROORKEE**
**ROORKEE – 247667 (INDIA)**
**FEBRUARY, 2020**

# MASS TRANSFER ASPECTS OF CELL CULTURE IN A BIOREACTOR

**A THESIS**

***Submitted in partial fulfilment of the requirements for the award of the degree***

***of***

**DOCTOR OF PHILOSOPHY**

***in***

**CHEMICAL ENGINEERING**

***by***

**SOHAIL RASOOL LONE**

**DEPARTMENT OF CHEMICAL ENGINEERING**
**INDIAN INSTITUTE OF TECHNOLOGY ROORKEE**
**ROORKEE – 247667 (INDIA)**
**FEBRUARY, 2020**

# INDIAN INSTITUTE OF TECHNOLOGY ROORKEE

## CANDIDATE'S DECLARATION

I hereby certify that the work presented in the thesis entitled **"MASS TRANSFER ASPECTS OF CELL CULTURE IN A BIOREACTOR"** is my own work carried out during a period from December, 2014 to February, 2020 under the supervision of Dr. Vimal Kumar, Associate Professor, Department of Chemical Engineering, Indian Institute of Technology Roorkee, Roorkee.

The matter presented in the thesis has not been submitted for the award of any other degree of this or any other Institute.

Sohail

**Dated:** 26/02/2020 **(SOHAIL RASOOL LONE)**

## SUPERVISOR'S DECLARATION

This is to certify that the above mentioned work is carried out under my supervision.

**Dated:** 26/02/2020 **(Vimal Kumar)**
**Supervisor**

The Ph. D Viva-Voce Examination of Mr. Sohail Rasool Lone, Research Scholar, has been held on 26/02/2020

S.K. Upadhyay

**Chairperson, SRC** **Signature of External Examiner**

This is to certify that the student has made all the corrections in the thesis.

26/2

**Signature of Supervisor** **Head of the Department**

# ABSTRACT

The widespread use of stirred tank bioreactors (STBRs) with agitation system as their core elements can be explained by their long tradition. STBRs being multiphase reactors are most widely used in industrial applications including chemical, biochemical, pharmaceutical and biological processes owing to their excellent operational flexibility and mixing capability. They play a vital role in the biopharmaceutical industry, particularly in aerobic bioprocesses and can find applications in fermentation and cell culture systems. STBRs have attracted much greater attention in the bioprocesses owing to their potential for integrating the development of high value-added products and thus replacing the need for conventional chemical based processes. STBRs have huge industrial importance as nearly 50% of the chemical reactants and products have passed through stirred tank reactors at one stage or the other and thus translating into over USD 1200 billion turnover per annum worldwide. To enhance the heat and mass transfer in such systems, baffles and impeller and other internals for specific applications are used. The oxygen transfer in such systems is an important parameter for determining their efficiencies and successful scale-up and is generally characterized by volumetric mass transfer coefficient, $k_La$ being recognized as the most important parameter characterizing gas-liquid mass transfer in STBRs. It also serves as an important transport characteristic used in the scale-up, design and performance optimization of STBRs.

The oxygen transfer is often considered as a rate limiting factor for the bioprocesses due to its low solubility in the liquid medium and therefore controlling dissolved oxygen in the liquid medium, i.e. broth is essential for cell growth. It is generally affected by agitation or (stirring) rate, aeration or (air flow rate) rate, media properties, different impeller types and their configurations, etc. Power consumption is also very important parameter in STBRs. It is an indispensable and the mostly used parameter to describe hydrodynamics, mixing and mass transfer and is also important scaling up parameter in stirred tank reactors.

In this work, experiments have been carried out in stirred tank bioreactors of different volumes, i.e. 7.5 L, 5 L and 1 L. Dissolved oxygen concentration for the prediction of volumetric mass transfer coefficient, $k_La$ has been measured by using the most widely used physical method, i.e. dynamic gassing-out-gassing-in method. It was observed that with an increase in scale of the reactor, irrespective of the impeller configuration, the $k_La$ decreases when employing the same

agitation speed (50-800 rpm) and aeration rate (0.5-3.5 L/min.). The effect of other parameters such as impeller diameter, liquid volume inside the reactor, liquid medium viscosity on $k_La$ has also been studied. The power input per unit volume is also studied for single and dual Rushton turbine systems. It is observed that the power consumption in aerated system is lower than the unaerated system, because the transfer of power from impeller to the fluid is greatly influenced by aeration. It may also be attributed to the formation of cavities behind the impeller blades and the fluid having different density under gassed and ungassed conditions. The difference between gassed and ungassed power inputs is more pronounced at higher agitation rates (400-800 rpm).

A new correlation has been proposed for $k_La$ and $P/V_L$ based on a mathematical and statistical approach using response surface methodology (RSM) with Box-Behnken design (BBD) of experiments. This correlation includes the effect of various parameters such as agitation rate (50-800 rpm), air flow rate (0.5-3.5 L/min.) and temperature (10-40 °C) for different impeller configurations. Among the operating parameters, the most significant variable affecting $k_La$ was found to be agitation rate, followed by aeration rate and temperature. The effect of temperature in most cases was insignificant. This may be most likely due to the range of temperature examined in this study was relatively narrow, typically used in commercial bioreactors. Among the investigated impeller configurations, dual Rushton turbine demonstrated the highest value of $k_La$. However, taking into account both $k_La$ and shear force generated by agitation, the pitched blade turbine appears to be most effective for aerobic fermentation and cell culture applications. Models developed using RSM successfully interpreted experimental $k_La$ and have been further validated under other operating conditions. More importantly, it is also observed that, compared with conventional power-law models, the RSM approach enables a more efficient correlation procedure and formulates simplified models with comparably high accuracy.

Further to study the effect of impeller spacing on $k_La$ and power input per unit volume ($P/V_L$), RSM-BBD study has been carried out considering three factors, i.e. agitation rate (100-600 rpm) and aeration rate (1-12 L/min.) and impeller spacing (4-8 cm) for dual Rushton and mixed impeller (Rushton-marine propeller) configurations. It is found that $k_La$ and $P/V_L$ were mainly affected by agitation rate, however the interaction between agitation rate and aeration rate is significant for both configurations. It is also observed that the effect of impeller spacing on $k_La$ and $P/V_L$ was insignificant. Correlations developed using RSM for $P/V_L$ have been found to better predict as compared with the available correlations in the literature. It is also established that $P/V_L$ is lower for mixed impeller, thus suggesting its wide applicability in cell culture applications. A new power-law correlation is proposed for the mixed impeller configuration. Higher level of accuracy for both the original and simplified RSM models is observed as compared with conventional power-law models. Finally, the proposed simplified models successfully validated with the experimental data. A power-law correlation proposed for dual Rushton turbine has been found to well predict $k_La$ and comparison has also been made with the available correlations in the literature and the RSM models, both original and simplified.

Further, mass transfer and rheological behavior are characterized during the growth of *E. coli* BL21 in a stirred tank bioreactor. During the culture of *E. coli* BL21 in a 1 L stirred tank bioreactor, effects of various key operating variables such as agitation rate (50-600 rpm), aeration rate (0.5-2 L/min.), impeller diameter (4-5 cm), bioreactor working volume (0.25-0.75 L) for different impeller configurations on $k_La$ has been investigated. It is observed that $k_La$ increases with all the examined operating variables except the bioreactor working volume. Among the impeller configurations investigated, pitched blade turbine showed the highest $k_La$ value (2.72 $min^{-1}$), suggesting that it is promising for its successful cell culture as it also generates relatively less shear force owing to its low power number. A comparison evaluating mass transfer with and without cells has also been investigated in this study. A new impeller type, i.e. dislocated Rushton turbine has been investigated for its mass transfer performance having same dimensions as that of the standard Rushton turbine and is found to display superior mass transfer performance for *E. coli* BL21 culture, thus showing its potential for its application in bioprocess industry. Further, $k_La$ for different impeller configurations is also correlated using dimensionless groups such as Reynolds, Froude and Flow numbers, suggesting this approach can be used for predicting $k_La$ in different scale of stirred tank bioreactors. To understand rheological properties of the culture medium, in the present work, samples of the liquid medium with a dual Rushton turbine have been collected at specific time intervals, and their viscosity is evaluated. The rheological analysis showed that the viscosity of the liquid medium used in this study is independent on the shear rate, indicating that it behaves as a Newtonian liquid. Further, it is also observed that the shear stress linearly increases with the shear rate, which indicates that the liquid medium can be classified as a Newtonian liquid.

# ACKNOWLEDGEMENT

Research, they say, is the romance of the mind. It is an unconditioned/mysterious- sometimes wild and vicious- journey into the realms of the unknown and unbelievable, and a mere thesis is not its destination but a new beginning.

A study like this calls for professional acumen and encouragement, intellectual nourishment, and spiritual sapience along the road. At the very outset, I must thank Almighty Allah, the Supreme Spring of all Knowledge and Wisdom for all that I, the blessed rendezvous of body, mind and soul, have been endowed with.

There have been many sincere and generous people who have helped me walk the talk, and a mere mention of them after a milestone won't do justice with their contribution that is surely going to sustain into an eternity. A very special note of thanks and gratitude is extended to my supervisor, research advisor, and intellectual mentor, **Dr. Vimal Kumar** (Associate Professor, Department of Chemical Engineering, Indian Institute of Technology Roorkee). This incredible journey in fact started with his sheer faith in my capabilities and capacities *ab-initio*. Dr. Vimal Kumar has taught me how to be a successful researcher, academician, and above all, a good human being. I appreciate his willingness to help and encourage me to complete this thesis, and the doctoral program. This would not have been possible without Dr. Kumar's remarkable and incessant mentorship.

My sincere thanks are due to **Prof. Shishir Sinha**, Chairman, Student Research Committee (SRC) and Head, Department of Chemical Engineering, IIT Roorkee, for providing me constructive advice on my thesis as well as my study at the institute. I am also grateful to **Prof. Basheshwer Prasad**, Internal Member, SRC, Department of Chemical Engineering, IIT Roorkee, and **Prof. Sanjoy Ghosh**, External Member, SRC, Department of Biotechnology, IIT Roorkee for giving valuable suggestions in enhancing the quality of the present research work and giving their valuable time in offering new perspectives. Moreover, I wish to express my sincere thanks to all the faculty members of the Department of Chemical Engineering, IIT Roorkee for their continuous encouragement and help during the course of my research. I would also like to thank the non-teaching staff of the Department for their cooperation and support.

I would also like to take this opportunity to thank and fully acknowledge **Dr. Jeffrey R. Seay**, Associate Professor, **Dr. Hyun-Tae Hwang**, Assistant Professor and **Dr. Derek L. Englert**, Assistant Professor, Department of Chemical and Materials Engineering, University of Kentucky

(UK), Paducah, Kentucky, United States under whose able guidance I worked as a Visiting Scholar at the University of Kentucky as part of the collaboration between the University of Kentucky and the Indian Institute of Technology Roorkee for their valuable suggestions and support during the course of this thesis work. I would also like to thank **Dr. Sergiy Markutsya**, Assistant Professor, Department of Mechanical Engineering, University of Kentucky, Paducah, Kentucky, United States for his valuable guidance and support. I also thank office staff of the Department of Chemical & Materials Engineering, University of Kentucky, Paducah, United States especially **Marc K. Invergo**, **Chelsea Hansing**, **Stephanie Bowlin Mahan**, **Alex Sherwood**, **Todd Cowan** for all their help and support during my stay at UK.

I sincerely thank the Indian Institute of Technology Roorkee and the Ministry of Human Resource Development (MHRD), Government of India for providing me the financial support to undertake this research work. I would also like to thank the University of Kentucky for providing me the opportunity to be a Visiting Scholar at its Paducah Extended Campus, Kentucky and also for providing financial support to attend the 2017 AIChE Annual Meeting at Minneapolis, Minnesota, United States to present my research.

I also take this opportunity to thank the Indian Institute of Technology Roorkee for providing me the financial support for attending the 71$^{st}$ Annual Session of the Indian Institute of Chemical Engineers (IIChE), CHEMCON-2018 at the National Institute of Technology Jalandhar, Punjab, India to present my research. I would also like to thank the Council of Scientific and Industrial Research (CSIR), Government of India for providing me the travel grant and the Indian Institute of Technology Roorkee for the financial support to attend the 14$^{th}$ International Conference on Gas-Liquid and Gas-Liquid-Solid Reactor Engineering (GLS-14) at Guilin, China.

It is a great opportunity to thank my grandfather **Haji Ghulam Qadir Lone** and my grandmother **Zooni Begum** for their prayers and blessings and continuous support and encouragement. I truly appreciate the sacrifice made by my beloved father **Haji Ghulam Rasool Lone**, who always wanted me to pursue this degree. Although it's never enough, but sincere thanks to my beloved mother **Zareefa Banoo** for everything she has done and is still doing for me. I consider my mother to be the real graduate of my academic journey. It is my parents that this thesis is dedicated to. In addition, my brother **Suhaib Rasool Lone** and sisters **Sufora Rasool, Saba Rasool and Saalihah Rasool** have been tremendous sources of encouragement, support, empathy and motivation for me. A special thanks to my father-in-law **Haji Ghulam Hassan Lone**, mother-in-law **Hajira Begum**, and my brother-in-law's **Javid Ahmad Sofi, Irshad-Ul-Hassan Lone**, **Aijaz Hassan Lone**, **Mohd. Ashraf Lone** for their constant support and well wishes. I would also like to thank my uncle **Mushtaq Ahmad Lone** and aunt **Saleema Begum**, cousin brother **Zubair Mushtaq Lone** and cousin sisters **Snobar Mushtaq Lone** and **Farhat Mushtaq Lone** for their encouragement, empathy and motivation.

Of course I can't express in words the deep appreciation for my beloved, my wife **Mrs. Shahzada Lone**. Her constant support has made this adventure possible and bearable. For that I am eternally grateful. Shahzada has been a wonderful companion during this journey.

I am also thankful to all my friends especially my lab mates **Dr. Hemant Kumar**, **Dr. Nilambar Bariha**, **Mr. Vikas Vashisth**, **Mr. Naveen Kushwaha**, **Ms. Ravisha Goswami, Mr. Abhishek Sharma, Dr. Parul Tyagi** who have always been encouraging, cooperative and helpful. I am also thankful to **Dr. Shailendra Singh Khichi**, **Mr. Kartik Gehlot** and **Ms. Shivani Singh Rajput** for their help, cooperation and support.

Since this has been a long journey, my dear friends outside the department "walls" have also been important, letting me constantly know that my life consists of more than the PhD work. I thank them all especially Rafiq Ahmad Malik, Abdul Raqib Bhat, Zubair Aziz, Tariq Ahmad Lone, Abdul Qayoom Bhat, Shabir Ahmad Dar. I truly value their friendship. All my Kashmiri friends here at IIT Roorkee (Assif Assad, Khalid Muzamil Gani, Jhon Mohammad Wani, Shahbaz Ahmad Lone, Shahnawaz Ahmad Baba, Lateef Ahmad Wani, Qazi Inam-Ul-Qadir, Zeeshan Bhat, Khalid Bashir, Manzoor Ahmad, Dr. Tawseef Ahmad Dar, and Dr. Aadil Hussain Bhat also deserve special appreciation for the wonderful memories we have had together. I would also like to specially thank **Dr. Jamid-Ul-Islam** for being a wonderful mentor more than a friend and for extending his help every time I have asked him for.

It is difficult to thank everybody who has directly or indirectly facilitated me in reaching this pinnacle of academic achievement. I will never be able to repay them other than to provide the similar directions for my students in the future.

**(SOHAIL RASOOL LONE)**
**FEBRUARY, 2020**

# CONTENTS

# LIST OF TABLES

# LIST OF FIGURES

# NOMENCLATURE

| Symbol | Description |
|---|---|
| $a$ | interfacial area ($m^2/m^3$) |
| $b$ | coefficient of independent variable in coded unit |
| $B$ | coefficient of independent variable in actual value |
| $C$ | dissolved oxygen concentration in liquid phase ($kg/m^3$) |
| $C^*$ | liquid phase dissolved oxygen saturation concentration ($kg/m^3$) |
| $C_x$ | biomass concentration ($kg/m^3$) |
| $d_i$, $D_i$, $T$ | Impeller or stirrer diameter (cm) |
| $D_L$ | diffusivity of the liquid ($m^2/s$) |
| $D_t$ | vessel or tank diameter (m) |
| $F_l$ | Flow number |
| $F_r$ | Froude number |
| $g$ | acceleration due to gravity ($m/s^2$) |
| $H$ | Henry's constant ($Pa \cdot m^3/kg$) |
| $k_L$ | liquid phase mass transfer coefficient (m/min) |
| $k_La$ | volumetric mass transfer coefficient (1/min) |
| $M$ | torque before gassing (N.m) |
| $M_g$ | torque after gassing (N.m) |
| n | number of factors |
| N | number of experimental runs |
| $N_c$ | number of the central points |
| $N_{cd}$ | impeller agitation rate at complete dispersion (rev./min.) |
| $N_i$, $N_R$ | impeller agitation rate (rpm) |
| $N_P$ | power number of impeller |
| $P_g$ | gassed power input (W) |
| $P_g/V$ | gassed power input per unit liquid volume ($W/m^3$) |
| $P_{ug}$ | ungassed power input (W) |
| $Po_2$ | partial pressure of oxygen (Pa) |

| | |
|---|---|
| $qo_2$ | specific oxygen uptake rate (mol $O_2$/$m^3$/s) |
| $Q$, $Q_g$ | air flow rate (L/min.) |
| $R_e$ | Reynolds number |
| $t$ | time (min.) |
| $V$, $V_L$ | volume of the liquid in the vessel (L) |
| $u_{sg}$,$v_{sg}$ | superficial gas velocity (m/s) |
| $W_i$ | impeller blade width (cm) |
| $x$ | coded unit of independent variable |
| $X$ | actual value of independent variable |
| $Y$ | response of the model |
| $R_e$ | Reynolds number |
| $R^2$ | correlation coefficient |
| $\alpha$ | empirical constant |
| $\beta$ | empirical constant |
| $\gamma$ | empirical constant |
| $\delta$ | empirical constant |
| $\upsilon$ | kinematic viscosity ($m^2$/s) |
| $\sigma$ | interfacial tension (N/m) |
| $\rho$, $\rho_L$ | density of liquid (kg/$m^3$) |
| $\mu$, $\mu_L$ | viscosity of liquid (Pa.s) |
| $\mu_a$ | apparent viscosity (Pa.s) |
| $\mu_c$ | viscosity according to Casson model (Pa.s) |
| $\lambda$ | Characteristic material time (s) |
| $i$, $j$ | representing independent variables interaction |

## Abbreviations

| | |
|---|---|
| STR | stirred tank reactor |
| STBR | stirred tank bioreactor |
| BBD | Box-Behnken design |
| CCD | central composite design |
| RSM | response surface methodology |

| | |
|---|---|
| RPM | revolutions per minute |
| SRT | standard Rushton turbine |
| DRT | dislocated Rushton turbine |
| MP | marine propeller |
| PBT | pitched blade turbine |
| OTR | oxygen transfer rate |
| OUR | oxygen uptake rate |
| OAR | oxygen absorption rate |
| DO | dissolved oxygen |
| ANOVA | analysis of variance |
| DF | degree of freedom |
| CV | coefficient of variation |
| PLA | poly-lactic acid |
| VVM | volume of gas per unit volume of liquid per minute |
| PRESS | predicted residual error sum of squares |

# CHAPTER 1

# INTRODUCTION

## 1.1 BACKGROUND

The wide spread use of the stirred tank bioreactors (STBRs), with agitation systems as their core elements, can be explained by their long tradition. STBRs are not only used in the chemical industry, but also find wide applications in biologics, pharmaceutical, food and oil, cosmetics, etc., since they offer flexible operation and better mixing (Williams, 2002; Nienow, 2014; Butcher and Eagles, 2002). They have attracted much greater attention in the bioprocesses owing to their potential for integrating the development of high value products and thus replacing need for conventional chemical processes (Nauman, 2008; Jossen et al., 2017). The STBRs are comprised of baffles and an agitator and other internals with specific applications, which also significantly influence the heat and mass transfer characteristics. Agitator is generally used for enhancing the gas-liquid interfacial area as it breaks the large gas bubbles into smaller ones. In the present time, stirred tank bioreactors (STBRs) have become more popular, due to well mixing mechanism, which helps in achieving necessary substrate contact, uniform pH and temperature control and uniform cell distribution (Branyik and Vicente, 2005; Hoffmann et al., 2008). Due to their low capital and operating costs, they are widely used in the bioprocess and biotechnological industries (Williams, 2002). They offer unmatched flexibility and control over various transport processes occurring inside the reactor. The oxygen transfer in such systems has been recognized as an important parameter for determining their efficiencies and successful scale-up. It is generally affected due to various factors, e.g. agitation rate, aeration rate, media and reactor properties, etc. The mass transfer characteristics are also significantly affected by different types of impellers and their configurations in a bioreactor.

Aeration of liquid (medium) in mechanically agitated contactors is the most widely used reactor configuration for different biochemical and chemical processes (Puthli et al., 2005; Gogate et al., 2000). Dissolved oxygen concentration is a significant constraint in stirred tank bioreactors as it can affect the cell proliferation rate, which demands that air or oxygen should be continuously supplied to the reactor and thus the importance of oxygen transfer in its design and scale-up. The dissolved oxygen concentration in the broth, being respiring microorganism’s suspension and the liquid medium, depends on the oxygen transfer rate (OTR), and the oxygen uptake rate (OUR). Therefore, in such systems, its control is crucial for its growth. Initially, oxygen is first transferred to the liquid phase, finally it is absorbed and consumed by the cell. The oxygen transfer in such aerobic bioprocesses is often considered as a limiting factor owing to its low solubility in the liquid medium (Garcia-Ochoa et al., 2010; Schaepe et al., 2013). Thus, to increase the mass transfer rate between the phases, either the liquid phase mass transfer coefficient ($k_L$) and/or interfacial area ($a$) should be enhanced. In stirred tank bioreactors, it is difficult to measure the interfacial area available for mass transfer. However, the term $k_La$, is mostly used to express the mass transfer effectiveness in such reactors and is more readily measured. Thus, $k_La$ is most often used as a measure of the efficiency of the stirred tank bioreactors.

In aerobic bioprocesses, as described above, oxygen transfer being the controlling step for the microbial growth and affects the evolution of bioprocesses. Thus the transfer of oxygen from the gas to the liquid phase and its subsequent consumption by microorganism continues to have a decisive importance in such reactors and work in this direction is still in progress and numerous studies have been carried out for enhancement of oxygen transfer. The hydrodynamic conditions in the stirred tank bioreactors strongly influences the gas-liquid oxygen transfer process and hence the yield of the cells or biomass. Such conditions generally being a function of energy dissipation depend on the operational conditions of the reactor, the culture properties, the geometry of the reactor and it is also affected by the oxygen consuming cells (Garcia-Ochoa et al., 2010; Garcia-Ochoa and Gomez, 2009).

In many biological processes employing stirred tank bioreactors, the limiting nutrient transport generally governs the rate of product formation. It has been widely reported that the transport rate of oxygen to the cells is considered a limiting factor in aerobic fermentation systems due to its low solubility in water. The hydrodynamics of the bubbles influence the oxygen transfer as bubble size distribution (BSD) is a key factor responsible for the oxygen transfer (Garcia-Ochoa and Gomez, 2009), as it governs the interfacial area for oxygen transfer. Therefore, the design and scale-up of stirred tank bioreactors should meet the oxygen requirements necessary for the growth of the cells as well as maintaining low shear rates and controlled flow patterns. Gas hold-up and mass transfer coefficient have been recognized as the most important parameters commonly used for characterizing oxygen transfer in the stirred tank bioreactors. Therefore, for improving the gas-liquid mass transfer, it has attracted the attention of many scientific researchers and engineers. The better gas dispersion performance is an essential requirement of the agitator generally being responsible for bubble breakup and coalescence so as to break the larger bubbles to increase the gas-liquid mass transfer to achieve efficient gas-liquid mixing. Several types of impellers exist, and have been continuously designed and developed, to meet various industrial needs. The standard Rushton turbine has been most widely used since 1950s due to the high mass transfer coefficient exhibited for the gas-liquid dispersion. It has been used as a measuring yardstick to which the other types of agitators are generally compared. However, despite its versatility, it is not the perfect one and many weaknesses have been identified, although it is still the most widely used agitator (Dhanasekharan et al., 2005). The most common features of a stirred tank reactor are shown in Figure 1.1.

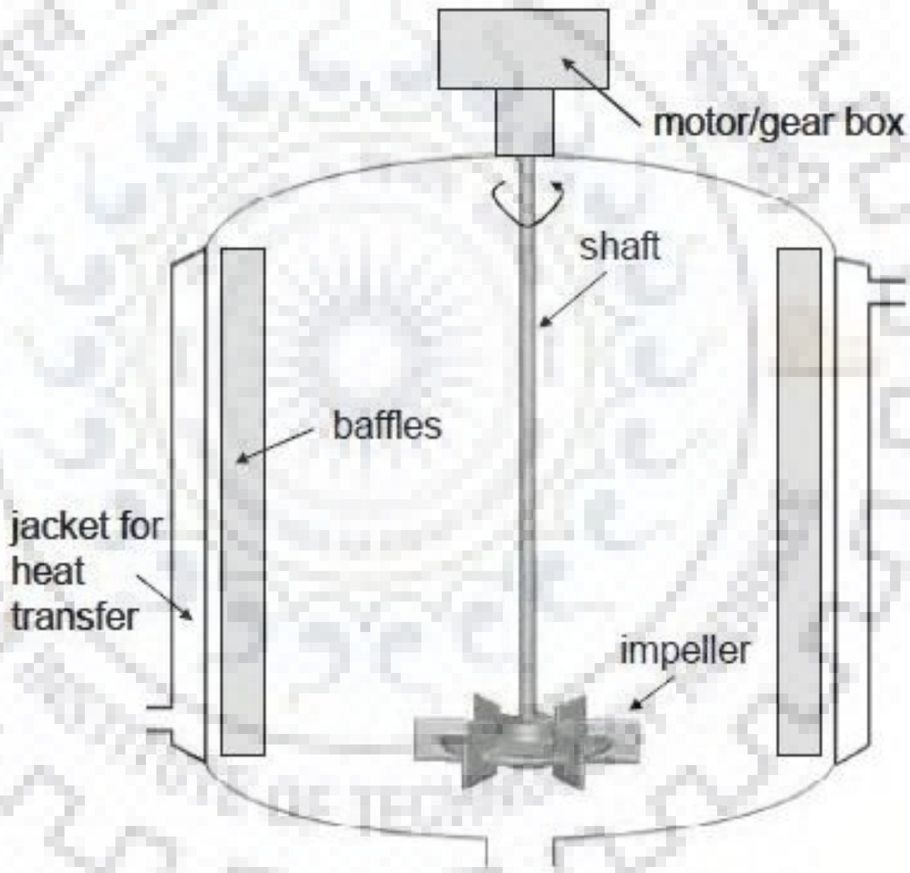


Figure 1.1. Common features of a standard stirred tank bioreactor

### 1.2 OXYGEN TRANSFER RATE (OTR)

The transfer of oxygen to the liquid phase is often a challenging task for the reactor engineering (Jesus et al., 2017), as it is plays an important role in its design and scale-up to ensure sufficient oxygen transfer (McClure et al., 2015). When designing and engineering bioreactors, it is often a challenging task, due to its low solubility in water at 37°C. Owing to the strong dependence of aerobic bioprocesses on the oxygen transfer, it is most widely found in the literature. The OTR is given as

$$OTR = k_L a.(C^* - C) \tag{1.1}$$

Owing to low solubility in water, its transfer rate thus becomes an essential consideration for its design and operation. Mass transfer in a gas-liquid process is often complex as it is influenced by a large number of factors such as the superficial gas velocity, the geometric design and the media properties (McClure et al., 2015). The oxygen transfer rate governs the microbial growth in a bioreactor and it is mostly used to predict the growth behavior. The mass transfer coefficient represents its quantitative magnitude. Figure 1.2 shows the schematic diagram of mass balance of oxygen transfer in a unit liquid volume.

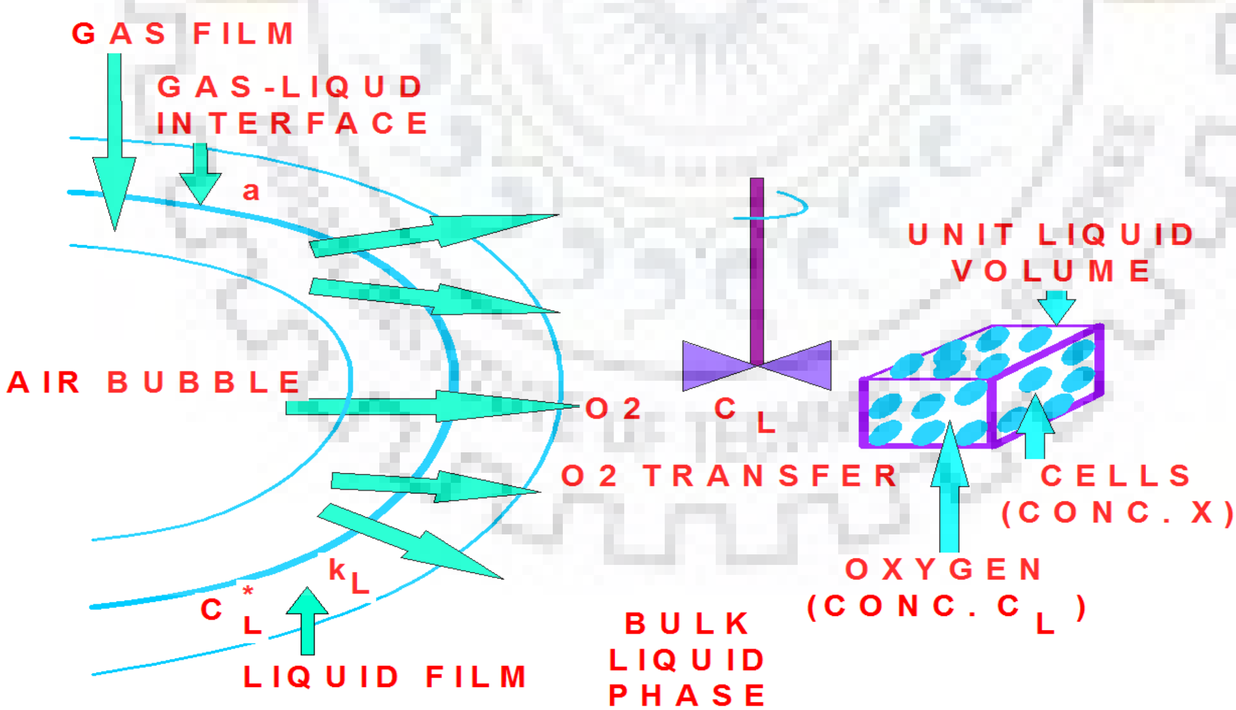


Figure 1.2. Schematic representation of the mass balance of oxygen transfer in a unit liquid volume

Several techniques are used to measure dissolved oxygen and its transfer rate in stirred tank bioreactors. Among them, zirconia, electrochemical, and laser cells, etc. have been used for measuring its concentration in the liquid medium. Optical sensors have also been found to be the better choice to determine oxygen concentration in the stirred tank bioreactors. Sulfite oxidation and gassing-out methods are mostly employed with a Clarke-type electrode for OTR measurements (Suresh et al., 2009). The oxygen absorption rate (OAR) was earlier determined, to study the effect of oxygen on the microbial growth. Nowadays, OTR is mostly used for determining the transfer of oxygen and several resistances encountered during such process (Suresh et al., 2009).

During most of the aerobic bioprocesses, the oxygen transfer requirements provided by sparging air bubbles serves an important constraint in achieving high cell density cultivations. Oxygen transfer is not an issue with low cell concentrations inside the reactor. However, as the cell concentration increases, it becomes difficult to ensure the necessary oxygen demand of the cells and thus limiting its growth (Schaepe et al., 2013). Several examples of limiting oxygen transfer rates have been discussed in the literature. The power input per unit volume also affects the gas-liquid flow in the culture and thus influencing the oxygen transfer. The gas-liquid flow is governed by the agitator and the compressor used to aerate the culture and thus strongly affecting the oxygen transfer rate.

## 1.3 VOLUMETRIC MASS TRANSFER COEFFICIENT ($k_La$)

The volumetric mass transfer coefficient, $k_La$, has been recognized as the most important parameter characterizing the gas-liquid mass transfer. It also serves as an important transport characteristics used in the scale-up, design and performance optimization of the stirred tank bioreactors (Labík et al., 2017). The processes which involve gas-liquid mass transfer as the controlling phenomenon, it becomes a key parameter (Garcia-Ochoa and Castro-Gomez, 2001). The bioreactor performance is greatly reduced due to insufficient oxygen transfer, and thus it becomes a crucial factor governing the bioreaction rate (Kantarci et al., 2005). The $k_La$ is a strong function of energy dissipation mode and the liquid media properties and thus its determination is essential in any fermentative aerobic bioprocess (Shukla et al., 2001; Jesus et al., 2017). Once the reactor is deaerated by sparging with some inert gas such as nitrogen, air is again sparged into it and the dissolved oxygen concentration measured as a function of time is used for calculating the

$k_La$. The dissolved oxygen concentration is measured until it is saturated (Kerdouss et al., 2008; Azargoshasb et al., 2016). The rate of change in the dissolved oxygen concentration in the liquid phase is given as follows:

$$\frac{dC_L}{dt} = k_L a.(C^* - C_L) \tag{1.2}$$

where $C^*$ and $C_L$ are dissolved oxygen concentration at saturation and at time t, respectively. The saturation concentration is given as follows:

$$P_{o_2} = H.C^* \tag{1.3}$$

Integrating Eq. 1.2 between two different times such as $t_1$ and $t_2$ gives as follows:

$$\ln\left(\frac{C^* - C_2}{C^* - C_1}\right) = -k_L a.(t_2 - t_1) \tag{1.4}$$

Finally, experimental $k_La$ can be obtained from the slope in Eq. 1.4. However, $k_La$ has also been determined using the following equation (Ashley et al., 1991 and Isailovic et al., 2015):

$$k_L a = \ln\left(\frac{DO^* - DO_{20}}{DO^* - DO_{80}}\right).\frac{1}{(t_{80} - t_{20})} \tag{1.5}$$

where DO* is its value at saturation, $DO_{20}$ and $DO_{80}$ represent 20% and 80% of DO*, respectively, and $t_{20}$ and $t_{80}$ are the times at which these are reached. The independent measurement of $k_L$ and $a$ separately is often considered as a difficult experimental task in general and particularly for those systems which are operated at heterogeneous flow regime with higher superficial gas velocities. However, the attempts have been made to measure the single bubble mass transfer by utilizing advanced visualization techniques which can separately measure $k_L$ and $a$ (Azargoshasb et al., 2016). Such techniques can be applied only for relatively low superficial gas velocity giving a high degree of insight into the process. In the literature, most of the published studies have reported the product of $k_L$ and $a$, i.e., the volumetric mass transfer coefficient, $k_La$ (Azargoshasb et al., 2016).

## 1.4 METHODS OF MEASUREMENT OF $k_La$

The volumetric mass transfer coefficient determination is essential for an efficient bioreactor design and to study the effect of different variables on the dissolved oxygen. There are several methods available in the literature, which are used for estimating the oxygen transfer rate (Van’t Riet, 1979). Among these methods, while some are applicable to other gases also, some are specific for oxygen transfer measurements only. The factors that must be taken into account, when selecting a method are:

1) type of aeration and homogenization system used,
2) the bioreactor type and its mechanical design,
3) the medium composition, and
4) the effect of the of microorganisms.

The dissolved oxygen mass balance in a well-mixed liquid phase can be established as:

$$\frac{dC}{dt} = OTR - OUR = k_L a.(C^* - C_L) - q_{o_2}.C_x \tag{1.6}$$

where *dC/dt* represents the accumulation rate of oxygen in the liquid phase, OTR represents the transfer of oxygen from the gas to the liquid, as described in Eq. (1.1), and OUR is the oxygen uptake rate due to the presence of the microorganisms. The application of the various methods is generally made on the basis of whether this measurement is carried out in the absence of microorganisms or dead cells or with biomass, which may consume oxygen during the course of measurement. The methods for the measurement of $k_L a$ can be broadly classified as:

1) Chemical methods (when no cells are present),
2) Physical methods (with and without cells), and
3) Dynamic methods.

### 1.4.1 Chemical Methods

Although these methods were the first to be used with wide acceptability. However, these methods in general should not be used for $k_L a$ determination in sparged bioreactors as the addition of the chemicals may lead to changes in the physico-chemical behavior of the liquids, especially coalescence. It also affects liquid film resistance due to the chemical reaction. In addition, the chemicals such as sodium bisulphate cannot be used inside the bioreactor as it might be harmful for the microorganisms. This method predicts higher values than the real ones, because the fast chemical reactions may influence the absorption rate, so the experimental conditions should be kept within the limits (Garcia-Ochoa and Gomez, 2009).

### 1.4.2 Physical Methods

They are the most widely used based on the oxygen probe response, as the concentration of the dispersed gas in the medium changes under non-stationary conditions. Also, they are the most widely used methods nowadays for the $k_La$ estimation since they are based on the dissolved oxygen concentration measurement during the absorption or desorption of oxygen in the solution (Baird et al., 1993; Garcia-Ochoa and Castro, 1998; Sanchez et al., 2000; Puthli et al., 2005; Zhan et al., 2006; Clarke et al., 2006).

### 1.4.3 Dynamic Method

The most widely used physical method for the measurement of $k_La$ is the gas-out gas-in dynamic method. In this method, first, the dissolved oxygen electrode is calibrated and then the nitrogen is sparged into the bioreactor to deaerate it until the dissolved oxygen reaches near zero. As the dissolved oxygen (DO) concentration reaches zero, it is aerated again and then the DO concentration is recorded with respect to time until it reaches saturation. Once a step change is introduced in the inlet gas, there appears to be a dynamic change in the dissolved oxygen concentration, which can be analyzed. Equation 1.6 can be again used for this method, in this case OUR is considered to be zero and thus integrating between two different times results:

$$\ln\left(\frac{C^* - C_2}{C^* - C_1}\right) = -k_L a.(t_2 - t_1) \tag{1.7}$$

Although, the physical methods are widely used in bioreactor systems, however they demand either the measurement of oxygen uptake rate independently or the accurate interfacial concentration determination (Ozbek and Gayik, 2001). The OUR can be determined by performing an experiment on a sample in a separate laboratory unit. It is often difficult to measure the interfacial oxygen concentration as it depends on the broth composition, the local pressure, and the oxygen concentration, which keeps on changing as the bubbles rise through the broth. The “gas out-gas in” method avoids such problems as it directly determines the $k_La$ in the microbial broth. This technique has been mostly employed to study the effect of operational conditions on $k_La$ (Garcia-Ochoa and Castro, 1998; Sanchez et al., 2000; Puthli et al., 2005; Djelal et al., 2006). Nevertheless, the response time, τ, of the dissolved oxygen probe is an important parameter and should be taken into account for the accurate determination of the dissolved oxygen concentration. It is usually recommended that $\tau << (1/k_La)$ in order to have reasonably accurate values.

## 1.5 POWER CONSUMPTION IN STIRRED TANK BIOREACTORS

Power consumption is a very important parameter for the stirred tank bioreactors. It is an indispensable and one of the most used parameter for describing the hydrodynamics, mixing and mass transfer performance in the stirred tank reactors. The power input per unit volume ($P/V_L$), also known as specific power input, is an important scaling-up parameter usually measured through the torque acting on the impeller shaft assembly under rotation. In order to make the correct measurement of power consumption, the losses during this process should be subtracted (Gill et al., 2008a). The necessary electrical power, required for the stirred tank bioreactors, the shaft design, and ensuring the mixing operations is directly governed by the specific power input (Puthli et al., 2005). Generally, it is expressed as the dimensionless number, which depends on the fluid property and the impeller geometry. For stirred tank bioreactors, the power input can be calculated as follows:

$$P = P_o \rho N^3 d_i^5 \tag{1.8}$$

In Eq. (1.8), $P_o$ is the dimensionless power number and depends on the geometric configuration and number of baffles, Reynolds number, Froude number and the aeration rate. Experimentally, specific power input can be determined using torque (M) measured on the stirrer shaft as follows:

$$\frac{P}{V_L} = \frac{2\pi NM}{V_L} \tag{1.9}$$

The impeller Reynolds number is determined as follows:

$$\mathrm{Re} = \frac{\rho_L N d_i^2}{\mu_L} \tag{1.10}$$

The power input per unit volume ($P/V_L$) associated with the liquid volume is most often used for process characterization and for scale-up. It has been used as a scale-up criterion for stirred tank bioreactors as many engineering process parameters remain constant during scale-up such as mass transfer and shear conditions and has been proven for cell culture applications. Thus, its measurement provides necessary and valuable information for characterizing the power capability of stirred tank bioreactors. The gassing power number is given as follows:

$$P_o = \frac{P}{\rho_l N^3 d_i^5} \tag{1.11}$$

P is the power consumption before gassing determined from the torque equation as:

$$P = 2\pi NM \tag{1.12}$$

where M is the net torque before gassing. In case of the aerated mixing, it is calculated as follows:

$$P_g = \frac{P^{'}}{\rho_l N^3 d_i^{\,5}} \tag{1.13}$$

where $P^{'}$ is the power consumption estimated using the following torque equation:

$$P^{'} = 2\pi N M_g \tag{1.14}$$

where $M_g$ is the net torque after gassing. It has been reported that power consumption is lower for the aerated systems compared to unaerated as the transfer of power from the impeller to the fluid may be affected by aeration (Luong and Volesky, 1979). This may be attributed to the fact that the aeration has the effect of lowering the liquid viscosity compared to the ungassed systems, which leads to the lesser power consumption. This power reduction may also be possible because of the cavity formation behind the impeller blades (Riet and Smith, 1973). The influence of aeration on the power consumption has been widely reported in the literature (Oosterhuis and Kossen, 1981; Warmoeskerken and Smith, 1981; Yawalkar et al., 2002) for single impeller systems. It has also been shown that the gassed power input is usually 30-40% of the ungassed power input, which depends on impeller type and aeration system used (Gill et al., 2008b).

## 1.6 MIXING IN STIRRED TANK BIOREACTORS

In a mixing operation, two materials are usually forced to collide to achieve a pre-defined value of mixing. It is the most common operation usually performed using mechanical agitation in the stirred tank bioreactors with the aim to achieve a homogeneity, faster heat exchange and component transport, and chemical reaction intensification (Magelli et al., 2013; Ascanio, 2015). The mechanically agitated tank is the most commonly used equipment in chemical and bioprocess industries to realize several elementary processes. With homogeisation as the key aim and the mixing time being a parameter of interest, it is mostly used for defining the liquid mixing time scale inside the stirred tank bioreactors (Taghavi et al., 2011). Mixing, being a physical process generally aims to reduce the non-uniformities in the fluids by removing the gradients of concentration, and other properties, is almost central to every bioreactor. It is indispensable in biotechnology as it defines the environment during cultivation inside the bioreactor. Mixing is a key engineering aspect since it ensures homogeneity of the culture affecting both the performance and the scale-up of the bioreactor. Efficient mixing is essential to avoid any kind of gradients that can be harmful for the cell growth (Hadjiev et al., 2006). Mixing time, being a key characterizing parameter to analyze the performance and hydrodynamics in stirred tank bioreactors, is the time required to achieve a certain degree of homogeneity of the tracer injected into it. Although maximizing the yield in any industrial bioprocess is a key consideration, however, it has been found that as the process is scaled-up, the yield starts decreasing (Bonvillani et al., 2006). This may be attributed to the substrate gradients, which can be caused by the poor mixing. Thus, mixing is of immense importance for the process optimization, scale-up and the product quality. It is one of the fundamental aspects of the process performance, which profoundly affects the blending, heat and mass transport and reaction phenomenon in a stirred tank reactor (Bonvillani et al., 2006). Consequently, it also affects the power input and operating efficiency. From the standpoint of macro-mixing, the bulk mixing time is defined as the time to get the material in the vessel uniformly distributed, while the local mixing time defines mixing in a particular localized region of the vessel depending on local turbulence (Mcclure et al., 2016). Therefore, the local measurements are time and space dependent, while the bulk mixing is based on time dependent, i.e. (temporal) measurements. In its non-dimensional form, mixing time can be expressed as:

$$N\theta_m = K \tag{1.15}$$

where $\theta_m$ is the mixing time in second (s), N is the impeller speed in revolutions per minute (rpm), and K being a constant, depend on the size, geometry of the tank and flow regime. Several experimental techniques used for determining the mixing time in stirred tank bioreactors are:

1) Colorimetry,
2) Electrical Resistance Tomography (ERT),
3) Planar Laser-Induced Fluorescence (pLIF),
4) Thermography, and
5) Conductometry and pH

In addition to the above mentioned experimental techniques, several researchers have used the experimental data and developed correlations for determining the mixing time. Although, such correlations have proved to be useful, however, they do not have the wide acceptability and when applied to other systems may often produce the inaccurate results. Therefore, it is the need of the hour is to develop a universal method for the prediction of the mixing time in stirred tank bioreactors, which is independent of the scale.

## 1.7 SCALE-UP OF STIRRED TANK BIOREACTORS

In general, the scale-up of a bioprocess involves transferring the new process developed at the laboratory scale to the production scale and it has gained much attention in the recent years owing to the hydrodynamics complexity and its possible impact on the transport characteristics. Apart from the bubble columns, mostly the larger scale processes are carried out in stirred tank reactors with one or several Rushton type turbines, as shown in Figure 1.1. With the increasing volumes of the products being manufactured in industrial processes over the last few decades, it has necessitated the use of larger and larger reactors (Bashiri et al., 2016). As a consequence, it has become a challenging task for the process engineers to develop substantial rules for their scale-up from the laboratory scale to the industrial scale due to the fact that their design and scale-up is not an easy task owing to the complexity of the momentum and mass transfer mechanisms. Currently, it is generally based on empirical correlations, best practices (know-how routines), and rules of thumb. With conventional scale-up procedures, it is generally assumed that the hydrodynamic parameters are constant inside reactor ("well-mixed" assumption). However, in reality, the values of such parameters such as mass transfer coefficient may vary significantly especially at the production scale. Dudukovic (2007) summarizes scale-up issue as follows: "Once the reactor system is successfully run in the laboratory to produce the desired conversion, yield, and selectivity, reproducing these results at the commercial scale is a real challenge" (Youssef et al., 2014). To accomplish this, Euzen et al. (1993) listed three types of experimental studies to be performed to supplement each other: laboratory scale, pilot plant, and mock-up (cold flow models) studies. The thermodynamic and kinetic assessment and their subsequent experimental verification at the laboratory scale units encompasses the first category. The next involves the analysis of physical and chemical mechanisms and implying that the mathematical models that can be transposable to industrial units. The last category includes, e.g., the use of dimensional similarity, residence time distribution (RTD) measurements through tracer studies, assessment of the hydrodynamics similarity and validation of computational fluid dynamics (CFD) studies.

Most of the times the correlations available in the literature are developed for small scale systems, so the scale-up of the stirred tank reactors is a challenging task. It is generally suggested that to get sufficient mass transfer in large scale reactors mostly bioreactors, they should be operated using the heterogeneous regime, however, the correlations developed for small scale and heterogeneous regime cannot be directly applied for scale-up. Based on the parameter analysis, several scale-up strategies have been suggested, however, each parameter is assumed to remain constant from laboratory to industrial scale (Nauha et al., 2015). These parameters for scale-up are as follows:

1) Global parameters:
    a. Volumetric mass transfer coefficient ($k_La$),
    b. Power input per unit volume (P/V),
    c. Impeller tip speed (T), and
    d. Mixing time ($\theta_m$).
2) Local parameters:
    a. Bubble distribution, and
    b. Velocity fields

Considering a simple stirred, aerated fermenter, no simple solution for the scale-up of aeration-agitation exists, which has the high probability of success for all fermentation processes. Most of the time, they are based on the aeration efficiency ($k_La$) or power input per unit volume (P/V). Impeller tip speed can also be used as basis for scale-up if a shear sensitive organism is used. Furthermore, constant mixing time as a basis for scale-up is not practically applicable as there exists no correlation between mixing time and aeration efficiency. However, the mixing time analysis for homogeneity (probably under aerated conditions) can be quite effective tool for scale-up, though not considered or reported to date and furthermore, time taken for constant mass transfer can also be considered. The correlation between these is that the constant mass transfer in well mixed tank (homogeneous) gives constant and less spatial variations of dissolved oxygen (DO), which is a critical parameter for cell viability (Nauha et al., 2015).

As already mentioned, the scale-up and design of larger reactors is mostly dependent on the correlations, best practices and rules of thumb. It is mostly relying on first carrying out the experiments at the laboratory scale and then increasing the scale to the bench scale (1-10 L) by validating results and trying to reproduce the laboratory scale results, then taking the next level to pilot scale (50-300 L) and if successful, then finally to the full production scale. Being the main criterion for the scale-up, oxygen transfer rate (OTR) should be optimized at every scale. Although, a scale-up ratio of 1:10 is typically used, however, if scale-up to 100 $m^3$ is required, then a pilot plant of 10 $m^3$ would be needed, which is practically not feasible, thus higher ratios are generally used. Various approaches have been recognized for the scale-up (Garcia-Ochoa and Gomez, 2009), which are, fundamental and semi-fundamental methods, dimensional analysis and rules of thumb. Fundamental methods involve the physical modeling of the large scale bioreactor systems, and thus eliminating the need for carrying the experiments at large scale. Among such methods, computational fluid dynamics, CFD is the most widely used method for modeling the stirred tank reactors. Many approaches have been recommended for scale-up using physical modeling. Despite the fact that CFD is a powerful tool for predicting the performance of stirred reactors, it has its own limitations such as complex interphase interactions, large number of computational grids requirement and longer computational times. The additional computational complexity is caused as the gas phase is introduced and the hydrodynamics gets complex. Therefore, the scale-up methods based on fundamental calculations are generally time consuming and need vast expertise and thus simpler methods are mostly used.

On the other hand, semi-fundamental methods involve solving simplified fundamental equations, which leads to scale-dependence. Scaling-up using dimensional analysis needs to keep dimensionless groups constant, which is not possible and thus choices should be made to select the dimensionless group, which mostly affects the scale-up. Mostly, thumb rules are employed for the scale-up and they vary with different sources. The scale-up method mostly found in the literature is to keep gas volume flow per unit of liquid volume per minute (vvm or vol $vol^{-1}$ $min^{-1}$) and the power input per unit volume (P/V) constant (Garcia-Ochoa and Gomez, 2009). However, constant vvm is a stoichiometric approach, and it is questionable from the viewpoint of hydrodynamics. Scale-up by keeping constant volumetric mass transfer coefficient, $k_La$, has also been found in the literature and is mostly based on the empirical correlations. Such correlations can be dimensional and non-dimensional. Dimensional correlations are mostly function of superficial gas velocity, $v_s$, or vvm, stirring rate, N, or power input per unit volume, P/V, and viscosity, $\mu_a$. The correlations are mostly in the following form:

$$k_L a = \alpha.(\frac{P_g}{V_L})^{\beta}.v_{sg}{}^{\gamma} \tag{1.16}$$

where the exponents β and γ depend on system geometry and impeller used and may range from 0.3 to 0.7 and 0 to 1.0, respectively (Stenberg and Andersson, 1988; Rushton and Bmbinet, 1968). The correlations of the form of Eq. (1.16) are generally scale dependent and should incorporate some additional terms for scale-up. The latter correlations are developed using dimensionless numbers such as Reynolds, Weber, Flow and Froude numbers. These take various forms and also include system dependent exponents, the use of which makes these correlations both system and scale independent. Very little evidence to their application in large scale reactors has been published (Amanullah, 2004). Such correlations are only applicable to the range they are developed for and not universally acceptable.

## 1.8 DIFFERENT IMPELLER TYPES USED IN STIRRED TANK BIOREACTORS

The design and choice of impellers plays a critical role to maintain proper hydrodynamic conditions and mass transfer rates in stirred tank bioreactors. They are responsible for mixing, and bubble breakage and coalescing. Figure 1.3 shows a schematic of the most commonly used impeller types. They are generally classified based on mixing regimes, i.e. laminar or turbulent mixing. Owing to poor momentum transport in laminar flow, the impeller diameters approach the diameter of tank, however, as turbulent flow transports momentum well, impeller diameters in this flow (Re >$10^4$) are usually one-fourth to one-half of the tank diameter. Typical laminar impellers include helical ribbons and screws, and anchor impellers. Discs, paste rollers, high shear and gate impellers are also used in laminar mixing.

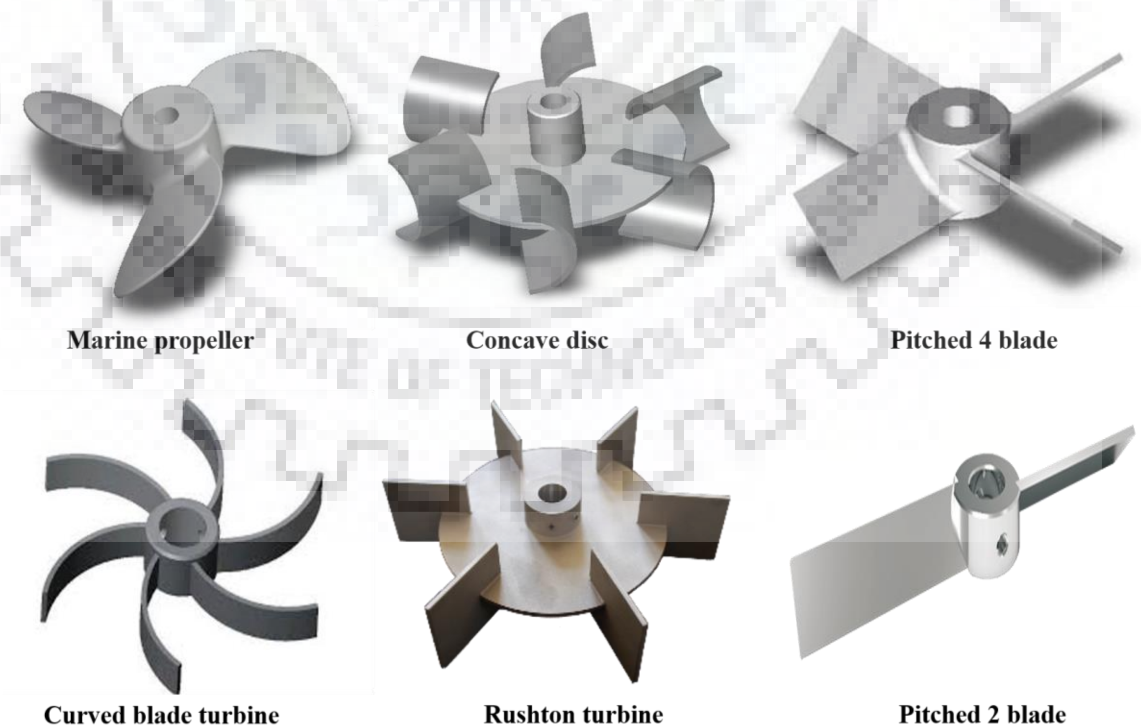


Figure 1.3. Different types of impellers used in the stirred tank bioreactors

Turbulent flow impellers mostly used in fermentation applications may further be classified into radial and axial flow impellers based on flow direction as shown in Figure 1.4. Typical radial flow impellers include: disc style, flat blade turbine (Rushton turbine) and curved blade impellers. The pitched-blade turbines and propellers are mostly axial or mixed flow impellers. Several types of impellers exist and are continuously being developed to meet various needs. The standard Rushton turbine, a radial type is the most widely used impeller since 1950s (Nienow, 1996). It delivers high mass transfer coefficient (Williams, 2002) and it is used as measuring yardstick to which other impellers are generally compared (Kadic and Heindel, 2014).

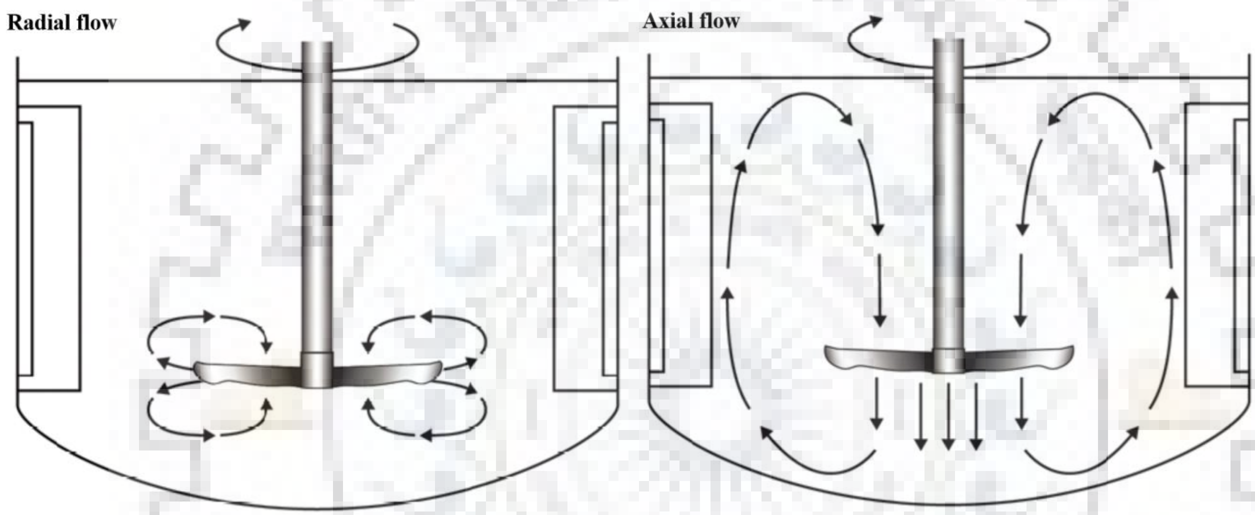


Figure 1.4. Radial and axial flow patterns in stirred tank bioreactors (*Source: Mirro and Voll, 2009*)

However, despite its versatility, it is not the perfect one and several weaknesses are reported, e.g. its axial pumping capacity is low and is not sufficient for necessary bulk flow for satisfying oxygen transfer requirements. It mostly disperses gas in the regions adjacent to the impeller and uniform dispersion of gas is hard to achieve. It can generate hydrodynamic shear, which can adversely affect the cultivation of animal cells with no protecting cell wall. Owing to its sweeping action, low-pressure trailing vortices can be observed at rear of the blades, resulting in great power drop after gas is introduced and thus the gas handling capacity is also affected due to flooding (Gelves et al., 2014; Kadic and Heindel, 2014). Yang et al. (2015) investigated the dislocated Rushton turbine, an exact variant of the standard Rushton turbine with same component dimensions except that blades are placed above and below impeller disc alternatively. It was concluded that dislocated Rushton turbine outperforms the standard Rushton turbine and thus indicates the promising potential of dislocated Rushton turbine in gas-liquid mixing in the stirred tank bioreactors.

On the other hand, pitched blade turbines generate mixed flow and the extent of axial flow actually depends on the blade or pitch-angle. Now-a-days, they are mostly used in cell culture applications due to less hydrodynamic shear. Recently, a new impeller, i.e. Chemineer Concave disc (CD-6) has been introduced and it has revolutionized the field of gas-liquid dispersion. Couper et al. (2005) reported that gas-handling capacity of this new impeller is 200% more than six bladed disk turbines, before flooding and even at flooding condition power reduction is around 30%. Ghotli et al. (2013) reported that curved blade impellers consume less power in both aerated and un-aerated states as compared to Rushton turbine.

## 1.9 MOTIVATION FOR RESEARCH

Stirred tank bioreactors have revolutionized the field of biotechnology due to the lot of thrust on bioprocesses for being ecofriendly and economically viable. Although a multitude of bioreactors used for cultivation of animal and human cell cultures have been introduced to the market over the past few decades, there is still a lack of engineering data. The thorough understanding and predictive performance of stirred tank bioreactors still remains a challenging problem owing to their complex hydrodynamics on account of so many different internal rotating elements. Their accurate design and operation is crucial for the profitability of the process due to its influence on the overall yield and productivity. Traditionally, it is mostly based on the empirical correlations describing macroscopic parameters, e.g. power demand, mass transfer coefficient and gas hold-up. The oxygen transfer in such systems has been recognized as the important parameter for determining their efficiencies and successful scale-up. It is mostly affected by various factors, e.g. agitation rate and aeration rate, media properties and reactor properties, etc. The mass transfer characteristics in a STBR are also significantly affected by different impeller types and their configurations. The power-input per unit volume is an important parameter for describing their hydrodynamics, mixing, mass transfer and most importantly scale-up. Stirred tank bioreactors from small- to large- scale for various applications have been developed over the past several decades, however, there is still a great scope and need for further research in this area.

## 1.10 RESEARCH OBJECTIVES

The overall objective of the proposed work is to characterize the performance of Rushton, pitched blade and marine propeller impellers and their different combinations on the volumetric mass transfer coefficient, $k_La$, considering with and without cell culture in a stirred tank bioreactor. The specific objectives of the proposed research work are as follows:

- To study the effect of various parameters such as agitation speed and aeration rate, impeller configurations, power input per unit volume, scale of reactors, viscosity, impeller diameter and liquid volume inside reactor, on the volumetric mass transfer coefficient, $k_La$, in the absence of cell culture in a stirred tank bioreactor.
- To study the effect of various parameters such as agitation rate and aeration rate, impeller configurations, impeller diameter, bioreactor working volume, on the volumetric mass transfer coefficient, $k_La$, in the presence of cell culture in a stirred tank bioreactor.
- To study the rheology of cell culture, i.e. *E. coli* BL21 inside the stirred tank bioreactor.
- Develop empirical correlations (dimensional and dimensionless) between volumetric mass transfer coefficient $k_La$ and the parameters considered for different impeller configurations.
- Mass transfer performance of a newly developed dislocated Rushton turbine (designed and fabricated using 3-D printing technology) and its comparison with the standard Rushton turbine.

## 1.11 THESIS ORGANIZATION

Based on the objectives of the proposed work, thesis has been organized into six chapters as follows:

The introduction, motivation, research objectives, and the structure of this thesis have been explained in Chapter 1.

Chapter 2 explains the critical review regarding the stirred tank bioreactors with emphasis on hydrodynamics, mass transfer, mixing, power consumption and scale-up. Some basic concepts regarding stirred tank bioreactors have also been explained in this chapter.

Chapter 3 addresses the experimental details of stirred tank bioreactors used, fabrication of different impellers using 3-D printing, method used for the experimental determination of $k_La$, preparation of solid and liquid LB medium for *E. coli* BL21, preparation of inoculum have been explained. Statistical modeling using design of experiments is also explained in this chapter. Rheological characterization for studying the flow behavior of *E. coli* BL21 has also been explained.

Chapter 4 covers mass transfer characterization in stirred tank bioreactors of different volumes. Further, the effect of different parameters on volumetric mass transfer coefficient ($k_La$) and power input per unit volume, ($P/V_L$); statistical modeling and analysis of volumetric mass transfer coefficient, $k_La$ and power input per unit volume, $P/V_L$ in stirred tank bioreactors for different impeller configurations; and comparison of RSM based correlations with the existing correlations have been reported in this chapter.

Chapter 5 covers the mass transfer and rheological characterization for cell culture, i.e. (*E. coli* BL21) in a stirred tank bioreactor for different impeller configurations and operational parameters, development of dimensionless correlations for different impeller configurations.

In Chapter 6, the research outcomes are summarized and concluded. In addition, the possible recommendations helpful for further study are suggested.

# CHAPTER 2

# LITERATURE REVIEW

## 2.1 GENERAL

This chapter aims to review the various aspects of the stirred tank reactors/bioreactors viz. hydrodynamics, mass transfer, power consumption, mixing and scale-up. The main focus of the collated literature is on the stirred tank reactors/bioreactors equipped with an agitation system and other accessories to have an understanding of the hydrodynamics and mass transfer in such systems. The literature review also provides the brief details of the recent work that has been carried out on the stirred tank reactors/bioreactors.

## 2.2 STIRRED TANK BIOREACTORS

Mechanically agitated vessels are mostly used in process industries for multiple operations such as biotechnological, pharmaceuticals, metallurgical and petrochemical (Kerdouss et al., 2008; Nauman, 2008; Bolic et al., 2016; Tervasmaki et al., 2016; Bach et al., 2017; Jossen, 2017) processes. The mixing operation in stirred tank reactors can either be simple fluid mixing or involve complex operations, and it can be carried out either with a single or multiphase systems based on the process. They have attracted much greater attention especially in the bioprocess owing to their potential for integrating the development of high value products and thus replacing the need for conventional chemical processes. Generally, a gas sparger is provided at the bottom of the reactor for sparging gas into the reactor. To enhance the heat and mass transfer in such systems, the baffles and agitator(s) and other internals with specific applications are used. Agitator is generally used for enhancing the gas-liquid interfacial area as it breaks the large gas bubbles into smaller ones. The oxygen transfer in such systems has been recognized as an important parameter for determining their efficiencies and successful scale-up. It is generally affected due to various factors, e.g. agitation rate, aeration rate, media properties and reactor properties, etc. Further, impeller types and their configurations also significantly influence the mass transfer characteristics in stirred tank bioreactors.

## 2.3 GAS SPARGED STIRRED TANK BIOREACTORS

In several industrial processes such as fermentation, oxidation, hydrogenation, chlorination, gas sparged stirred tank reactor is employed. They can be operated either in two phase or sometimes an additional phase can also be used such as catalyst in some cases or a microorganism can also be used for producing industrially important bio-products. To ensure that the phases are properly mixed, impeller agitation rate and type play an important role in their design. The bio-applications involving microorganisms, shear speed should be considered to avoid any harm to them.

The commonly used gas sparged stirred tank bioreactor includes a shaft provided with one or more impellers, baffles, and a sparger for aeration purpose. Aspect ratio, i.e. the ratio of reactor height to diameter (H/D), varies depending on the application, e.g. systems requiring more gas residence time demand higher aspect ratio and more than one impeller is used on the same shaft. For maintaining temperature inside the reactor vessel, heater and chiller is used. Rushton turbine is the most commonly used impeller type in the industry developed by Rushton and co-workers and is considered as standard impeller design (Rushton et al., 1950). A standard reactor configuration comprises of a cylindrical vessel made of either high quality glass or stainless steel with flat or dished bottom of depth H, with diameter of vessel equal to T, and baffle width, B = 0.1T. The ratio of impeller to tank diameter is 1/3, being centrally mounted with clearance C = 0.33H, the said reactor configuration is shown in Figure 2.1. The major advantage of the Rushton turbine is the strength gained from the impeller disc compared to open-bladed paddle, and it also avoid by passing the gas through the shaft. However, it also has drawbacks because of higher power consumption and less axial flow. Thus, considering its drawbacks, other impeller types such as pitched blade, marine propeller, Smith impeller, CD6, Scaba impeller have been designed and developed over the years. Table 2.1 summarizes a few of the studies carried out in stirred tank bioreactors considered by the researchers for different applications.

### 2.3.1 Applications of Stirred Tank Bioreactors in Bioprocesses

One of the most important and frequent application is as bioreactors, where they are used for treating the microorganisms in a completely safe environment utilized for producing industrially important products, e.g. enzymes, proteins, and antibiotics, etc. A few such studies utilizing STR’s as bioreactors are presented in Table 2.2. Bandaiphet and Prasertsan (2006) used *Enterobacter cloacae* WD7 and studied the effect of aeration rate and agitation rate and scale-up on the volumetric mass transfer coefficient, $k_La$ for production of exopolysaccharide. Elqotbi et al. (2013)

numerically performed the production of gluconic acid by *Aspergillus niger* strain by using a two-phase stirred bioreaction system by employing the Euler-Euler model. Gabelle et al. (2012) using *Trichoderma reesei* studied the effect of rheology on the volumetric mass transfer coefficient in the growth phase in STBRs of different volumes for the production of a variety of economically important proteins such as cellulase enzymes. Liu et al. (2017) reported the production of fumaric acid by immobilized *Rhizopus arrhizus* RH 7-13-9 # on loofah fiber and provided a new method for the production fumaric acid in a STBR. Pereira et al. (2017) carried out the production of biosurfactant using *Aureobasidium pullulans* in a stirred tank bioreactor. Abdella et al. (2016) reported the production of β-glucosidase from wheat bran and glycerol using *Aspergillus niger* in stirred tank and rotating fibrous bed bioreactors. Siedenberg et al. (1997) studied the production of xylanase on synthetic medium in stirred tank and airlift loop reactors using *Aspergillus awamori*.

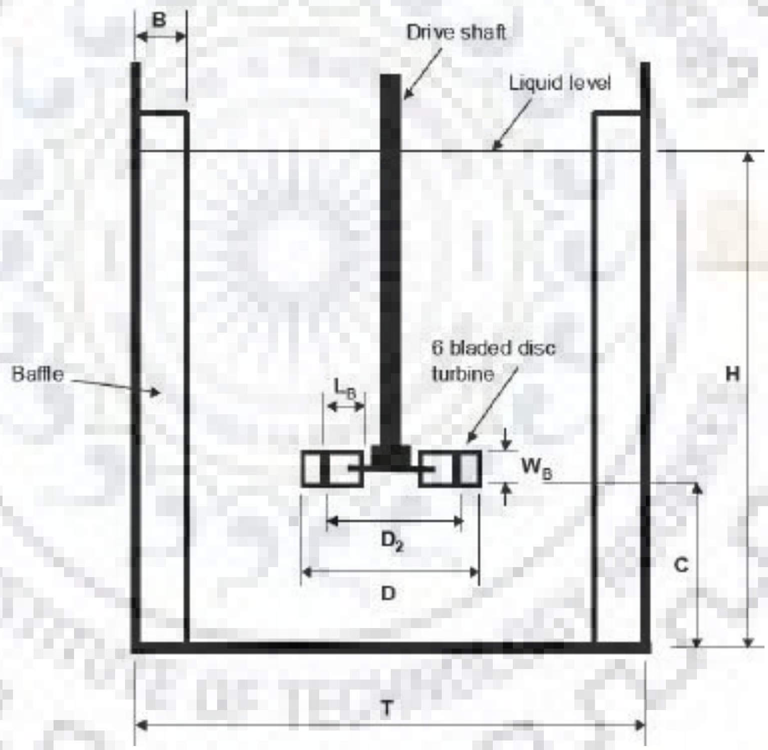


Figure 2.1. Standard configuration of stirred tank bioreactor with a Rushton turbine

Table 2.1 Summary of the literature reviewed on stirred tank bioreactors

| Investigator | Objective (s) | Study; Fluid; System | Parameters investigated | Remarks |
|---|---|---|---|---|
| Pedersen et al. (1994) | Mixing time characterization in stirred bioreactors | Experimental<br>Fluids: Air, water, NaOH solution<br>System: Stirred tank reactor (3 L) | Mixing time | Studied liquid mixing STBRs of different volumes (7, 15, and 41 L)<br>Mixing was characterized under both aerated and unaerated conditions for both aqueous and viscous medium for a 15 L reactor.<br>Mixing time was compared for different volume reactors at real process conditions, i.e., an aerated viscous medium. |
| Wernersson and Tragardh (1999) | Scale-up of Rushton turbine agitated tanks | Experimental and Computational<br>Fluids: Air, water<br>System: Three different stirred with diameters 0.8, 1.88, 2.09 m equipped with 2, 3 and 4 Rushton impellers respectively, baffles used. | Turbulent kinetic energy, local energy dissipation rate, power consumption | Developed empirical correlations for scale-up purposes considering three different reactors.<br>Influence of the ratio of bulk zone volume to impeller zone volume on the distribution of the power supplied to the reactor. |

| | | | | |
|---|---|---|---|---|
| Puthli et al. (2005) | Gas-liquid mass transfer studies on a laboratory scale bioreactor for triple impeller system | Experimental<br>Fluids: Air, water, and other chemicals to alter the physico-chemical properties of the liquid phase.<br>System: Laboratory scale glass bioreactor with a volume of 2L and 0.13m diameter and 0.22m height, four baffles, air sparger, different impeller configurations.<br>Impeller agitation rates: 300-600 rpm,<br>Aeration rates: 8.92-33.81 $cm^3/s$. | Mass transfer coefficient ($k_La$) | It was reported that process variables such as agitation and aeration rates, impeller configuration, and fluid viscosity affect the $k_La$.<br>Triple impeller system delivered highest $k_La$ values with least power consumption. |
| Bandaiphet and Prasertsan (2006) | Effect of aeration, agitation rates and scale-up on mass transfer coefficient in exopolysaccharide production using *Enterobacter cloacae WD7* | Experimental<br>Fluids: Air, water<br>System: Two stirred tank reactor with 5L and 72 L volumes, impellers with six flat blades used,<br>Impeller agitation rate: 200-800 rpm<br>Air flow rate: 0.5-1.75 vvm. | Dissolved oxygen concentration (% sat.), biopolymer yield, dry cell weight, oxygen uptake rate (OUR), oxygen transfer rate (OTR), mass | Biopolymer yield increased with agitation and aeration rates for the pilot plant scale, but decreased with increasing agitation rate at bench scale due to shear thinning behavior (from 3.07 to 2.28 g/g over the range 200-800 rpm) and increased with aeration rate (from 2.79 to 3.07 g/g over the range 0.5 to 1.25 vvm, respectively).<br>$k_La$ values in the exponential and stationary phases increased with agitation |

| | | | | |
|---|---|---|---|---|
| | | | transfer coefficient, viscosity | and aeration rates to 9.97 and 9.72 $h^{-1}$ at aeration rate of 1.25 vvm of bench scale fermentation and 9.68 and 9.50 $h^{-1}$ in exponential and stationary phases at aeration rate of 1.75 vvm at pilot plant scale, respectively. |
| Hadjiev et al. (2006) | Mixing time in aerated bioreactors | Experimental<br>Fluids: Air, sucrose solution of different concentrations<br>System: Stirred tank reactor, torque meter | Mixing time | Studied the effect of various parameters on the mixing time and Influence of geometry of reactor on mixing time.<br>A new correlation for estimating the mixing times in stirred reactors is proposed. |
| Gill et al. (2008) | Quantification of power consumption and oxygen transfer characteristics of a STBR for scale-up | Computational and Experimental<br>Fluids: Air, water, medium | $P/V_L$, $k_La$, growth curves | Developed correlations to predict $k_La$ and power consumption.<br>Reported $k_La$ as the most suitable criterion for the scale-up of miniature STBRs. |
| Kerdouss et al. (2008) | Mass transfer coefficient determination in a | Experimental and computational<br>Fluids: Air, water<br>System: 3 L stirred tank reactor | Gas volume fraction, Sauter mean diameter, | The model predicts spatial distribution of gas hold-up, Sauter mean bubble diameter and $k_La$. |

| | | | | |
|---|---|---|---|---|
| | stirred vessel using CFD | equipped with a pitched blade impeller and ring sparger. | mass transfer coefficient ($k_La$) | Reported good agreement between experimental and numerical results for $k_La$. |
| Zadghaffari et al. (2009) | Mixing study in dual Rushton stirred tank | Experimental and computational<br>Fluids: Air, water<br>System: Flat bottomed glass cylinder with diameter 0.30 m and four vertical baffles, two Rushton turbines, Rhodamine-B fluorescent tracer particles, Impeller agitation rates: 225, 300, 400 rpm. | Flow field, pumping number, mixing time | Numerically investigated the flow fields, power and mixing time.<br>Numerical predictions were validated with experimental results for velocity of liquid phase using particle image velocimetry (PIV) and planar laser-induced fluorescence (PLIF) technique. Reported reduction in mixing time and increase in stirring power input with increasing agitation speed. |
| Ranganathan and Sivaraman (2011) | Hydrodynamics and mass transfer investigation in a gas-liquid stirred reactor using CFD coupled with PBM | Computational<br>Fluids: Air, water<br>System: Fully baffled Perspex vessel with 0.292m dia. and 0.584 m height. Two Rushton turbines with dia. 0.0973 m | Gas hold-up, Sauter mean diameter, specific interfacial area | Reported local hydrodynamic parameters such as gas holdup, Sauter mean bubble diameter and interfacial area.<br>The predicted gas holdup, Sauter mean diameter and $k_La$ values were in good agreement with the reported experimental data (Alves et al., 2002a, b, 2004). |

| | | | | |
|---|---|---|---|---|
| Taghavi et al. (2011) | Experimental and CFD investigation of power consumption in a dual Rushton stirred tank | Experimental and computational<br>Fluids: Air, water<br>System: Cylindrical flat bottomed plexiglass with diameter 0.3 m, four baffles used with width 0.03 m,<br>Impeller agitation rates: 200-600 rpm,<br>Air flow rates: 100-800 L/h. | Flow field, power number, power consumption | Studied the flow regime behavior, local and total power consumption of a single and gas–liquid phase systems.<br>Developed new empirical correlations for estimating power consumption and flow regime transitions in stirred tank bioreactors. |
| Gabelle et al. (2012) | Impact of rheology on mass transfer coefficient in stirred tank bioreactors | Experimental<br>Fluids: Air, water, xanthan gum as model fluid.<br>System: Stirred tank reactors of 3 and 20 L volumes, double flux-specific impeller used in 3 L reactor, a Rushton and pitched blade turbine used in 20 L reactor, ring sparger used. | Growth curves, apparent viscosity, mass transfer coefficient | Measured mass transfer coefficients during the growth phase in bioreactors of 3 and 20 L and compared with those measured with water and model fluids. Gas–liquid mass transfer is strongly impacted by the rheology of the media, especially when biomass concentration exceeds approximately 15 g/ L. |
| Karimi et al. (2013) | Oxygen transfer in a stirred tank bioreactor for environmental purposes | Experimental<br>Fluids: Waste gases including benzene, toluene, xylene and air<br>System: Cylindrical glass vessel with semi-circle bottom with diameter 10 cm with 1.77 L working volume, four | Volumetric mass transfer coefficient | Twin Rushton turbine configuration showed superior mass transfer performance (23-77% enhancement in $k_La$) compared with other impeller configurations.<br>Sparger type has negligible effect on |

| | | | | |
|---|---|---|---|---|
| | | baffles, air sparger, Rushton turbine, pitched blade with 4 and 2 blades,<br>Impeller agitation rates: 400-800 rpm,<br>Air flow rates: 1-5 L/min. | | oxygen transfer.<br>Agitation rates in the range of 400-800 rpm are the most efficient for oxygen transfer in stirred tank bioreactor. |
| Magelli et al. (2013) | Mixing time in high aspect ratio stirred reactors | Experimental and computational<br>Fluids: Water<br>System: Stirred tank reactors of three different vessel sizes, different impellers used,<br>Impeller agitation rates: 120-2000 rpm | Mixing time | Impeller number and spacing strongly affect mixing time.<br>Proposed an empirical correlation for mixing time.<br>Zoning and non-zoning impeller configurations are successfully analyzed. |
| Petitti et al. (2013) | Simulation of coalescence, break-up and mass transfer in a gas-liquid stirred tank | Experimental and computational<br>Fluids: Air, water<br>System: Flat bottomed stirred tank equipped with a Rushton turbine and a porous sparger.<br>Impeller agitation rates: 155-250 rpm<br>Air flow rate: 0.018-0.093 vvm | Sauter mean diameter, specific interfacial area, mass transfer coefficient, oxygen concentration in the liquid and gas phase | Bubble coalescence, break up and mass transfer have been considered with CQMOM (Multi-variate population balance model).<br>Predictions for mean bubble size, Sauter mean diameter and mass transfer are in good agreement with experiments. |

| | | | | |
|---|---|---|---|---|
| Lee and Dudukovic (2014) | Flow regime and gas hold-up study in gas-liquid stirred tanks | Experimental<br>Fluids: Air, water<br>System: Flat bottomed stirred tank reactor with a Rushton turbine and a ring sparger.<br>Impeller agitation rates:126-830 rpm;<br>Air flow rate: 2.08 to 30 $ft^3/h$ | Gas hold-up, bubble count profiles, flow regime | Identification of flow regime in gas-liquid stirred tanks.<br>Linear relationship of the Froude number with gas hold-up quantified.<br>Air-water system has been used in this study, however, this technique can be used for all gases and liquids. |
| Scargiali et al. (2014) | Mass transfer and hydrodynamic characteristics of stirred reactors without baffles | Experimental<br>Fluids; Air, water<br>System: PMMA made cylindrical stirred tank with diameter 19 cm and height 30 cm, six different turbine types used.<br>Impeller agitation rates: 100-1300 rpm. | Mass transfer coefficient, power number, power dissipation | Mass transfer performance of unbaffled systems is mainly affected by specific power consumption.<br>Among the different impeller geometries investigated, a simple PBT was found to provide better oxygen transfer performance and is therefore widely used in fermentation processes particularly for shear-sensitive cultures. |
| Bao et al. (2015) | Influence of impeller diameter on overall gas dispersion properties in a | Experimental and computational<br>Fluids: Air, water<br>System: Cylindrical stainless steel dished bottom tank with diameter 0.48 m, four baffles used, three impellers and | Flow field, relative power demand (RPD), gas hold-up | Studied the effect of the impeller diameter on gas dispersion.<br>As D/T increases, relative power demand (RPD) decreases slightly. At low superficial velocity (0.0078 $m.s^{-1}$), the gas |

| | | | | |
|---|---|---|---|---|
| | stirred tank | a ring sparger used.<br>D/T: 0.30-0.40<br>Aeration rates: 5-59 $m^3/h$ | | hold-up increases with D/T. However, at high superficial velocity and at D/T=0.33, good balance is observed between liquid recirculation and liquid shearing rate, resulting in highest gas holdup among four different D/T. |
| Montante and Paglianti (2015) | Gas hold-up distribution, mixing time analysis in stirred tanks | Experimental<br>Fluids: Air, water<br>System: Cylindrical flat bottomed vessel with diameter 0.232 m and height 0.28 m provided with four equally spaced baffles. Rushton turbine, pitched blade turbine upward pumping, Lightnin A310 impeller used. Porous membrane used for gas sparging | Gas hold-up distribution, mixing time | Used electrical resistance tomography for gas-liquid system analysis.<br>Effect of bubbles on liquid mixing time is studied.<br>Mixing quality is quantitatively related to the flow regime.<br>ERT allows the analysis of gas-liquid systems without limitation on gas loading. |
| Mounsef et al. (2015) | The effect of aeration conditions characterized by $k_La$ on fermentation kinetics of *Bacillus* | Experimental<br>Fluids: Air, water, CMB, LB broth<br>System: Stirred tank reactor with 2 L volume,<br>Impeller agitation rates: 340-500 rpm<br>Aeration rate: 0.033-1 vvm. | Cell concentration, spore concentration, maximum specific oxygen | Aeration has been identified as a key factor for *Bacillus thuringiensis* growth and is generally characterized by $k_La$.<br>For reasonable values of the aeration rate, the best toxin proteins productivity was reached in the 6% CMB culture medium |

| | | | | |
|---|---|---|---|---|
| | *thuringiensis* kurstaki | | uptake rate, productivity | for $k_La$ of 65.5 $h^{-1}$ suggesting that $k_La$ could be used as a scale-up criterion for its production. |
| Yang et al. (2015) | Gas-liquid hydrodynamics in a vessel using dual dislocated- blade Rushton turbines | Experimental and computational<br>Fluids: Air, water<br>System: Cylindrical vessel with elliptical bottom with diameter 0.21 m and four baffles, ring sparger, standard and dislocated Rushton turbine used<br>Impeller agitation rates: 300-700 rpm<br>Aeration rates: 0.4 and 0.6 $m^3$/h. | Flow field, gas hold-up, power consumption, dissolved oxygen | Dislocated Rushton turbine (DRT) is superior than the standard Rushton turbine (SRT) in gas-liquid mixing operations. The DO performance of DRT is higher than STR and the increase is up to 16% and gas hold-up is also higher by around 18%. Moreover, the power-consumption of DRT is 5% lower than SRT. |
| Azargoshasb et al. (2016) | Experiments and three phase CFD-PBE simulation of a stirred tank bioreactor for high cell density cultivation (HCDC) | Experimental and computational<br>Fluids: Air, water, LB broth.<br>System: Stirred tank bioreactor volume 5 L with baffles, Rushton, scaba and paddle impellers and a ring sparger used.<br>Impeller agitation rates: 50-1200 rpm,<br>Aeration rates: 1 vvm | Velocity vectors, liquid velocity, gas volume fraction, gas hold-up, air volume fraction, Sauter mean diameter, energy dissipation rate, | Gas-liquid-solid flow was modeled using Eulerian multiphase and $k$-$\epsilon$ model. Energy dissipation rate, gas holdup, flow patterns, Sauter mean diameter and $k_La$ have been investigated for different impeller types using multiple reference frame (MRF) model.<br>Studied the influence of aeration and agitation rates. |

| | | | | |
|---|---|---|---|---|
| | | | mass transfer coefficient, biomass and glucose concentrations | Scaba impeller results in higher $k_La$, and thus resulting in higher biomass concentrations.<br>Due to high consumption of substrate around the impeller, the best feeding spot is in the vicinity of the impeller. |
| Sarkar et al. (2016) | Mixing of multi-phase flow in a bioreactor using CFD-PBM | Experimental and computational<br>Fluids: Air, water<br>System: Cylindrical shaped bioreactor with spherical bottom, a Rushton and two three- blade type propeller impeller, four baffles, a pipe type sparger containing circular holes.<br>Impeller agitation rates: 50-300 rpm<br>Aeration rates: 2-6 L/min. | Turbulent kinetic energy dissipation rate, gas velocity, gas volume fraction, bubble distribu-tion, Sauter mean diameter, mass transfer coefficient, | To understand mixing in a bioreactor, a multiphase (Eulerian-Eulerian), with turbulent ($k$-$\epsilon$) CFD model integrated with population balance model (PBM) has been used.<br>Mixing plays a crucial role in scale-up. Predicted size distribution of bubbles as a function of process parameters. |
| Wutz et al. (2016) | Predictability of $k_La$ in stirred tank reactors under multiple operating conditions using | Computational<br>Fluids: Air, water<br>System: Two stirred tank reactors with volume 2.3 L with blade impeller with four blades and a macro-sparger and 80 | Flow field, turbulent dissipation rate, mass transfer coefficient | Two different scales show similar flow behavior under turbulent dissipation. Compared numerical predictions for $k_La$ with the experimental data for model evaluation. Results indicated that the |

| | | | | |
|---|---|---|---|---|
| | an Euler -Lagrange approach | L with blade impeller with six blades and a ring sparger. | | breakage does not play a major role in small-scale bioreactor with simulated bubble residence times of ~ 0.7 s. |
| Bach et al. (2017) | Evaluation of mixing and mass transfer in a stirred pilot scale bioreactor using CFD | Experimental and computational<br>Fluids: Air, water<br>System: Tori spherical bottomed cylindrical vessel with baffles, Impeller agitation rates: 150, 320 and 400 rpm<br>Aeration rate: 96, 200 and 400 NL/min. | Viscosity, mixing time, tracer response, bubble size, mass transfer coefficient | CFD model developed captures mixing and mass transfer mechanics.<br>An indirect method for bubble sizes based on experimental data is shown.<br>Mixing performance was simulated with CFD and the results showed good agreement with experimental data. |
| Zhang et al. (2017) | Power consumption and mass transfer in gas-liquid-solid stirred tank reactor | Experimental and computational<br>Fluids: Air, water<br>System: Stirred tank reactor with diameter 0.30 m and height 0.75 m, four baffles with width 0.03 m, ring sparger used,<br>Impeller agitation rates: 480-840 rpm,<br>Superficial gas velocity: 0.0039-0.039 m/s | Relative power demand (RPD), mass transfer coefficient, power consumption, flow field | Solid particles found to influence power consumption and $k_La$ in different ways.<br>$k_La$ in a three-phase system is smaller than in a two-phase system.<br>Different optimal impeller combinations found in two- and three-phase systems. NPG and $k_La$ correlations were regressed for five different triple-impeller combinations. |

| | | | | |
|---|---|---|---|---|
| Kaiser et al. (2018) | Power input measurements in laboratory scale bioreactors | Experimental<br>System: Flat bottomed cylindrical bioreactor (2L),<br>Impeller agitation rates: 1000-2000 rpm,<br>Aeration rate: 1-2 vvm | Torque, power input, power number | Power input in STBRs is an important scaling up parameter measured through torque acting on impeller shaft during rotation. Measurement of power inputs in benchtop scale bioreactors over a range of turbulence conditions can be described by the dimensionless Reynolds number.<br>Power-input of several multi- and single-use bioreactors is provided by dimensionless power number ($P_o$), which is found to be in the range of $P_o \approx 0.3$ to $P_o \approx 4.5$ at maximum Reynolds number. |
| Li et al. (2018) | Hydrodynamics, mass transfer and cell growth characteristics in a novel microbubble stirred bioreactor with porous metal plate as impeller and gas sparger | Experimental and computational<br>Fluids: Air, water, carboxyl methyl cellulose (CMC) solution<br>System: Stirred tank bioreactor with elephant ear impeller down pumping,<br>Impeller agitation rate: 0-500 rpm,<br>Aeration rate: 0-2 vvm | Mass transfer coefficient, power consumption, mixing time, | A novel microbubble-based stirred tank bioreactor (MSTBR) sintered porous metal plate (SPMP) impeller was developed.<br>The MSTBR showed increased $k_La$ and gas hold-up.<br>The MSTBR reduced mixing energy consumption and improved ARA (arachidonic acid) production. |

Table 2.2 Biochemical applications of stirred tank bioreactors

| Bioproduct | Biocatalyst | Reference |
|---|---|---|
| Exopolysaccharide | *Enterobacter cloacae WD7* | (Bandaiphet and Prasertsan, 2006) |
| Gluconic acid | *Aspergillus niger* | (Elqotbi et al., 2013) |
| Cellulase | *Trichoderma reesei* | (Gabelle et al., 2012) |
| Fumaric acid | *Rhizopus arrhizus RH 7-13-9 #* | (Liu et al., 2017) |
| Biosurfactant | *Aureobaisdium pullulans* | (Pereira et al., 2017) |
| β-glucosidase | *Aspergillus niger* | (Abdella et al., 2016) |
| Xylanase | *Aspergillus awamori* | (Siedenberg et al., 1997) |

Mostly, the research concerning stirred tank bioreactors focused on the following: gas hold-up studies (Yawalkar et al., 2002; Lee & Dudukovic, 2014; Montante & Paglianti, 2015; Tervasmäki et al., 2016), bubble size distribution (BSD) (Laakkonen et al., 2005; Kerdouss et al., 2006; Azargoshasb et al., 2015), mass transfer and mixing studies (Kerdouss et al., 2008; Gimbun et al., 2009; Zadghaffari et al., 2009; Delafosse et al., 2014; Ascanio, 2015; Sarkar et al., 2016; Tervasmäki et al., 2016), power consumption (Bouaifi & Roustan, 2001; Taghavi et al., 2011; Xie et al., 2014; Zhang et al., 2017), flow regime investigation (Mavros, 2001; Montante et al., 2013; Lee & Dudukovic, 2014; Lamotte et al., 2018), and computational fluid dynamic studies (Dhanasekharan et al., 2005; Deglon & Meyer, 2006; Kerdouss et al., 2006; Kerdouss et al., 2008; Wang et al. 2014; Azargoshasb et al., 2015). The effect of the tank dimensions and different tank geometries, internals design (impellers, aeration systems, baffles, etc.), the effect of the agitation rate and superficial gas velocity, rheology of the cell culture broth are commonly encountered in these studies. Several experimental studies have already been carried out towards the quantification of the effects of the operating conditions, stirred tank bioreactor dimensions and design of other internals such as agitator, sparger, etc. on the performance of the stirred tank reactors. Even though with several research studies existing in the literature, stirred tank bioreactors have not been fully understood yet as most of these studies deal with the smaller reactors, however, very few studies have been performed on larger sized industrial reactors. The addition of a second phase (gas) also causes considerable difficulties due to the complex nature of phase interactions.

## 2.4 STIRRED TANK BIOREACTORS: CONCEPTS

The various published studies have mostly focused on the fluid dynamics and regime analysis and characteristic parameters, especially gas hold-up, bubble characteristics, mixing time, power consumption and mass transfer coefficient. In this section, together with these concepts, the effects of superficial gas velocity, gas hold-up, gas distributor (sparger) design used are presented.

### 2.4.1 Fluid Dynamics and Regime Analysis

The fluid dynamic characterization has a significant impact on the operation and performance of STBRs. It is generally observed that, the experimental results depend on the flow regime inside the reactor. With only a single phase inside the reactor, the fluid flow is quite simple and easy to predict in the reactor and governed by the agitator. Once aeration (gas phase) is introduced, the flow field by the impellers is affected, thus complicating the system hydrodynamics. The flow regimes are generally divided into homogeneous and heterogeneous. In bubble columns, these flow regimes have also been observed. The flow field is considered homogeneous, if it is governed by mixing, while it is considered heterogeneous, if gas flow dictates the flow field. The large scale reactors are generally operated in the later regime. The term impeller flooding is governed by the flow regime transition, i.e. from homogeneous to heterogeneous. It is considered as an undesirable condition in which there is no proper gas dispersion. It is a function of agitation rate and aeration rate. When the flooding occurs inside the reactor, the gas distribution is not proper and efficient over the whole vessel, leading to the creation of dead zones and thus affecting the mass transfer. However, the flow regime transition is not the same as flooding transition. The beginning of heterogeneous flow regime may even take place at high agitation and aeration rates, when the impeller is not flooded. On the contrary, flooding may lead to a heterogeneous regime even at relatively low air flow rates. The onset of the flooding can be estimated by the correlation of the Froude number with the ratio of the impeller to tank radius or by a mechanistic model.

The flow regimes in stirred tank bioreactors are also differentiated according to the impeller Reynolds number inside the reactor. Three flow regimes are commonly encountered in stirred tank bioreactors, i.e. laminar, transitional and turbulent flow regimes. The laminar flow regime is obtained at a Reynolds number less than 10 and characterized by bubbles of relatively uniform sizes and rise velocities and gentle mixing inside the reactor. There seems to be no bubble coalescence or break-up in this regime and is governed by sparger design and other system properties. The turbulent flow regime is observed at Reynolds numbers greater than 10000 in stirred tank bioreactors. This flow regime is characterized by the chaotic form of the homogeneous gas-liquid system due to enhanced turbulence of gas bubbles and liquid recirculation and thus results in unsteady flow patterns and large bubbles with short residence times. It is also sometimes referred to as coalesced bubble flow regime, owing to the varied bubble sizes. This flow regime is frequently observed in industrial-size, large diameter reactors.

The transition from the laminar to turbulent flow and the investigation of the transition regime are quite important. With transition taking place, the hydrodynamics of system significantly changes. There exists an onset of liquid circulation in the reactor depending on the agitation system, as a result more gas entry takes place inside the reactor leading to higher gas hold-ups and improved mixing. Most industrial reactors are operated under turbulent conditions. Thus, their flow is characterized by the structures of various time and length scales, whose effects on physical phenomena such as mixing and mass transfer potentially depend on the reactor scale.

Apart from the type of impeller used and for gas flow rate entering the reactor, different flow regimes can be observed when the agitation speed is increased. Considering a standard reactor provided with baffles and a central Rushton impeller, there exist various flow regimes depending on the major bubble trajectories as shown in Figure 2.2. However, the literature has reported only three regimes i.e. flooding, loading and fully recirculated described using two dimensionless numbers, i.e. Flow number [*Fl*] and the Froude number [*Fr*] as defined below:

$$F_l = \frac{Q_g}{ND_i^3} \tag{2.1}$$

$$F_r = \frac{N^2 D_i}{g} \tag{2.2}$$

where $Q_g$ represents the gas flow rate entering the reactor, $N$, impeller agitation rate, $D_i$, the impeller diameter, and $g$, gravitational constant. As the $Fr$ increases the $Fl$ decreases, i.e., by increasing impeller agitation rate, the flow regime transitions from a less to a more dispersed state. The complete flow regime map for air-water system is shown in Figure 2.3.

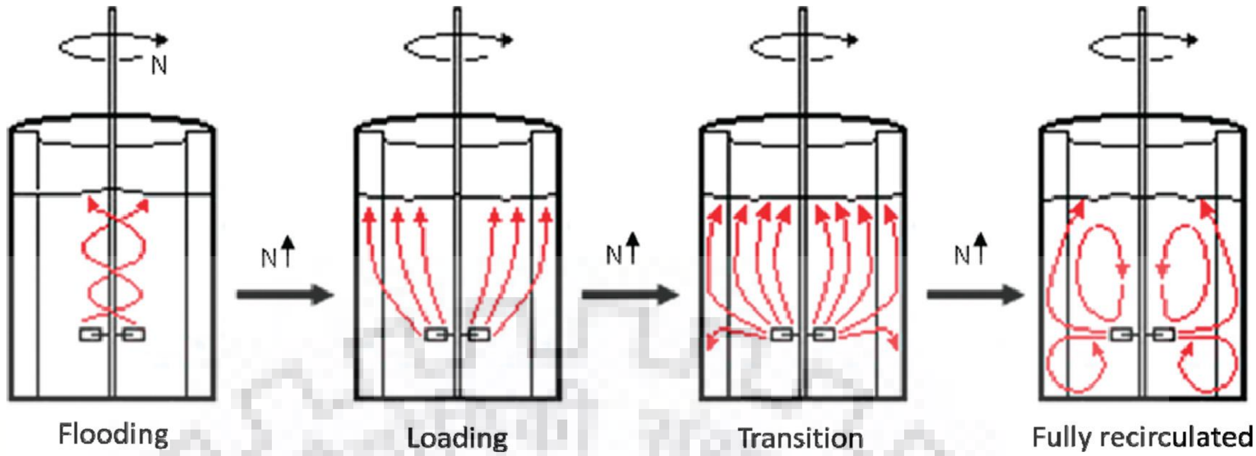


Figure 2.2. Flow regime transition from flooding to loading to the fully recirculated regime. (*Source: Lee and Dudukovic, 2014*)

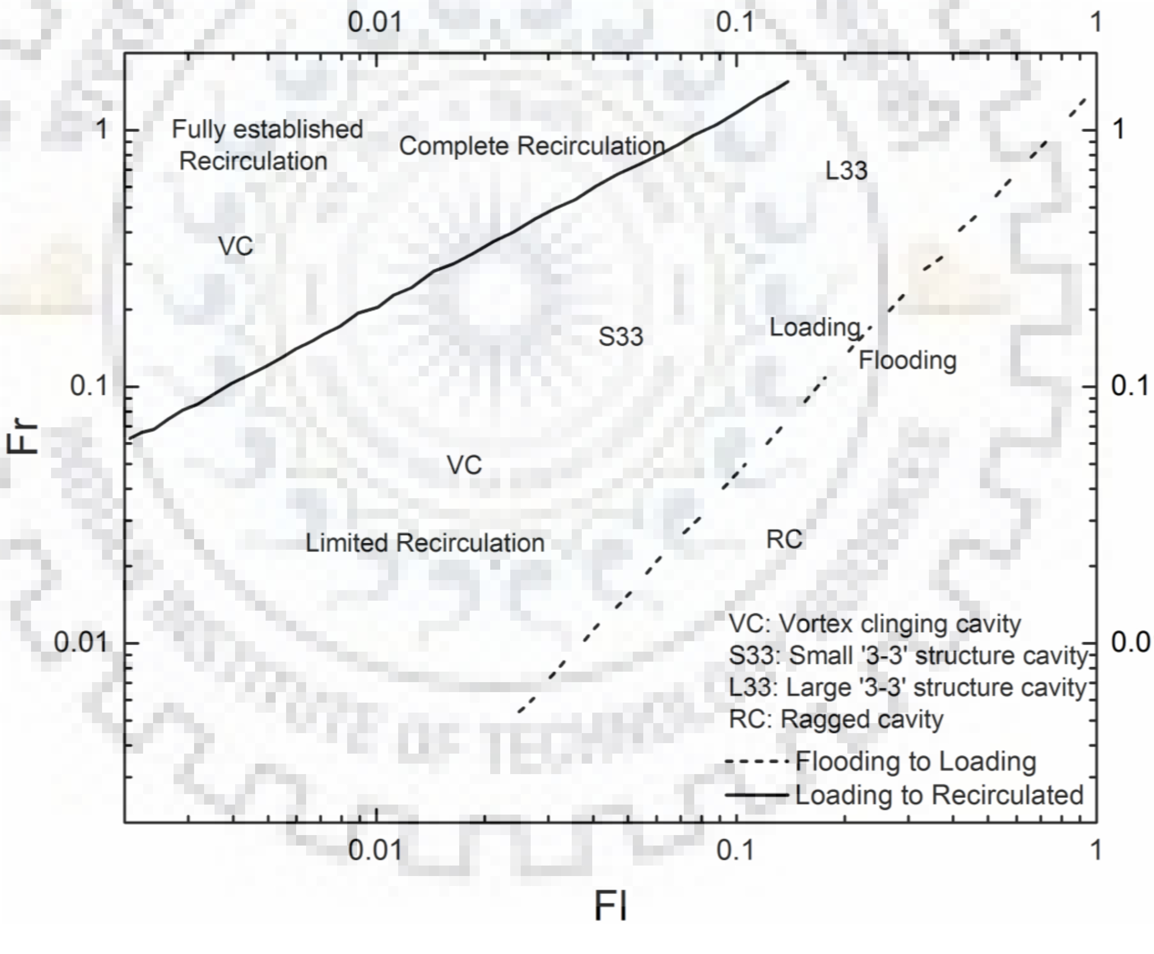


Figure 2.3. Flow regime map for a standard fully baffled air–water stirred tank reactor (*Source: Lee and Dudukovic, 2014*)

In Figure 2.3, VC, S33, L33 and RC refers to vortex clinging structure, small "3-3" structure, the large "3-3" structure, and ragged cavities, respectively. Further, from Figure 2.3 it can be seen that the cavity structures are related with each flow regime behind the impeller blades (Tatterson, 1991; Bombac et al., 1997). The two transition lines from flooding to loading and loading to fully recirculated regimes are determined by observing at which operating conditions dominant bubble trajectories changes, which is also confirmed by predicting the cavity structures. In dimensionless form it is represented as:

Flooding to loading regime transition= $Fl_F = 30F_r(T/D)^{-3.5}$ (2.3)

Loading to recirculated regime transition= $Fl_{CD} = 13Fr^2(T/D)^{-5}$ (2.4)

From the last few years, owing to increasing computational power, there are several computational fluid dynamic (CFD) models readily available, and thus the demand for reliable experimental techniques for flow regime identification has increased considerably. As concluded by, even detailed results obtained using CFD models need experimental validation, because of several assumptions and closure models used in CFD. Although much success in modeling stirred tank bioreactors has been reported, however, the results are not verified at varying operating conditions. Thus, it remains to be seen whether such models can be used over a range of operating conditions needs to be verified, mostly in loading and fully recirculated regimes since most processes are carried out in this regime and also near transition lines, where local flow properties are difficult to report.

### 2.4.2 Gas Hold-up

It is a key dimensionless parameter for designing the STBRs characterizing transport phenomena and also directly affects the mass transfer. It is one of the most indispensable hydrodynamic characteristic needed for performance estimation, design and scale-up of reactors. Therefore, it is one of the most widely studied parameters reported in the literature on STBRs (Veera et al., 2001; Yawalkar et al., 2002; Tervasmaki et al., 2016;). It is defined as how much of the gas phase is occupied by the gas bubbles expressed in terms of its volume fraction. The liquid and solid holdups are also defined in the similar way. However, most of the studies report gas hold-up, owing to its important role in design and analysis of STBRs. Several correlations have been developed over a period of time that relate the overall gas holdup to the operating conditions (Akita and Yoshida, 1974; Fan et al., 1987; Jiang et al., 1995). The overall gas hold-up is strongly affected by the gas and liquid properties, their superficial velocities, presence of solid particles (size, density and loading), gas distributor design, reactor internals (number of baffles, cooling coils, etc.) and power input. Most of the existing correlations available in the literature predict only an average or overall hold-up. Moreover, these correlations have been developed for air-water or other similar systems and hence their predictive capability for industrial scale operations is limited. Greaves and Barigou (1990), Rewatkar et al. (1993), Yawalkar et al. (2002) have summarized the work done by several researchers on the gas hold-up in STBRs. The correlations proposed can be broadly classified into two main categories: 1) based on dimensionless groups i.e., *Fr*, *Fl*, D/T ratio, etc., and 2) based on Kolmogoroff's theory on power dissipation. In the earlier days, the research was mostly based on small scale reactors. Thus, gas hold-up prediction from correlations based on smaller diameter reactors show wide deviation from actual hold-up in larger diameter reactors. The disagreement has been attributed to dependency of gas hold-up on a particular flow regime for operating conditions and specific geometric configuration.

To design reactors on a rational basis, it would be highly desirable to know the local values of the fractional gas hold-up and how this change with the operating conditions. Having this information, the local rates of heat and mass transfer can be estimated and the local bubble size can be predicted and successively the overall performance can be estimated. Limited research studies have been carried out for the local fractional gas hold-up in two/three phase STBRs, however, there have been many attempts to measure the bubble size distribution (BSD), specific interfacial area and overall average hold-up. Few attempts have been made to model the local gas hold-up profiles mathematically. Ranade et al. (1994) and Ranade and Deshpande (1999), have used numerical models to predict the gas hold-up distribution, however, these models have been found to be computationally intensive. Recently, Montante et al. (2015) used the electrical resistance tomography (ERT) to study the gas-liquid dispersion in STRs. The main aim of their study was to give a detailed information on spatial distribution of the gas phase and on the effect of the bubbles on the liquid homogenization dynamics. This experimental technique has been used to overcome the typical limitations of optical methods so as to gain insight into complex behavior of sparged stirred tanks as there is no restriction on upper gas hold-up value, and has been of interest for several chemical and biochemical processes.

### 2.4.3 Gas Sparger

Gas sparger type plays an important role in dictating the bubble characteristics and thus affects gas hold-up, which in turn may alter several other parameters characterizing STRs. Small orifice diameter plates result in formation of smaller bubbles. Various common type spargers used in STRs are ring sparger, nozzle sparger, porous sparger, pipe sparger, macro and micro spargers (Kerdouss et al., 2008; Petitti et al., 2013; Montante and Paglianti, 2015; Wutz et al., 2016). However, ring sparger is most widely used. Bouaifi et al. (2001) found that with smaller gas bubbles, the higher gas hold-up is attained and concluded that small orifice gas distributors result in higher gas hold-up. Luo et al. (1999) reported that gas hold-up strongly depends on the type of the gas sparger.

### 2.4.4 Superficial Gas Velocity

It is the average velocity of the gas sparged into the reactor being expressed as volumetric flow rate divided by overall cross-sectional area of reactor (Xu et al., 2017). It is a very important parameter to be calculated for considering the hydrodynamics of the stirred tank reactor. It has been observed that gas hold-up in stirred tank reactors mainly depends on superficial gas velocity and it increases with superficial velocity. In equation form, it is expressed as:

$$v_{sg} = \frac{Q_g}{A} \tag{2.5}$$

$$v_{sg} = \frac{4Q_g}{\pi D_t^2} \tag{2.6}$$

where $Q_g$ is the gas flow rate ($m^3/s$) entering the reactor and $A$ is the cross sectional area ($m^2$) of the reactor, and $D_t$ is the vessel diameter (m).

### 2.4.5 Theoretical Mass Transfer Coefficient Determination

Apart from the experimental determination of the volumetric mass transfer coefficient as described above, several empirical correlations have been developed by various researchers which take into account the various parameters affecting mass transfer inside the STBRs. As reported in literature, $k_La$ has been correlated either by using dimensionless groups or energy input criterion using Kolmogoroff's theory. Correlations employing dimensionless groups are of the form $k_La=f$ ($Fr$, $Fl_g$, $D/T$, etc.), while correlations using energy input criterion are in the form $k_La=f\,(P/V_L)^{\alpha}\,(u_{sg})^{\beta}$. Tables 2.3-2.5 show the brief summary of existing correlations.

Table 2.3 Mass transfer coefficient correlations for stirred tank bioreactors

| Investigator | Correlation | Parameters |
|---|---|---|
| Van't Riet (1979) | $k_L a = 0.026(\frac{P_g}{V_L})^{0.4}(u_{sg})^{0.5}$ (Air-Water System) | $500 W/m^3 < Power/V_L < 10,000 W/m^3$, $2 L < V_L < 2,600 L$, (Applicable for various types of impellers, vessel diameter and impeller diameter) |
| Van't Riet (1979) | $k_L a = 0.002(\frac{P_g}{V})^{0.7}(u_{sg})^{0.2}$ (Ionic System) | $500 W/m^3 < Power/V_L < 10,000 W/m^3$, $2 L < V_L < 2,600 L$ (Applicable for various types of impellers, vessel diameter and impeller diameter) |
| Montes et al. (1999) | $k_L a = 3.2\times10^{-3}(\frac{P_g}{V})^{0.35}(u_{sg})^{0.41}$ (Yeast Broths System) | Volume of vessels=2L, 5L and 15L |
| Vilaca et al. (2000) | $k_L a = 6.76\times10^{-3}(\frac{P_g}{V})^{0.94}(u_{sg})^{0.65}$ (Air-water-sulfite solution) | Vessel diameter, $d_T$=0.21 m, Impeller type= Rushton turbine, $d_i/d_T$=0.4 |
| Lineck et al. (2004) | $k_L a = 0.01(\frac{P_g}{V})^{0.699}(u_{sg})^{0.581}$ (Air-water system) | Vessel diameter, $d_T$=0.29 m, Impeller type= Rushton turbine, $d_i/d_T$=0.33 |
| Smith et al. (1977) | $k_L a = 0.01(\frac{P_g}{V})^{0.475}(u_{sg})^{0.4}$ (Air-water system) | Vessel diameter, $d_T$=0.61-1.83 m, Impeller type= Disc turbine, $d_i/d_T$=0.33-0.5 |
| Zhu et al. (2001) | $k_L a = 0.031(\frac{P_g}{V})^{0.4}(u_{sg})^{0.5}$ (Air-water system) | Vessel diameter, $d_T$=0.39 m, Impeller type= Disc turbine, $d_i/d_T$=0.33 |
| Kapic & Heindel (2006) | $k_L a = 0.04(\frac{P_g}{V})^{0.47}(u_{sg})^{0.6}$ (Air-water system) | Stirred tank reactor, Rushton impeller |
| Moucha et al. (2003) | $k_L a = 1.0813\times10^{-3}(\frac{P_{tot}}{V_L})^{1.19}(u_{sg})^{0.549}$ (Air-water system) | Stirred tank reactor, Rushton impeller |

| | | |
|---|---|---|
| Garcia-Ochoa & Gomez (2009) | $k_L a = 0.00067(\frac{P_g}{V})^{0.6}(u_{sg})^{0.67}(\mu_L)^{-0.67}$<br>$k_L a = 0.00172(N)^2(u_{sg})^{0.67}(\mu_L)^{-0.67}$<br>(Air-water system) | Stirred tank reactor |
| Yawalkar et al. (2002) | $k_L a = 3.35(\frac{N}{N_{cd}})^{1.464}(u_{sg})$<br>(Air-water system) | Stirred tank reactor, Rushton impeller |
| Puthli et al. (2005) | $k_L a = 1.38\times10^{-4}(\frac{P_g}{V})^{0.58}(u_{sg})^{0.43}$<br>(Single impeller (DT) and Air-water system)<br>$k_L a = 1.36\times10^{-4}(\frac{P_g}{V})^{0.61}(u_{sg})^{0.43}$<br>(Dual impeller (DT-PTD) and Air-water system)<br>$k_L a = 1.9\times10^{-4}(\frac{P_g}{V})^{0.67}(u_{sg})^{0.53}$<br>(Triple impeller(DT-PTD-PTD) and Air-water system)<br>$k_L a = 9.75\times10^{-5}(\frac{P_g}{V})^{0.68}(u_{sg})^{0.53}$<br>(for 0.25% (w/v) CMC (Carboxymethyl cellulose)<br>$k_L a = 9.35\times10^{-5}(\frac{P_g}{V})^{0.66}(u_{sg})^{0.54}$<br>(for 0.375% (w/v) CMC)<br>$k_L a = 2.16\times10^{-3}(\frac{P_g}{V})^{0.36}(u_{sg})^{0.56}$<br>(for 0.5% (w/v) CMC) | Stirred tank bioreactor, DT(Disc turbine) PBT (Pitched blade turbine down-flow), Different concentrations of CMC |
| | $k_L a = 1.3\times10^{-3}(\frac{P_g}{V})^{0.57}(u_{sg})^{0.54}(\frac{\mu}{\mu_w})^{-0.84}$ | |

Table 2.4 Dimensionless correlations for prediction of $k_La$ in stirred tank reactors for Newtonian fluids

| Investigator | Correlation (range of parameters) |
|---|---|
| Perez et al. (1974) | $\frac{k_L a T^2}{D_L} = 21.2.(\frac{\rho N T^2}{\mu_a})^{1.11}.(\frac{\mu_a}{\rho D_L})^{0.5}.(\frac{v_{sg} T}{\sigma})^{0.45}.(\frac{\mu_G}{\mu_a})^{0.69}$ |
| Yagi et al. (1975) | $\frac{k_L a T^2}{D_L} = 0.06.(\frac{\mu_a}{\rho D_L})^{0.5}.(\frac{T^2 N \rho}{\mu_a})^{1.5}.(\frac{\mu_a v_{sg}}{\sigma})^{0.6}.(\frac{N^2 T}{g})^{0.19}.(\frac{NT}{v_{sg}})^{0.32}$ ($v_{sg}$=0.381 m/s; N= 300 and 400 rpm) |
| Nishikawa et al. (1981) | $\frac{k_L a D^2}{D_L} = 0.368.(\frac{\rho N T^2}{\mu})^{1.38}.(\frac{\mu}{\rho D_L})^{0.5}.(\frac{\mu v_{sg}}{\sigma})^{0.5}.(\frac{N T^2}{g})^{0.367}.$ $(\frac{NT}{v_{sg}})^{0.167}.(\frac{T}{D})^{0.25}.(\frac{P/V}{\rho N^3 T^5})^{0.75}$ |
| Costa et al. (1982) | $\frac{k_L a T^2}{D_L} = 8.38.(\frac{\rho N^{2-n} T^2}{k})^{2/3}.(\frac{k}{\rho N^{1-n} D_L})^{1/3}.(\frac{\rho N^2 T^3}{\sigma})^{0.43}$ $\left[1+1.5.10^{-3}.(\frac{\rho N^2 T^3}{\sigma})\right].(\frac{NT}{v_{sg}})^{-0.4}.(\frac{T}{D})$ |
| Albal et al. (1983) | $\frac{k_L a T^2}{D_L} = 1.41.10^{-3}.(\frac{\mu_a}{\rho D_L})^{0.5}.(\frac{T^2 N \rho}{\mu_a})^{0.67}.(\frac{\rho N^2 T^3}{\sigma})^{1.29}$ (N= 800 to 1200 rpm) |
| Schluter et al.(1992) | $k_L a(\frac{\nu}{g^2})^{1/3} = C.\left[\frac{P/V}{\rho\left(\nu g^4\right)^{1/3}}\right]^{0.62}.\left[\frac{Q}{V}.\left(\frac{\nu}{g^2}\right)^{1/3}\right]^{0.23}$ (C= 7.94 (for Rushton turbines) and 5.89 (for intermig impellers) $0.5 \le P/V_L \le 16$ kW/m$^3$; $0.0038 \le q_G/V_L \le 0.027$ s$^{-1}$) |

Table 2.5 Dimensionless correlations for prediction of $k_La$ in stirred tank reactors for non-Newtonian fluids

| Investigator | Correlation (range of parameters) |
|---|---|
| Yagi et al. (1975) | $\frac{k_L a T^2}{D_L} = 0.06.\left(\frac{\rho N T^2}{\mu_a}\right)^{1.5}.\left(\frac{N^2 T}{g}\right)^{0.19}.\left(\frac{\mu_a}{\rho D_L}\right)^{0.5}.\left(\frac{NT}{u_{sg}}\right)^{0.32}.\left(\frac{\mu_a u_{sg}}{\sigma}\right)^{0.6}.\left[1+2(\lambda N)^{0.5}\right]^{-0.67}$ (vsg=0.381 m/s; N= 300 and 400 rpm) |
| Hocker et al. (1981) | $\frac{k_L a V}{Q} = 0.105.\left(\frac{P}{Q\rho\left[g\mu_a/\rho\right]^{2/3}}\right)^{0.59}.\left(\frac{\mu_a}{\rho D_L}\right)^{-0.3}$ |
| Nishikawa et al. (1981) | $\frac{k_L a D^2}{D_L} = 0.115.\left(\frac{T^2 N \rho}{\mu_a}\right)^{1.5}.\left(\frac{\mu_a}{\rho D_L}\right)^{0.5}.\left(\frac{\mu_a u_{sg}}{\sigma}\right)^{0.5}.\left(\frac{TN^2}{g}\right)^{0.37}\left(\frac{NT}{v_{sg}}\right)^{0.17}.\left(\frac{D}{T}\right)^2.\left(\frac{P_0}{N^3T^5\rho}\right)^{0.8}.\left[1+2(\lambda N)^{0.5}\right]^{-0.67} + 0.112.\left(\frac{P/V}{N^3T^5\rho+P/V}\right).\left(\frac{u_{sg}}{(gD)^{0.5}}\right).\left(\frac{k\left(Cu_{sg}\right)^{n-1}}{\rho D_L}\right)^{0.5}.\left(\frac{gD^2\rho}{\sigma}\right)^{0.66}.\left(\frac{gD^3\rho^2}{\left[k\left(Cu_{sg}\right)^{n-1}\right]^2}\right)^{0.42}.\left[1+0.18\left(\lambda\frac{v_b}{d_b}\right)^{0.45}\right]^{-1}$ |
| Garcia-Ochoa and Gomez (1998) | $\frac{k_L a T^2}{D_L} = 6.86.\left(\frac{\rho N^{2-n}T^2}{kK^{n-1}}\right)^{2/3}.\left(\frac{NT}{u_{sg}}\right)^{-2/3}.\left(\frac{\rho N^2 T^3}{\sigma}\right)$ <br> $\frac{k_L a T^2}{D_L} = 0.022.\left(\frac{\rho N T^2}{\mu_c}\right).\left(\frac{NT}{u_{sg}}\right)^{-2/3}.\left(\frac{\rho N^2 T^3}{\sigma}\right)$ <br> ($u_{sg}$=0.002 m/s; $\mu_{eff}$=0.008 to 0.03 Pa.s) |

## 2.5 SUMMARY

A detailed literature on stirred tank bioreactors covering the various aspects such as hydrodynamics, mass transfer, power consumption, mixing, scale-up, fluid dynamics and regime analysis has been discussed. Mostly the focus is on the stirred tank bioreactors equipped with agitation system and other internals for specific applications to understand their hydrodynamics and mass transfer. Stirred tank reactors are widely used in various industrial applications such as chemical, biochemical, pharmaceutical, metallurgical areas, etc. and thus understanding the hydrodynamics and mass transfer in such reactors is very essential for their successful operation. Mass transfer characterization is an essential aspect in stirred tank reactors being particularly used for cell culture and other similar applications. Even though several experimental studies have already been carried out, yet the understanding of stirred tank reactors is not complete as most of these studies have been carried out on smaller reactors, which cannot be directly applied to larger reactors. The addition of second phase (gas) is also challenging to understand the hydrodynamics of such a complex system involving interaction between the gas and liquid phase. The flow regime characterization has a significant effect on the operation and performance of STR's. Several correlations used for the estimation of volumetric mass transfer coefficient such as power-law, dimensionless correlations developed by several researchers have also been reported in this chapter. Apart from the experimental studies on stirred tank reactors, computational fluid dynamics (CFD) has also been used for studying the hydrodynamics, mixing and mass transfer in stirred tank reactors and few studies have been discussed.

# CHAPTER 3

# MATERIALS AND METHODS

## 3.1 GENERAL

In this chapter, experimental details including stirred tank bioreactors used, design and fabrication of impellers using 3-D printing, method used for the experimental determination of $k_La$, preparation of solid and liquid LB medium for *Escherichia coli* BL21, preparation of inoculum have been explained. Rheological characterization for studying the flow behavior of *E. coli* BL21 has also been reported. A detailed discussion about experimental design using response surface methodology (RSM) has also been included in this chapter.

## 3.2 EXPERIMENTAL DETAILS

### 3.2.1. Stirred Tank Bioreactors

#### 3.2.1.1 Stirred Tank Bioreactors with Single Impeller

The experiments were conducted in bioreactors of different volumes, i.e. 7.5 L, 5 L and 1 L with an operating working volume as 5 L, 3 L and 0.75 L, respectively. The schematic diagram and experimental setups of stirred tank reactors used are shown in Figures 3.1 and 3.2 (a-c), respectively. The bioreactors were typically cylindrical glass reactors with dished bottoms and equipped with heater and chiller for maintaining temperature inside the reactor vessel. For creating enough mixing inside the bioreactors, the impeller to tank diameter ratio was maintained greater than 1/3. The bioreactor dimensions are given in detail in Table 3.1. All the reactors had aspect ratio (H/D) greater than one. The bioreactors are typically baffled to promote effective mixing and prevent vortex formation and all the bioreactors in this study were provided with four baffles. The gas is supplied through a ring sparger with drilled holes. A dissolved oxygen (DO) probe with built in temperature probe was used to measure dissolved oxygen concentration and temperature simultaneously. The different impellers such as Rushton turbine, pitched blade turbine, marine propeller and their different configurations were used during the experimental study.

#### 3.2.1.2 Stirred Tank Bioreactors with Dual and Mixed Impellers

Experiments were conducted in a 7.5 L STBR with an operating working volume of 5 L. Distilled water was used as the liquid inside the reactor. The reactor was consisting of a heating coil and a chiller for maintaining temperature. The dual Rushton and mixed impeller (Rushton+ marine propeller) configurations were used separately to agitate the fluid mixture. For creating enough fluid mixing inside the STRs, the impeller to the reactor diameter ratio was maintained greater than 1/3 (Taskin-Ozcan and Wei, 2003; Liu, 2011). The baffles have been used to promote effective mixing and prevent vortex formation. The gas is supplied through a ring sparger with 6 holes of 1 mm diameter. A dissolved oxygen (DO) probe with built in temperature probe was used to measure dissolved oxygen concentration and temperature simultaneously. The schematic diagrams of the Rushton and marine propeller impellers used for mixed impeller (Rushton + marine propeller) and dual Rushton turbine configurations in the stirred tank bioreactor, as shown in Figure 3.3. Table 3.1 shows the specifications of the reactor used in this study along with impeller details. The specific power input ($P/V_L$) was measured for these different impeller configurations using the power meter.

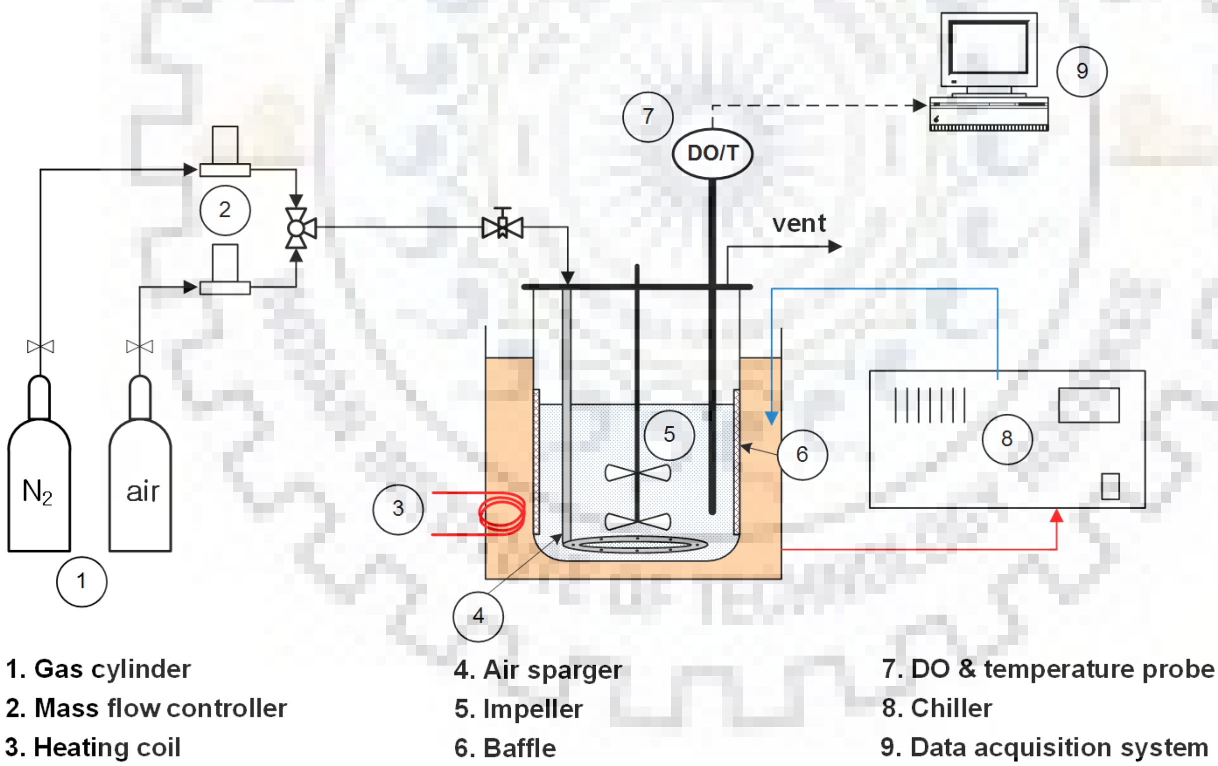


Figure 3.1 Schematic diagram of stirred tank bioreactor

Figure 3.2a Experimental Setup of 7.5 L Stirred Tank Bioreactor

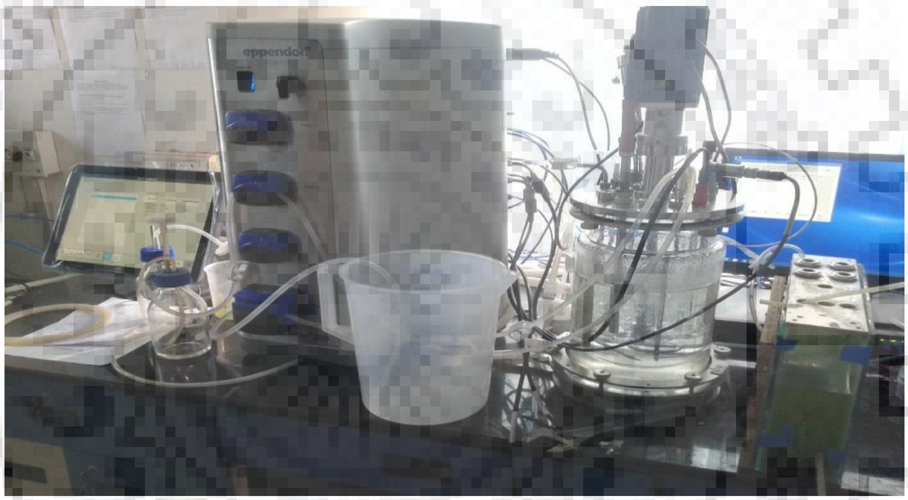


Figure 3.2b Experimental Setup of 5 L Stirred Tank Bioreactor

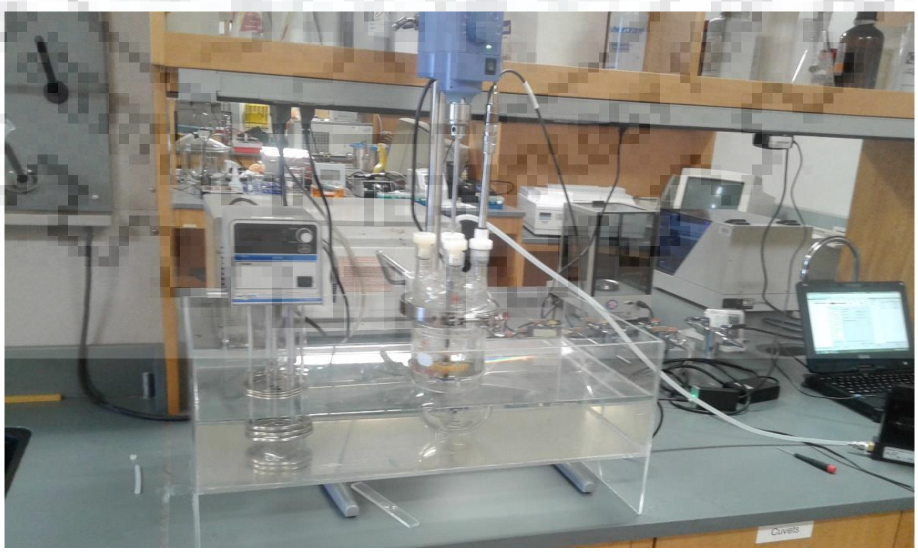

Figure 3.2c Experimental Setup of 1 L Stirred Tank Bioreactor


Figure 3.3 a) Mixed impeller and Dual Rushton configuration stirred tank bioreactor, and b) i) Rushton turbine and b) marine propeller.

### 3.2.2 Design and Fabrication of Impellers Using 3-D Printing Technology

All the impellers used in I L reactor in this study have been fabricated using 3-D printing technology (Ultimaker 2 Extended), where poly-lactic acid (PLA) was used as a fabricating material. The diameter of the impeller was constant at 5 cm in order to keep the diameter ratio of impeller to tank greater than 1/3. In general, if this ratio is less than 1/3, then it is most likely that the impeller is not able to generate enough flow inside the stirred tank to mix the different elements thoroughly (Ozcan-Taskin and Wei, 2003; Liu, 2011). The impeller printed using 3-D printing is cost-effective as compared to the stainless steel impellers generally used in stirred tank bioreactors. Figure 3.4 shows the dimensions of Rushton and pitched blade turbines used in the present study along with their designs.

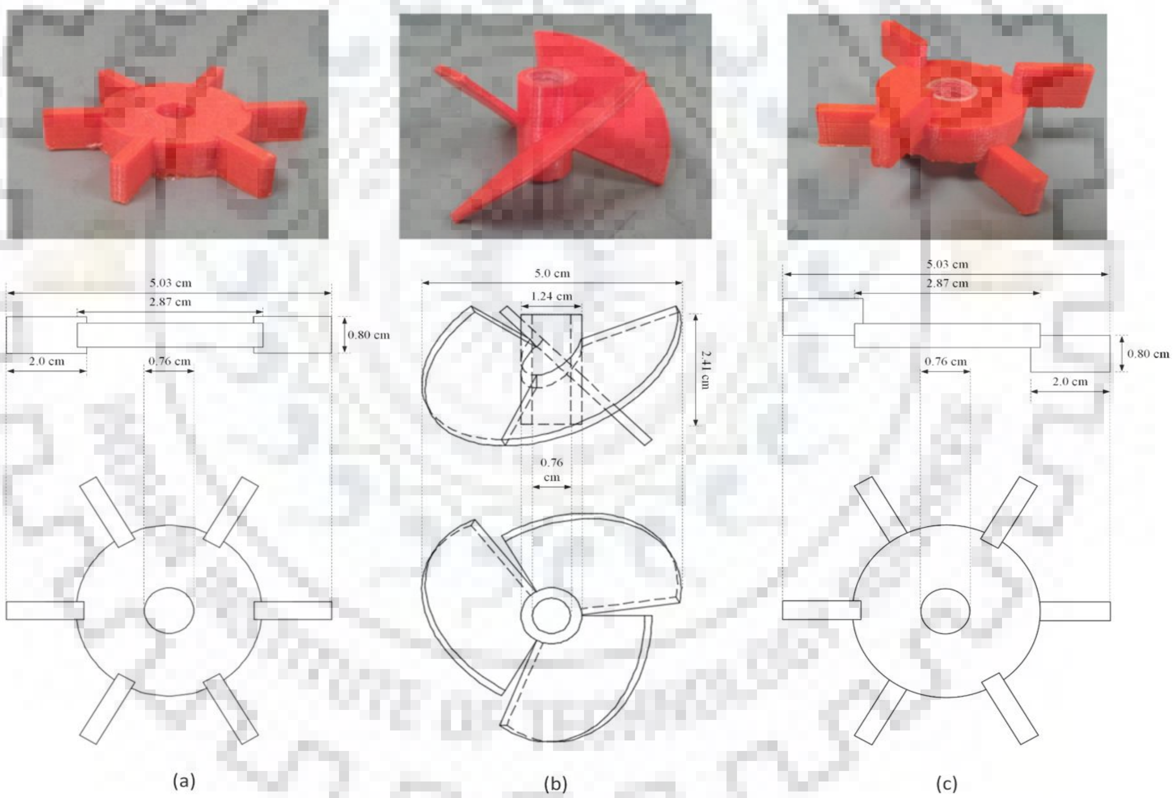


Figure 3.4. Actual pictures and dimensions of (a) Rushton turbine, (b) pitched blade turbine and (c) dislocated Rushton turbine

Table 3.1 Characteristics of the 7.5, 5 and 1 L stirred tank bioreactors

| Description | Unit | Value | | |
|---|---|---|---|---|
| | | **7.5 L** | **5 L** | **1 L** |
| Body of the vessel | - | Glass (dished bottom) | Glass (dished bottom) | Glass (dished bottom) |
| Diameter of the reactor ($D_t$) | m | 0.18 | 0.15 | 0.1 |
| Reactor height ($H_t$) | m | 0.28 | 0.23 | 0.17 |
| Aspect ratio ($H_t$:$D_t$) | - | 1.6:1 | 1.53:1 | 1.7:1 |
| Height of shaft | m | 0.25 | 0.255 | 0.24 |
| Total reactor volume | L | 7.5 | 5 | 1 |
| Operating (working) volume | L | 5 | 3 | 0.75 |
| Number of baffles | - | 4 | 4 | 4 |
| Baffle width | m | 0.018 | 0.015 | 0.01 |
| Impeller types | - | RT, MP | RT, PBT | RT, PBT |
| Rushton turbine (RT) diameter | m | 0.06 | 0.059 | 0.0505 |
| Pitched blade turbine (PBT) diameter | m | - | 0.069 | 0.0505 |
| Marine propeller (MP) diameter | m | 0.10 | - | - |
| Sparger type | - | Ring sparger | Ring sparger | Ring sparger |

### 3.2.3 Preparation of Cell Culture

The *E. coli* strain BL21 was cultured in LB (Lysogeny broth) liquid medium prepared by mixing sodium chloride (10 g/L), tryptone (10 g/L), and yeast extract (5 g/L) in deionized water. Similarly, solid LB medium was also prepared by mixing sodium chloride (10 g/L), tryptone (10 g/L), yeast extract (5 g/L), and agar (15 g/L) in deionized water. Both media were autoclaved at 121 °C and 15 psi for 20 minutes. The liquid medium was directly used in the reactor while the solid medium for preparing agar plates to grow the *E. coli* BL21, which can further be used to prepare the inoculum. An *E. coli* stock was prepared by streaking a fresh solid medium LB plate with an *E. coli* colony and then incubating at 37°C for overnight. As soon as the individual colonies were visible on the plate, it was stored in a refrigerator for reproduction. The inoculum is a suspension containing the living cells used to initiate the growth inside the stirred tank. An individual colony from a stock LB agar plate was added to liquid medium and then incubated at 37°C by adding antibiotic inside a shaker by maintaining a shaker speed of 200 rpm for approximately 12 hours. The inoculation ratio was maintained constant at 1% (v/v) during all the experimental runs.

### 3.2.4 Rheological Measurements

The flow and mixing characteristics of particulate suspensions have since long been the subject of academic interest. Particulate suspensions generally occur in industries such as food processing, polymer manufacturing, and pharmaceuticals, etc. Rheological characterization of such suspensions is often conducted to better understand their complex properties (Apostolidis and Beris, 2016). To understand the rheology of cell suspensions is especially important, because the cells in the culture can be extremely sensitive to shear and it is also important to design, develop and scaling-up such cell-culture processes. Submerged cultures of several organisms are widely used to produce several economically important bio products and one of the ways to increase their yields is to increase their concentration before production (Oolman et al., 1986; Gibbs et al., 2000; Nevalainen et al., 2005). Sometimes these cells in suspension form have viscous nature and may behave in a non-Newtonian manner, due to the interaction between them (Olsvik and Kristiansen, 1994). Rheology affects transport properties which lead to poor oxygen transfer making it difficult to achieve better mixing and aerated suspensions. Due to economic reasons, a high biomass concentration is needed to produce desired amount of bioproduts. However, at high concentrations of biomass, the media inside the reactor may become shear-thickening and this increase in viscosity creates limitations on mixing and mass transfer (Patel and Thibault, 2009) and thereby affecting efficiency of entire process. The logical step to overcome such limitations on oxygen transfer would be overcome by increasing the agitation speed or aeration rate. However, both would lead to an increase in investment and operating costs. In addition, it can create foaming and shear problems (Lejeune and Baron, 1995; Ahamed and Vermette, 2010;). It therefore appears from the literature that mass transfer in such systems is closely related to both the rheology and also biomass concentration and thus studying the rheology during such processes is very important for their successful operation.

Before conducting experiments for characterizing rheological properties of the liquid medium, the whole reactor vessel along with other accessories was sterilized inside an autoclave at 121°C and 15 psi for 20 minutes. After the sterilization, the reactor was taken out of the autoclave, and then the reactor was filled with prepared LB medium and inoculated with the *E. coli* BL21 to start the culture. A small amount of the liquid medium sample was collected at specific time intervals, and the rheological tests were performed using a controlled stress rheometer (AR2000 from TA Instruments). For accurate and uniform shear rate measurement, a plate and plate geometry was used. All the rheological tests were carried out at 25°C and the shear rate was varied from 100 to 3000 1/s. The viscosity and shear rate with varying shear stress were determined for all the samples collected at different time intervals.

### 3.3 MEASUREMENT OF VOLUMETRIC MASS TRANSFER COEFFICIENT, $k_La$

The volumetric mass transfer was determined initially in the absence of cells inside the bioreactors. Since it has been reported that $k_La$ is a strong function of agitation rate, aeration rate, impeller types and configurations, following parameters were used for characterizing the mass transfer in the stirred tank bioreactors: agitation speed, aeration rate, impeller diameter, liquid volume inside the reactor, liquid medium viscosity, different impeller types (single and dual Rushton, pitched blade, marine propeller, dislocated Rushton) and their different configurations.

The most widely used physical method for the measurement of $k_La$, i.e. dynamic gassing-out-gassing-in method, has been used in this study. In this method, the bioreactors were filled with the distilled water up to the level according to the operating volume used. First, the dissolved oxygen probe (VisiFerm DO Sensor, Hamilton) with built-in temperature sensor was calibrated between 0 and 100%. Once the calibration was over, the $k_La$ measurement was started. The $k_La$ was measured by deaerating the reactor vessel by sparging with inert gas (nitrogen used) until oxygen dissolved in the liquid medium reached zero (Kerdouss et al., 2008). To determine $k_La$, the dissolved oxygen mass balance inside the reactor was established using Eq. 3.1:

$$\frac{dC_L}{dt} = k_L a.(C^* - C_L) \tag{3.1}$$

where, $C^*$ and $C_L$ represent the concentration of dissolved oxygen in the liquid phase at saturation and time t, respectively. The saturation concentration is given by Henry's law as:

$$P_{o_2} = H.C^* \tag{3.2}$$

Equation (3.1) can be further integrated for time varying from $t_1$ to $t_2$ as follows:

$$\ln\left(\frac{C^* - C_2}{C^* - C_1}\right) = -k_L a.(t_2 - t_1) \tag{3.3}$$

Finally, experimental $k_La$ can be obtained from the slope in Eq. (3.3). However, $k_La$ can also be determined for dissolved oxygen (DO) values from 20% and 80% by the following equation (Ashley et al., 1991; Isailovic et al., 2015):

$$k_L a = \ln\left(\frac{DO^* - DO_{20}}{DO^* - DO_{80}}\right).\frac{1}{(t_{80} - t_{20})} \tag{3.4}$$

where $DO^*$ is a saturation value, $DO_{20}$ and $DO_{80}$ are 20% and 80% of $DO^*$, respectively and $t_{20}$ and $t_{80}$ are the corresponding times at which $DO_{20}$ and $DO_{80}$ are achieved.

## 3.4 DESIGN OF EXPERIMENTS USING RESPONSE SURFACE METHODOLOGY

Response surface methodology (RSM) is a mathematical and statistical tool, which defines the relationship between the response and independent variables. RSM, with polynomial models, reduces the number of experimental runs, when compared to conventional models RSM is a set of mathematical and statistical techniques quite useful for the multiple regression analysis, empirical model development and analysis of data involving multiple parameters, with response influenced by several variables (Myers et al., 2009). It was first proposed by Box and collaborators (Bezerra et al., 2008) in 1950s. Box-Behnken (BBD) and Central Composite (CCD) designs are mostly used response surface designs for optimization and correlation development. BBD is less expensive in experimentation than CCD since it includes lesser data points, however, both designs can accommodate second order terms. Further, it is a class of rotatable or nearly rotatable second-order-design based on a three-level incomplete factorial design (Box and Behnken, 1960).

It has been extensively used in number of applications, such as waste-water treatment (Kumar et al., 2007; Kumar et al., 2008), pharmaceutical drug delivery (Mujtaba et al., 2014), isomerization process for upgradation of catalytic fuels (Adzamic et al., 2013), fixed bed reactor performance optimization (Eppinger et al., 2014), optimized design of divided wall distillation columns (Sangal et al., 2012), emulsion process characterization and optimization (Kundu et al., 2015), optimization of enzymatic hydrogen peroxide production in a CSTR (Aghbolaghy and Karimi, 2014), supercritical extraction (Rai et al., 2016), etc. for process optimization and to identify significant process and geometrical parameters, which influence the response. RSM has two major advantages: 1) a relationship can be developed between independent operating parameters and a measured response, which can be further used to predict the response for other values of operating variables, and 2) determination of the significant and optimized conditions of the operating parameters for an optimum response over a predefined range of operating conditions. It reduces the experimental effort needed to assess performance in industrial devices. In such processes, a number of input variables are influence performance measures, known as the response. Design of experiments by RSM allows optimization of a response (output variable) influenced by independent variables (input variables) effectively by reducing the experimental efforts (Aghbolaghy and Karimi, 2014; Myers et al., 2009).

By developing a second order polynomial model (Eq. 3.5), the number of experimental runs were significantly reduced by BBD combined with RSM, which permits (a) estimation of the parameters of the quadratic model, (b) building of sequential design, (c) determination of the lack of fit of the model, and (d) use of blocks (Ferreira et al., 2007). It is basically a spherical design with all points lying on a sphere of radius $\sqrt{2}$, and no points at the vertices of the cubic region created by the upper and lower limits of each variable (Ferreira et al., 2007). The second order polynomial demonstrates the rapport between independent variables (e.g. impeller agitation rate, air flow rate, impeller spacing, and temperature in the present study) and dependent variable (e.g., the volumetric mass transfer coefficient and power input per unit volume). The following second order polynomial response equation has been used in the present work to correlate the dependent and independent variables:

$$Y = b_0 + \sum_{i=1}^{n} b_i x_i + \sum_{i=1}^{n} b_{ii} x_i^{\,2} + \sum_{j>i}^{n} \sum_{i=1}^{n} b_{ij} x_i x_j \tag{3.5}$$

where, $Y$ is the response, $x_i$ and $x_j$ are the coded experimental levels of the independent variables $i$ and $j$, respectively, $b_0$ is constant, $b_i$ is the influence of variable on the response (regression coefficient for linear effect), $b_{ii}$ is the parameter that defines the shape of the curve (regression coefficient for quadratic effect), and $b_{ij}$ is the effect of the interaction between the variables $i$ and $j$ (regression coefficient for the interaction effect). The accuracy and ability of above polynomial model could be evaluated by the coefficient of determination ($R^2$) and F-test.

In the present work, three factors (independent variables) with three levels of BBD levels were used for the analysis of design of experiments. As shown in Tables 3.2 and 3.3, the levels of factors chosen were represented as $x_1$, $x_2$, and $x_3$ and were prescribed into three levels coded as -1, 0 and 1 for low, central (or middle point), and high values, respectively.

Table 3.2 Experimental values and coded levels of the independent variables

| **Independent Variables** | **Code Units** | **Coded Levels** | | |
|---|---|---|---|---|
| | | -1 | 0 | 1 |
| Impeller agitation rate (rpm) | $x_1$ | 50 | 425 | 800 |
| Air flow rate (L/min) | $x_2$ | 0.5 | 2.0 | 3.5 |
| Temperature (°C) | $x_3$ | 10 | 25 | 40 |

Table 3.3 Coded levels of the independent parameters and their experimental values

| **Independent Variables** | **Code Units** | **Coded Levels** | | |
|---|---|---|---|---|
| | | -1 | 0 | 1 |
| Stirring rate (rpm) | $x_1$ | 100 | 350 | 600 |
| Aeration rate (vvm) | $x_2$ | 0.2 | 1.3 | 2.4 |
| Impeller spacing (cm) | $x_3$ | 4 | 6 | 8 |

The number of experimental runs ($N$) to be performed for the development of the RSM-BBD model is defined as $N$=2$n$($n$-1) +$N_C$, where n is the number of factors and $N_C$ is the number of the central points of each factor ($n$= $N_C$ = 3). Hence, a total of 15 experiments have to be performed for each impeller configuration (single and dual Rushton, pitched blade, and mixed turbines (Rushton + pitched blade and Rushton + marine propeller)). The central point is the parameter value between the lower and higher limit of each factor. Table 3.4a shows BBD experimental matrix with coded values for different impeller configurations. It is clearly seen that the experimental runs were randomized to reduce the potential for bias. It is also noteworthy that RSM requires reduced number of experimental runs as compared with traditional design of experiments, which can save both time and cost. Table 3.4 also shows the experimental and predicted response values of $k_La$

(Table 3.4b). Table 3.5-3.6 shows BBD experimental matrix for $k_La$ and $P/V_L$ for Rushton-Rushton and Rushton-Marine propeller configurations. The experimental design matrix, data analysis, and optimization procedure were performed using the JMP® statistical software package and Design Expert.

Table 3.4 (a) Box-Behnken Design matrix and (b) corresponding experimental and predicted response values of $k_La$ for different impeller configurations

(a)

| | Single Rushton | | | Dual Rushton | | | Pitched blade | | | Mixed | | |
|---|---|---|---|---|---|---|---|---|---|---|---|---|
| **Run** | $x_1$ | $x_2$ | $x_3$ | $x_1$ | $x_2$ | $x_3$ | $x_1$ | $x_2$ | $x_3$ | $x_1$ | $x_2$ | $x_3$ |
| 1 | 0 | 0 | 0 | 1 | 0 | 1 | 1 | 1 | 0 | 0 | 0 | 0 |
| 2 | 0 | -1 | -1 | 0 | 0 | 0 | 0 | 1 | -1 | 0 | 1 | 1 |
| 3 | 0 | 1 | 1 | 0 | 0 | 0 | -1 | -1 | 0 | -1 | 0 | 1 |
| 4 | 1 | 1 | 0 | 0 | 0 | 0 | 0 | 0 | 0 | 1 | -1 | 0 |
| 5 | 1 | -1 | 0 | 0 | 1 | 1 | 0 | -1 | -1 | 0 | -1 | -1 |
| 6 | 0 | -1 | 1 | -1 | 1 | 0 | 1 | -1 | 0 | 1 | 1 | 0 |
| 7 | 0 | 0 | 0 | -1 | 0 | -1 | 0 | 1 | 1 | -1 | 1 | 0 |
| 8 | 0 | 0 | 0 | -1 | 0 | 1 | 1 | 0 | -1 | 1 | 0 | -1 |
| 9 | 1 | 0 | -1 | 1 | 1 | 0 | -1 | 0 | -1 | 1 | 0 | 1 |
| 10 | -1 | -1 | 0 | -1 | -1 | 0 | 0 | 0 | 0 | -1 | 0 | -1 |
| 11 | -1 | 0 | 1 | 1 | 0 | -1 | 1 | 0 | 1 | -1 | -1 | 0 |
| 12 | 0 | 1 | -1 | 0 | 1 | -1 | -1 | 1 | 0 | 0 | 1 | -1 |
| 13 | -1 | 1 | 0 | 0 | -1 | 1 | 0 | -1 | 1 | 0 | 0 | 0 |
| 14 | 1 | 0 | 1 | 0 | -1 | -1 | 0 | 0 | 0 | 0 | 0 | 0 |
| 15 | -1 | 0 | -1 | 1 | -1 | 0 | -1 | 0 | 1 | 0 | -1 | 1 |

(b)

| | Single Rushton | | Dual Rushton | | Pitched blade | | Mixed | |
|---|---|---|---|---|---|---|---|---|
| **Run** | $k_La_{,expt.}$ | $k_La_{, pred.}$ | $k_La_{,expt.}$ | $k_La_{, pred.}$ | $k_La_{,expt.}$ | $k_La_{, pred.}$ | $k_La_{,expt.}$ | $k_La_{, pred.}$ |
| 1 | 0.911 | 0.911 | 3.311 | 3.304 | 2.818 | 2.921 | 1.998 | 2.074 |
| 2 | 0.577 | 0.493 | 1.563 | 1.570 | 1.431 | 1.469 | 3.018 | 3.150 |
| 3 | 1.203 | 1.287 | 1.686 | 1.570 | 0.177 | 0.073 | 0.596 | 0.754 |
| 4 | 1.880 | 1.911 | 1.462 | 1.570 | 1.479 | 1.451 | 0.780 | 1.071 |
| 5 | 1.429 | 1.483 | 2.226 | 2.308 | 0.872 | 0.866 | 1.294 | 1.162 |
| 6 | 0.813 | 0.875 | 0.671 | 0.548 | 1.858 | 2.005 | 3.385 | 3.438 |
| 7 | 0.911 | 0.911 | 0.368 | 0.373 | 1.705 | 1.711 | 0.646 | 0.355 |
| 8 | 0.911 | 0.911 | 0.659 | 0.699 | 2.735 | 2.594 | 2.212 | 2.054 |
| 9 | 1.398 | 1.428 | 3.611 | 3.535 | 0.359 | 0.468 | 3.439 | 3.254 |
| 10 | 0.178 | 0.146 | 0.208 | 0.284 | 1.380 | 1.449 | 0.364 | 0.549 |
| 11 | 0.489 | 0.458 | 2.395 | 2.355 | 3.027 | 2.918 | 0.202 | 0.1495 |
| 12 | 0.930 | 0.867 | 1.252 | 1.368 | 0.547 | 0.410 | 1.883 | 1.989 |
| 13 | 0.558 | 0.504 | 1.166 | 1.049 | 1.110 | 1.072 | 2.058 | 2.074 |
| 14 | 2.302 | 2.186 | 0.795 | 0.713 | 1.490 | 1.451 | 2.166 | 2.074 |
| 15 | 0.295 | 0.411 | 1.761 | 1.884 | 0.449 | 0.591 | 1.512 | 1.406 |

Table 3.5 Box-Behnken design for Rushton-Rushton configuration for $k_La$ and $P/V_L$

| Run | $x_1$ Stirring rate (rpm) | $x_2$ Air flow rate (vvm) | $x_3$ Impeller spacing (cm) | Response $k_La$ (min$^{-1}$) | $P/V_L$ (kW/m$^3$) |
|---|---|---|---|---|---|
| 1 | 350 | 1.3 | 6 | 1.098 | 0.202 |
| 2 | 350 | 2.4 | 4 | 0.658 | 0.112 |
| 3 | 600 | 2.4 | 6 | 2.228 | 0.904 |
| 4 | 350 | 0.2 | 8 | 0.616 | 0.218 |
| 5 | 350 | 1.3 | 6 | 1.056 | 0.208 |
| 6 | 600 | 0.2 | 6 | 1.769 | 1.304 |
| 7 | 350 | 0.2 | 4 | 0.413 | 0.098 |
| 8 | 600 | 1.3 | 8 | 1.898 | 1.486 |
| 9 | 350 | 2.4 | 8 | 1.161 | 0.208 |
| 10 | 100 | 0.2 | 6 | 0.146 | 0.054 |
| 11 | 100 | 1.3 | 4 | 0.635 | 0.046 |
| 12 | 600 | 1.3 | 4 | 1.954 | 0.954 |
| 13 | 100 | 1.3 | 8 | 0.676 | 0.024 |
| 14 | 100 | 2.4 | 6 | 1.021 | 0.074 |
| 15 | 350 | 1.3 | 6 | 0.986 | 0.212 |

Table 3.6 Box-Behnken design for Rushton-marine propeller configuration for $k_La$ and $P/V_L$

| Run | $x_1$ Stirring rate (rpm) | $x_2$ Air flow rate (vvm) | $x_3$ Impeller spacing (cm) | Response $k_La$ (min$^{-1}$) | $P/V_L$ (kW/m$^3$) |
|---|---|---|---|---|---|
| 1 | 100 | 1.3 | 8 | 0.637 | 0.008 |
| 2 | 100 | 1.3 | 4 | 0.766 | 0.008 |
| 3 | 350 | 2.4 | 4 | 1.481 | 0.126 |
| 4 | 350 | 1.3 | 6 | 1.127 | 0.202 |
| 5 | 600 | 0.2 | 6 | 1.858 | 1.380 |
| 6 | 350 | 1.3 | 6 | 1.091 | 0.202 |
| 7 | 100 | 0.2 | 6 | 0.175 | 0.018 |
| 8 | 350 | 2.4 | 8 | 1.291 | 0.240 |
| 9 | 600 | 1.3 | 8 | 1.339 | 1.200 |
| 10 | 350 | 1.3 | 6 | 1.195 | 0.202 |
| 11 | 100 | 2.4 | 6 | 0.977 | 0.004 |
| 12 | 350 | 0.2 | 8 | 0.575 | 0.220 |
| 13 | 350 | 0.2 | 4 | 0.615 | 0.206 |
| 14 | 600 | 1.3 | 4 | 2.017 | 1.134 |

# CHAPTER 4

# MASS TRANSFER CHARACTERIZATION IN STBRs

## 4.1 GENERAL

The effectiveness of heat and mass transfer in stirred tank bioreactors is significantly influenced by flow pattern generated by the type of impeller used (Gogate et al., 2000). In this study, the volumetric mass transfer coefficient was determined experimentally for different impeller configurations including single Rushton, dual Rushton, pitched blade turbine, marine propeller, mixed turbine (Rushton + pitched blade, Rushton + marine propeller) in three different STBRs and the effect of different parameters on $k_La$ has been investigated. In the present work, the volumetric mass transfer coefficient and power input per unit volume determined experimentally for different types of impellers including single Rushton, dual Rushton, pitched blade, and mixed (Rushton + pitched blade, Rushton + marine propeller) configurations have been analyzed statistically using RSM. Furthermore, the correlation models developed by the RSM were simplified and validated experimentally. Finally, the models developed using RSM were compared with power-law correlations.

## 4.2. MASS TRANSFER IN 7.5, 5 AND 1 L STIRRED TANK BIOREACTORS

The experimental study has been carried out on the 7.5, 5 and 1 L stirred tank bioreactors for different impeller agitation rates (50-800 rpm) and air flow rates (0.5-3.5 L/min.). The impeller configurations used were single Rushton, dual Rushton, pitched blade, marine propeller and mixed impeller (Rushton + marine, Rushton + marine propeller). The volumetric mass transfer coefficient has been determined using the method as described previously.

### 4.2.1 Single Rushton Turbine

Single Rushton turbine has been employed to study the effect of agitation speed and aeration rate on the volumetric mass transfer coefficient inside the STBRs of different volumes. The temperature has been maintained constant (around 25°C) during this study. From Figure 4.1 it can be observed that $k_La$ increased with an increase in agitation rate and aeration rate for all the reactors. At the lower agitation rate, i.e. 50 and 100 rpm, the increase in $k_La$ is not appreciable.

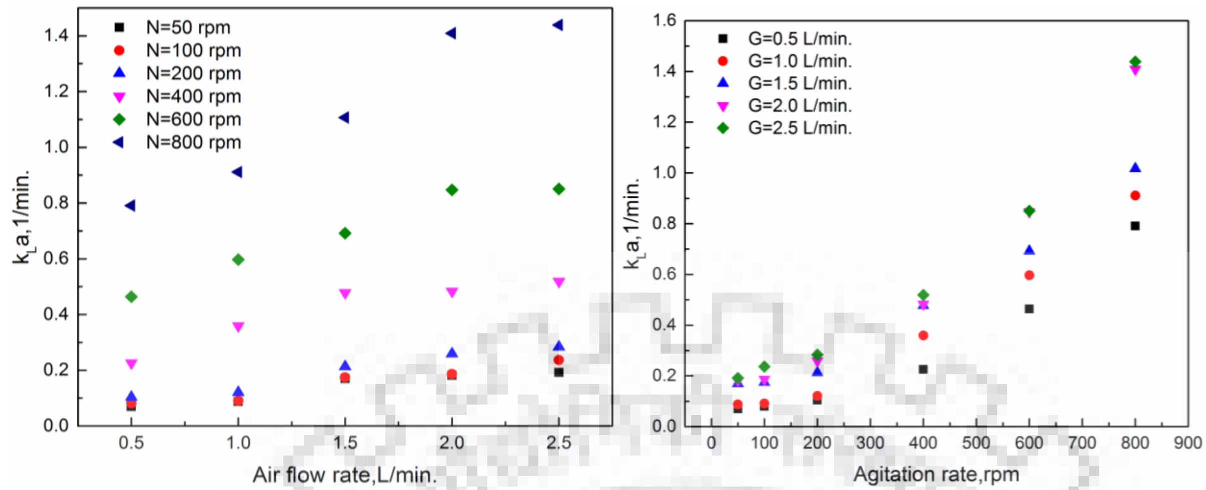


(a)

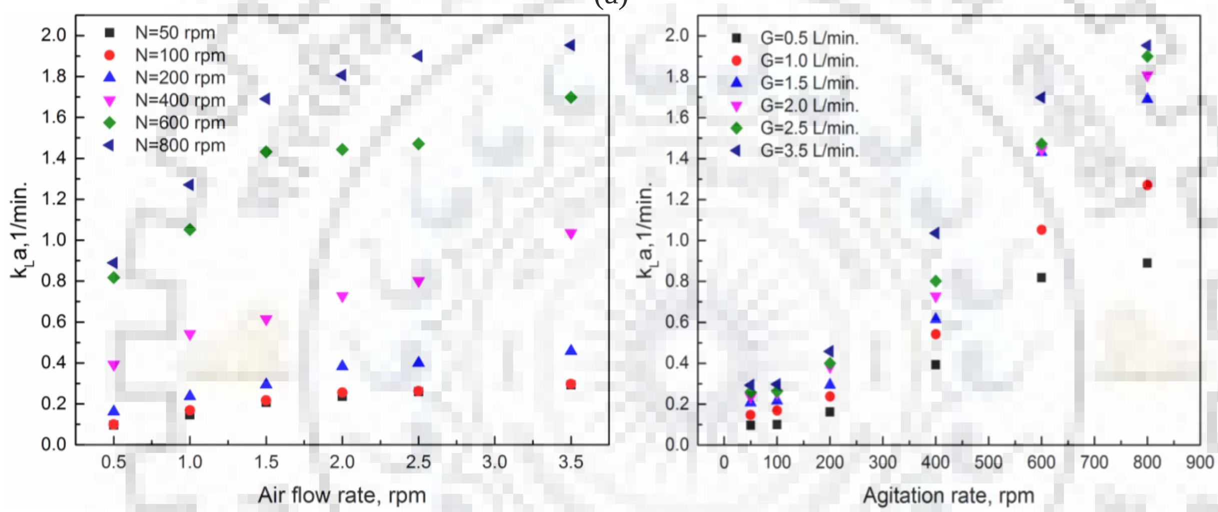


(b)

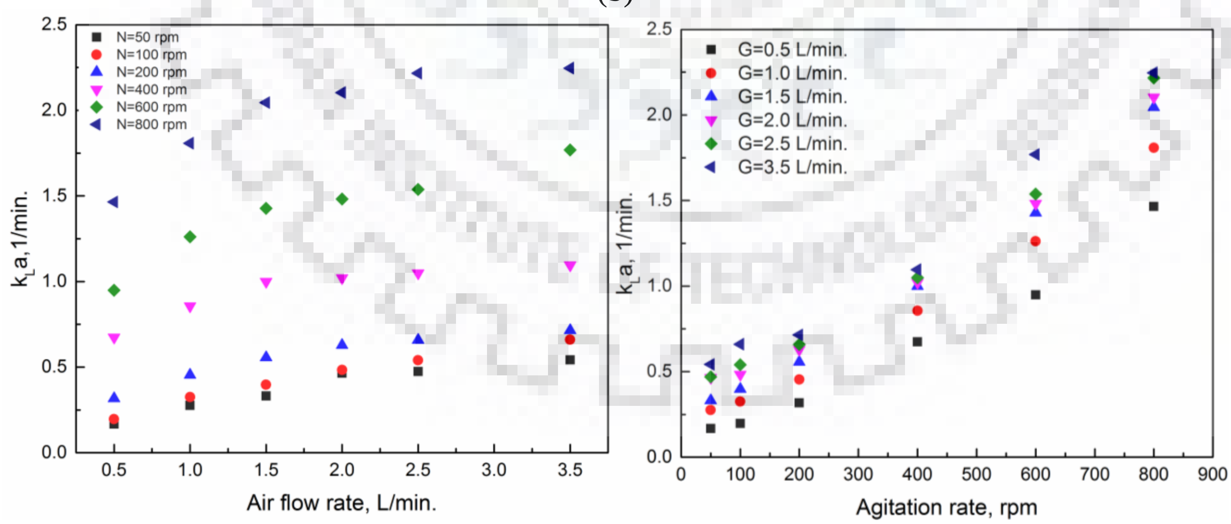


(c)

Figure 4.1. Effect of agitation rate and air flow rate on $k_La$ for single Rushton turbine in (a) 7.5 L, (b) 5 L and (c) 1 L stirred tank bioreactors

With increase in agitation rate, there is an increase in gas-liquid interfacial area, which increases the overall volumetric mass transfer coefficient. However, increase in aeration rate may lead to an increase in gas hold-up, which increases the interfacial area and thus increases the volumetric mass transfer coefficient, $k_La$. With single Rushton turbine used in three STBRs of different volumes, it has been observed that the lowest $k_La$ was observed in 7.5 L STBR and the highest $k_La$ was obtained in 1 L STBR under same conditions of agitation rate and aeration rate. Thus, an increase in scale of the reactor leads to decrease in $k_La$.

### 4.2.2 Dual Rushton Turbine

The dual Rushton turbine configuration has been utilized for studying the mass transfer coefficient in STBRs of different vessel volumes using the same ranges of agitation and air flow rates as were used for the single Rushton turbine and results obtained are shown in Figure 4.2. Normally, it would be expected that higher $k_La$ values would be obtained using dual Rushton turbine due to better mixing conditions created using two impellers, however, it was observed that $k_La$ values are only slightly higher than that obtained for the single Rushton turbine, as shown in Figure 4.1. This may be attributed to the fact that there may be an improper mixing inside the reactor using two Rushton turbines as it may also depend on the spacing between the impellers. Also, it has been observed that increasing the spacing between the impellers beyond a critical level would lead to an ineffective agitation region between the adjacent impellers and thus results in reduction in mass transfer. However, as observed for the single Rushton turbine, higher $k_La$ has been obtained in 1 L STBR and lower $k_La$ has been obtained in 7.5 L, which could be attributed to the lower surface-to-volume ratio in a larger reactor and thus leading to a lower $k_La$.

### 4.2.3 Pitched Blade Turbine

The pitched blade turbine with three curved blades, being an axial impeller has been used to study the effect of agitation and air flow rates on the volumetric mass transfer coefficient in 1 and 5 L STBR. In case of 1 L STBR, the impeller printed using 3-D printer using poly-lactic acid (PLA) as the fabricating material has been used. Higher $k_La$ values were observed as compared to single and dual Rushton turbine configurations above as shown in Figure 4.3. It has been reported that axial impellers have lower power number as compared to radial impellers, and thus consume lesser power, which in turn produces lesser hydrodynamic shear detrimental for the cell damage. In addition, it also delivered higher volumetric mass transfer coefficient, which would actually help to achieve higher yield of the biomass inside the bioreactor and thus increase the yield of the final bio-products.

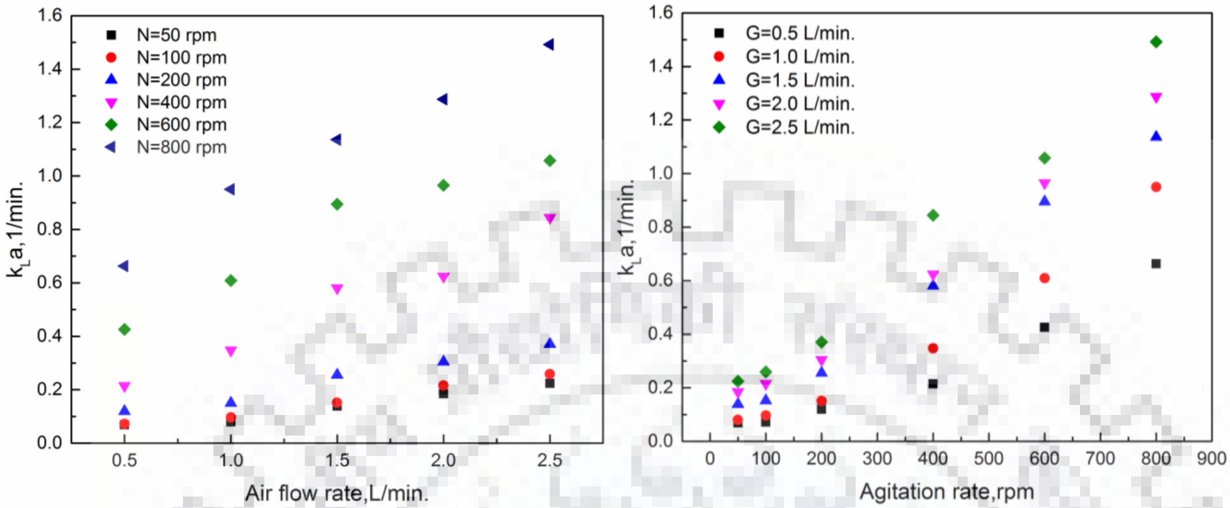


(a)

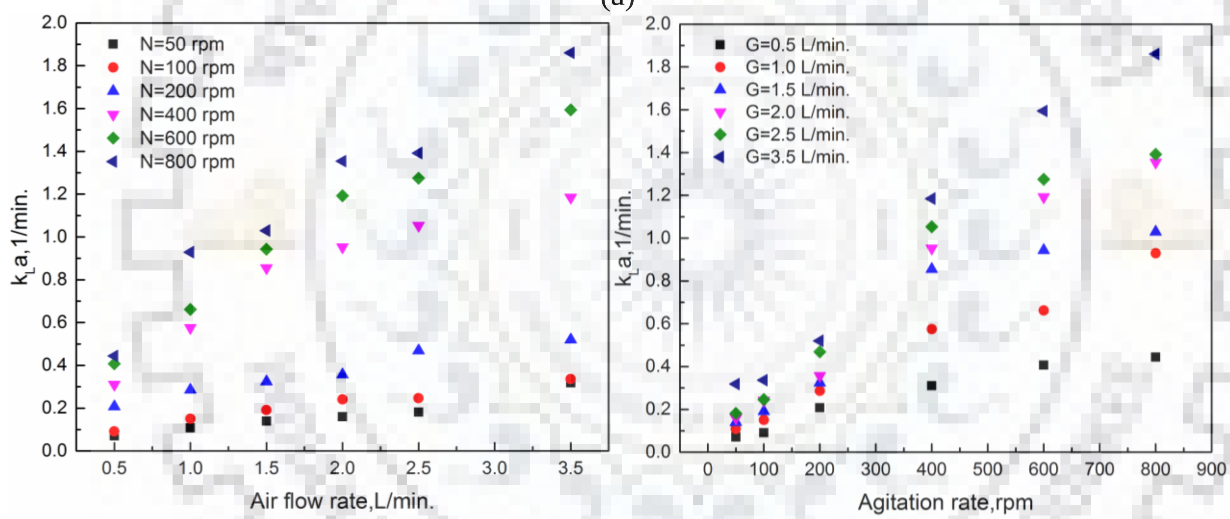


(b)

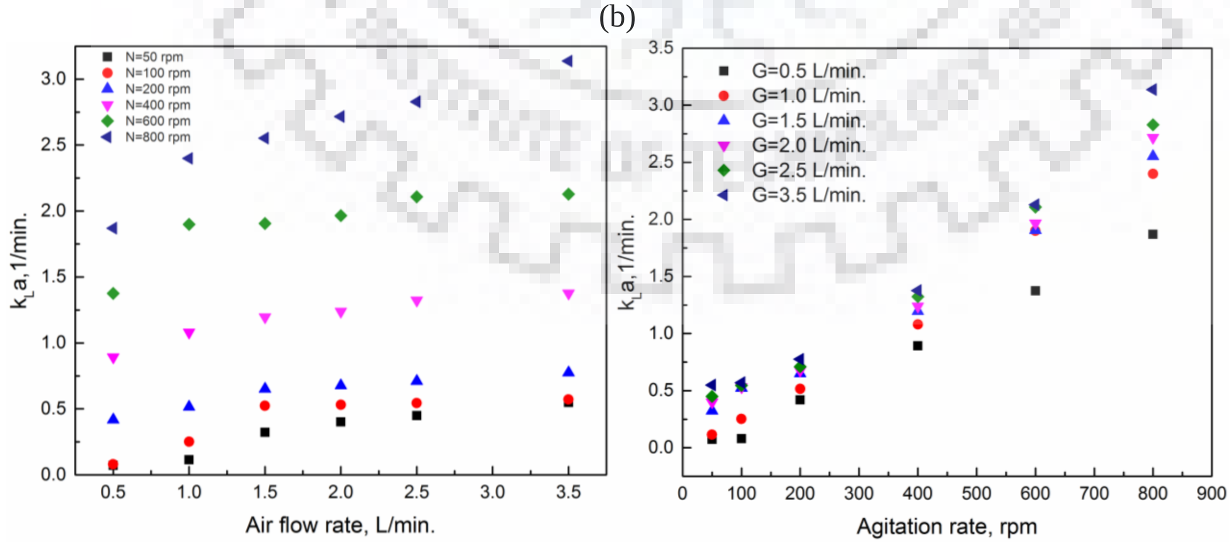


(c)

Figure 4.2. Effect of agitation rate and air flow rate on $k_La$ for dual Rushton turbine in (a) 7.5 L, (b) 5L and (c) 1L stirred tank bioreactors.

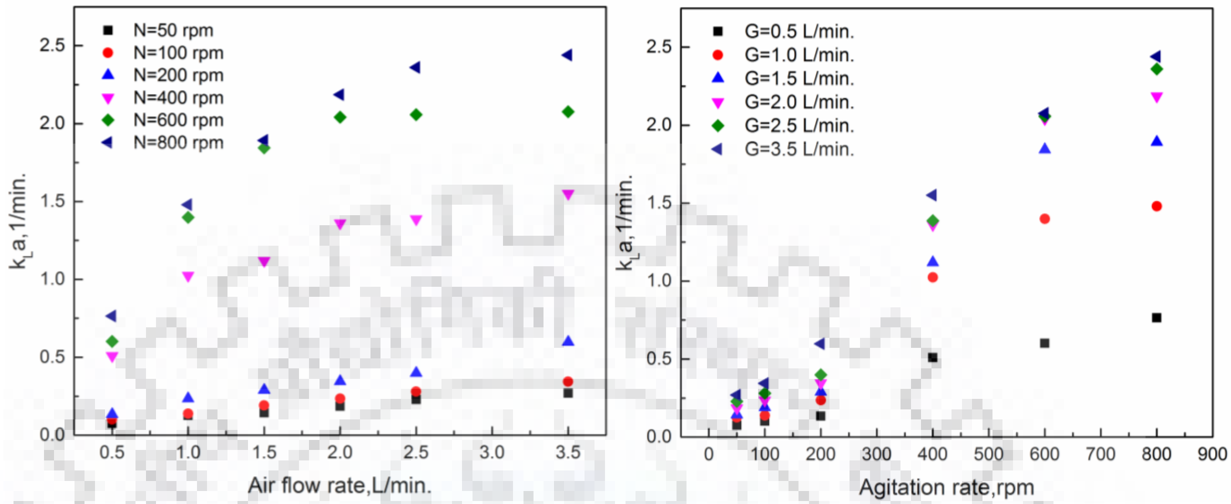


(a)

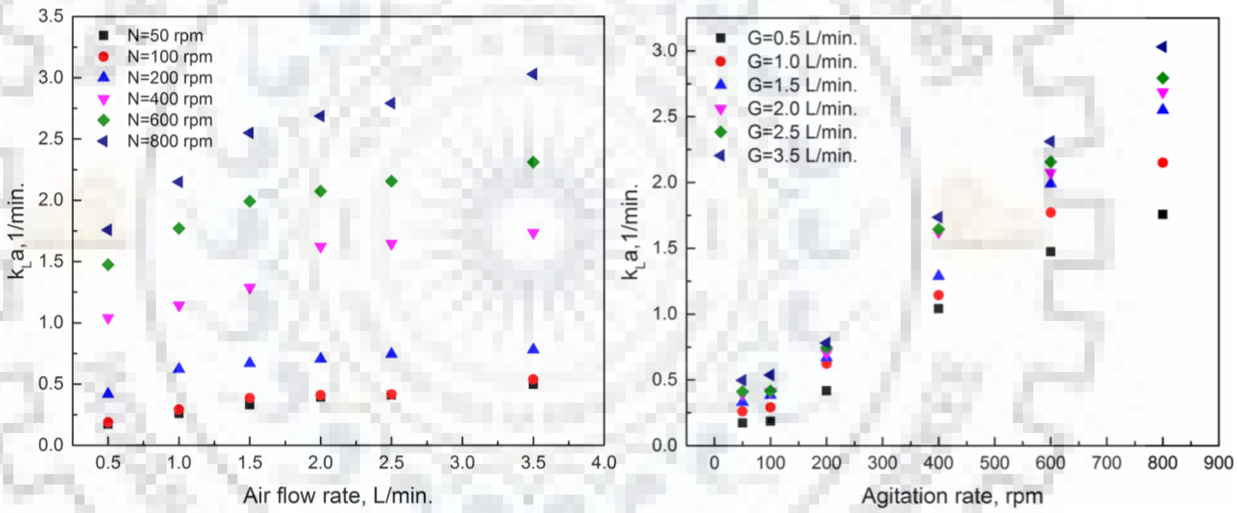


(b)

Figure 4.3 Effect of agitation rate and air flow rate on $k_La$ for pitched blade turbine in (a) 5 L and (b) 1 L stirred tank bioreactors

### 4.2.4 Marine Propeller

Marine propeller being an axial impeller has also been used to study its effect on the volumetric mass transfer coefficient inside the STBRs at different agitation rate and air flow rate in a 7.5 L stirred tank bioreactor. Almost similar $k_La$ values were observed as obtained in case of single and dual Rushton turbine configurations, as shown in Figure 4.4. As reported in the literature, marine propeller being an axial impeller has lower power number as compared to radial impeller such as Rushton type. Therefore, even if it has delivered lower $k_La$, it has an added advantage that due to its low power number, the power consumption would be less and that would be actually beneficial for the cells in terms of the shear damage.

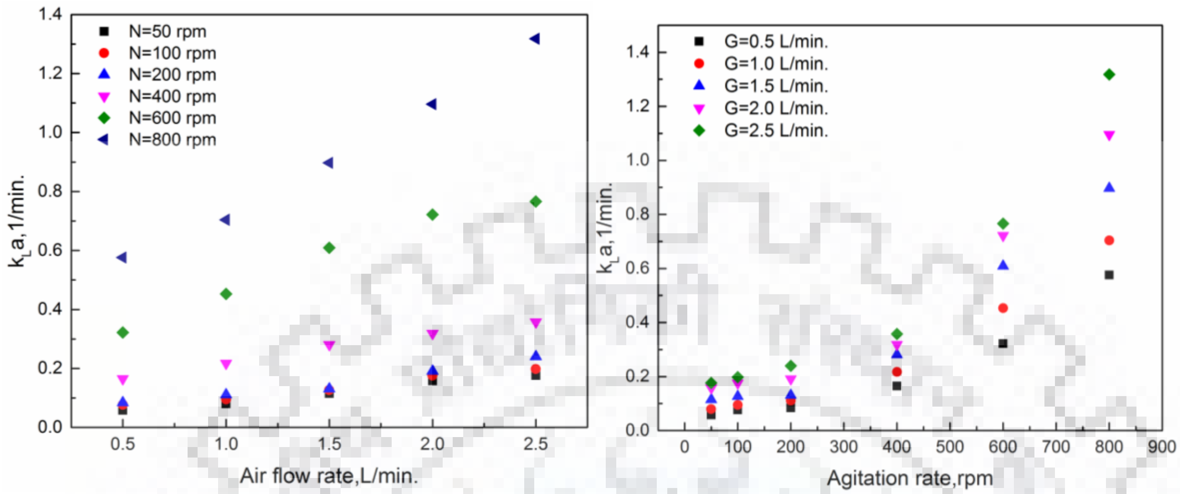


Figure 4.4. Effect of agitation rate and air flow rate on $k_La$ for marine propeller in 7.5 L stirred tank bioreactor

### 4.2.5 Mixed Impeller

Mixed impellers configured by Rushton and marine propeller, and Rushton and pitched blade turbines have been used to study its effect on the volumetric mass transfer coefficient at varying agitation rate and air flow rate. Due to the combined axial and radial flow exhibited by mixed impeller, the $k_La$ values were found to be higher than single and dual Rushton turbines and marine propeller, as discussed above and shown in Figure 4.5. The combination of two different impellers was found to exhibit higher $k_La$ value owing to mixed flow (axial and radial), which lead to better mixing and thus increased the volumetric mass transfer coefficient inside the bioreactor.

As mentioned earlier, axial flow impellers such as pitched blade and marine propellers owing to their low power number generate less shear as compared with radial flow impellers and thus would not be harmful for the cells. Thus, mixed impellers may be considered as most suitable impellers for cell culture and other similar applications.

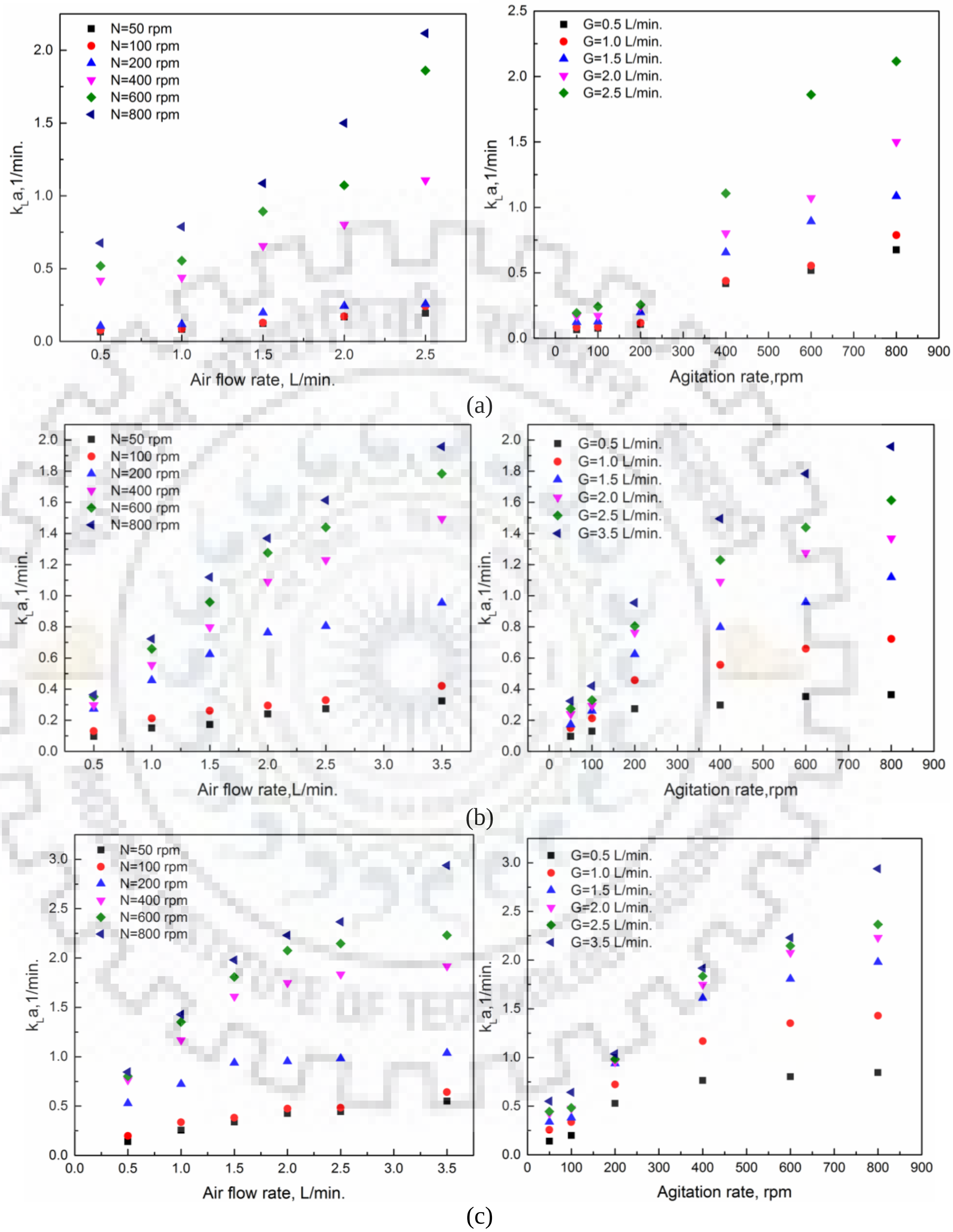


Figure 4.5. Effect of agitation rate and air flow rate on $k_La$ for mixed turbine (a) 7.5 L (Rushton + marine propeller), (b) 5 L (Rushton + pitched blade turbine) and (a) 1 L (Rushton + pitched blade turbine) stirred tank bioreactors

### 4.2.6 Effect of the Impeller Diameter on $k_La$

Impeller diameter is one of the important variables in the stirred tank bioreactors, which may influence the volumetric mass transfer coefficient as it may affect the power input per unit volume dissipated inside the bioreactor. The three Rushton turbine impellers of different diameters, ranging from 4 cm to 5 cm, were used to study their influence on the mass transfer coefficient keeping the impeller to tank diameter ratio greater than 0.33 and at the same air flow rate and temperature. It was found that $k_La$ was increasing with an increase in the impeller diameter as shown in Figure 4.6, however, the impeller diameter cannot be increased beyond the impeller to tank diameter ratio greater than 0.5. Therefore, it can be suggested that the impeller to tank diameter ratio should be kept as maximum as possible, but not greater than 0.5.

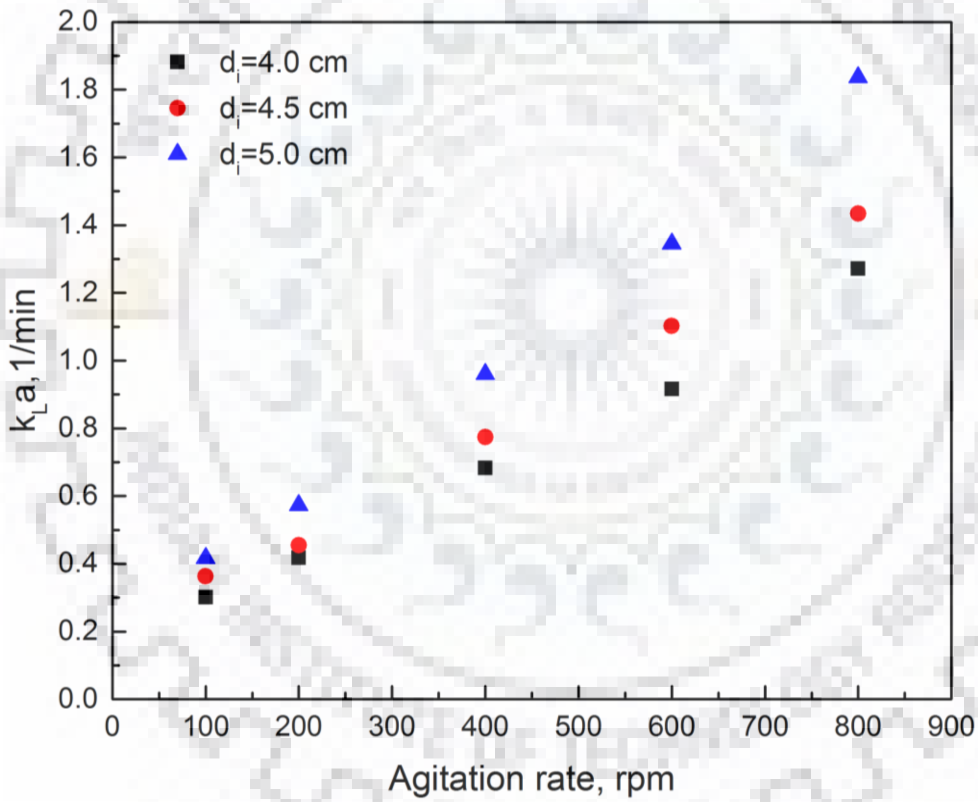


Figure 4.6. Effect of impeller diameter on $k_La$ in stirred tank bioreactor

### 4.2.7 Effect of the Liquid Volume on $k_La$

The liquid working volume has also been reported to affect the volumetric mass transfer coefficient. Three different liquid working volumes, ranging from 0.35 L to 0.9 L, were used inside the bioreactor for the prediction of volumetric mass transfer coefficient. It was found that $k_La$ was decreasing with an increase in the liquid volume inside the bioreactor as shown in Figure 4.7. This decrease in the $k_La$ may be attributed to the fact that with an increase in the liquid volume, the interfacial area may be decreasing at the same agitation speed, and thus decreasing the volumetric mass transfer coefficient. The decrease in liquid volume would lead to better mixing inside the bioreactor and thus the mass transfer coefficient would increase.

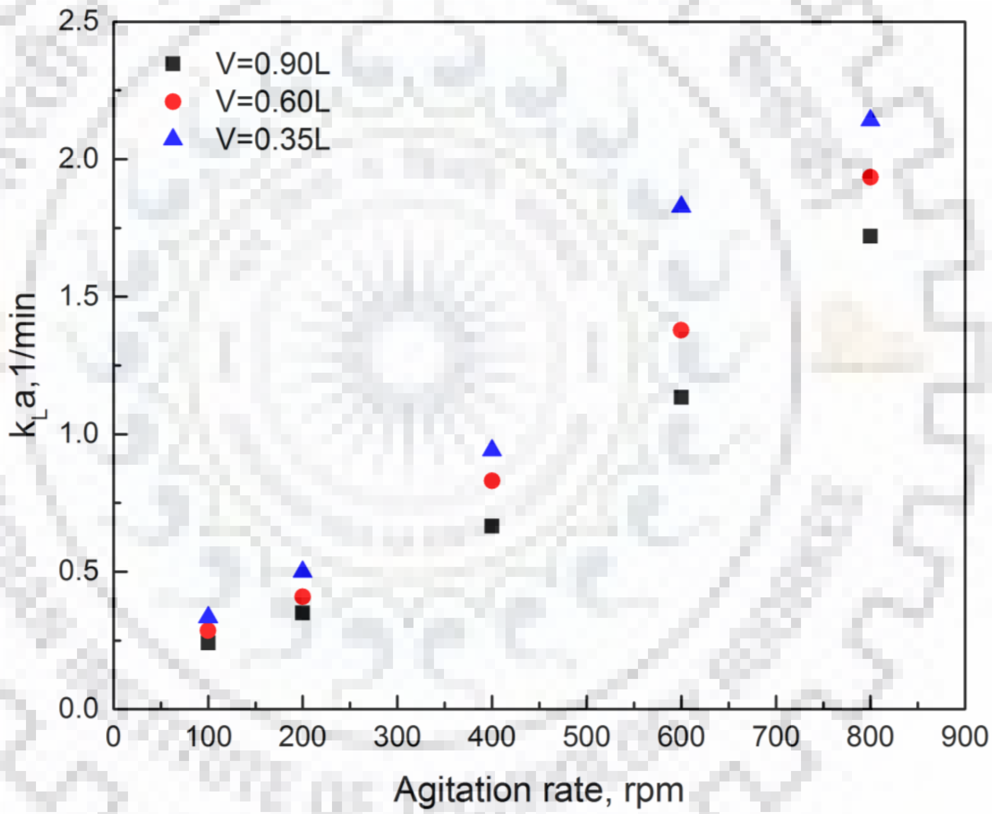


Figure 4.7. Effect of the liquid volume on $k_La$ in stirred tank bioreactor

### 4.2.8 Effect of Liquid Viscosity on $k_La$

Viscosity is a key parameter and thus plays an important role in a variety of biotechnological and chemical processes, such as in the production of biopolymers and in fermentations of filamentous microorganisms. In such processes, the viscosity could be changed during the process. Thus, it is necessary to study the effect of viscosity on the volumetric mass transfer coefficient in stirred tank bioreactors for the better understanding and successful operation of such processes. Liquid viscosity was increased by adding weighed amounts of glycerol to distilled water. Experimental results show that $k_La$ decreases with an increase in the viscosity of the liquid medium, as can be observed from Figure 4.8. In stirred tank bioreactor, the interfacial area can be considered almost constant and accordingly any decrease in $k_La$ with an increase in viscosity may be due to decrease in liquid phase mass transfer coefficient, $k_L$. It has also been reported that an increase in viscosity decreases turbulence at the gas-liquid surface, which decreases the surface-renewal rate, and consequently $k_L$, thus leading to an overall decrease in $k_La$.

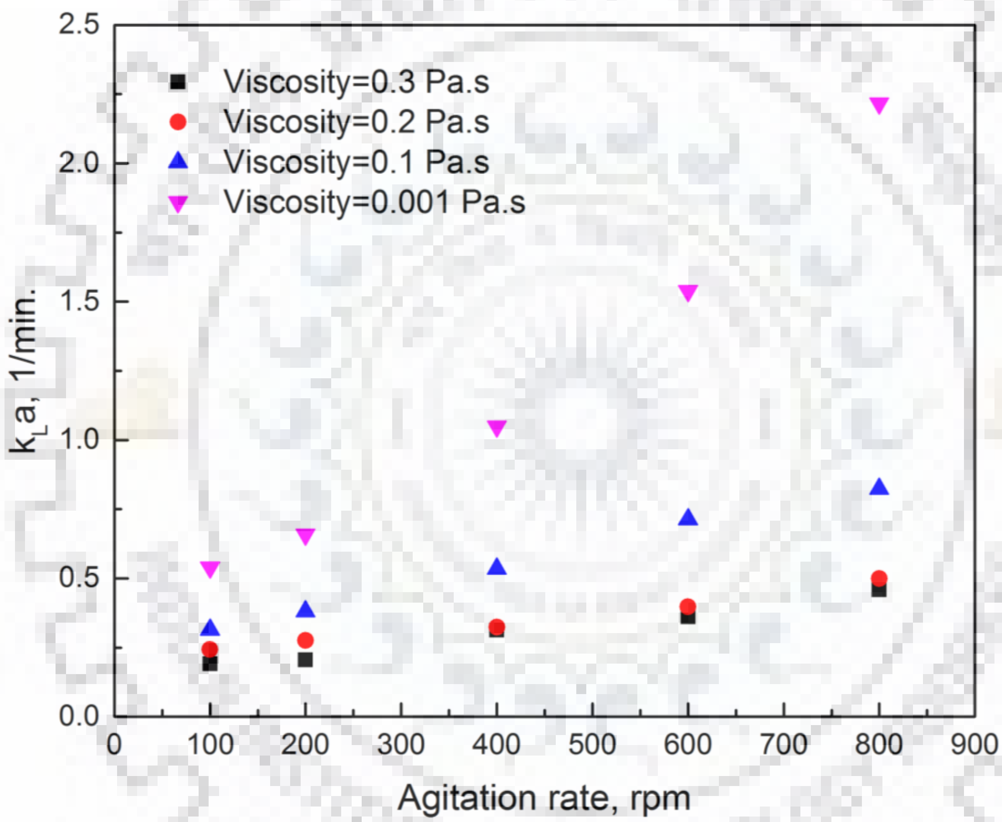


Figure 4.8. Effect of the liquid medium viscosity on $k_La$ in stirred tank bioreactor

### 4.2.9 Effect of the Standard and Dislocated Rushton Turbine on $k_La$

Although the standard Rushton turbine (SRT) is the widely used impeller type in STBRs since 1950's and is considered as a measuring yard stick to which other types of impellers are compared. However, several weaknesses have been reported in this turbine such as low axial pumping capacity, large shear stress, low-pressure trailing vortices resulting in power drop. To overcome these challenges, several efforts have been made for the modification of the standard Rushton turbine (SRT) over the past few years and many new designs of Rushton turbine have been developed. In this study, a dislocated Rushton turbine (DRT), Figure 3.4c, has been investigated for its mass transfer performance in a stirred bioreactor having the same dimensions as that of the SRT, except that the blades have been mounted above and below the impeller disc alternatively, i.e.

- three alternative blades are above the impeller disc with bottom edge of each blade aligned to bottom surface, and
- other three are below the impeller disc with their top edges parallel to top surface of disc.

It can be observed form Figure 4.9 that the dislocated Rushton turbine has shown better mass transfer performance than the standard Rushton turbine for gas-liquid mixing in stirred bioreactors. The improvement in kLa was approximately 10 – 15 % as compared to the conventional Rushton turbines. These results lay the foundation for its application in chemical and biochemical process industries.

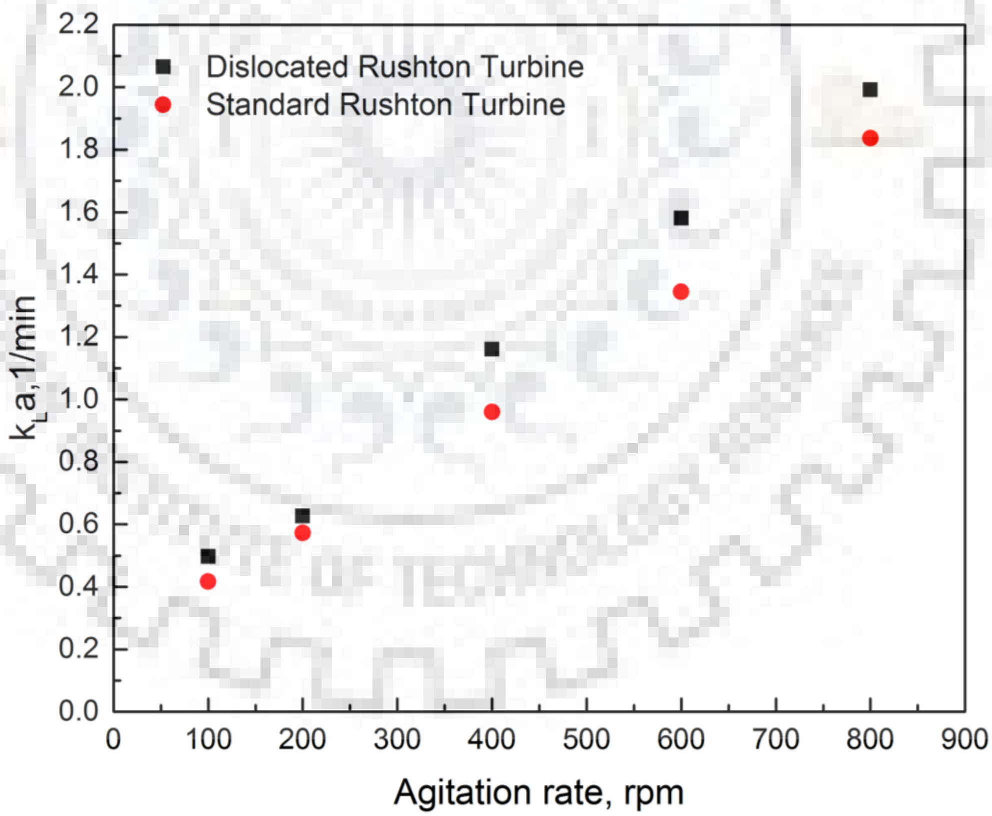


Figure 4.9. Effect of the different designs of Rushton turbine on $k_La$

### 4.2.10 Effect of Aeration Rate on Power Input per unit Volume ($P/V_L$)

Power consumption is a very important parameter for the STBRs. It is an indispensable and one of the most used parameter for describing hydrodynamics, mixing and mass transfer in STBRs. The power input per unit volume ($P/V_L$), also known as specific power input, is an important scaling-up parameter usually measured through the torque acting on the impeller shaft assembly under rotation. However, its experimental determination in small scale vessels is still a challenging task owing to frictional losses due to bearings and/or shaft seals. In the present study, the power input for gassed and ungassed conditions was calculated using Eqs. (4.3) and (4.4), respectively, for single and dual Rushton turbines. The agitation rate was varied from 50-800 rpm and the aeration rate was varied between 0.5-3.5 L/min. It can be seen from Figure 4.10 that the power consumption in aerated system is lower than in the unaerated system, because the transfer of power from impeller to the fluid is greatly influenced by aeration. The results in Figure 4.10 also show that the calculated power consumption for the single and dual Rushton turbines increases exponentially with agitation rate. It may also be attributed to the formation of cavities behind the impeller blades and the fluid having different density under gassed and ungassed conditions (Van't Riet and Smith, 1973). It can be observed that the power consumption for ungassed conditions is higher than the gassed power consumption. The difference between gassed and ungassed power inputs is more pronounced at higher agitation rates (400-800 rpm). The effect of aeration has been extensively studied by Nienow et al. (1977), Oosterhuis and Kossen (1981), Warmoeskerken and Smith (1981) and Yawalkar et al. (2002) and reported that the gassed power input is generally 30-40% of the ungassed power input depending on impeller types and aeration rate (Oosterhuis and Kossen, 1985).

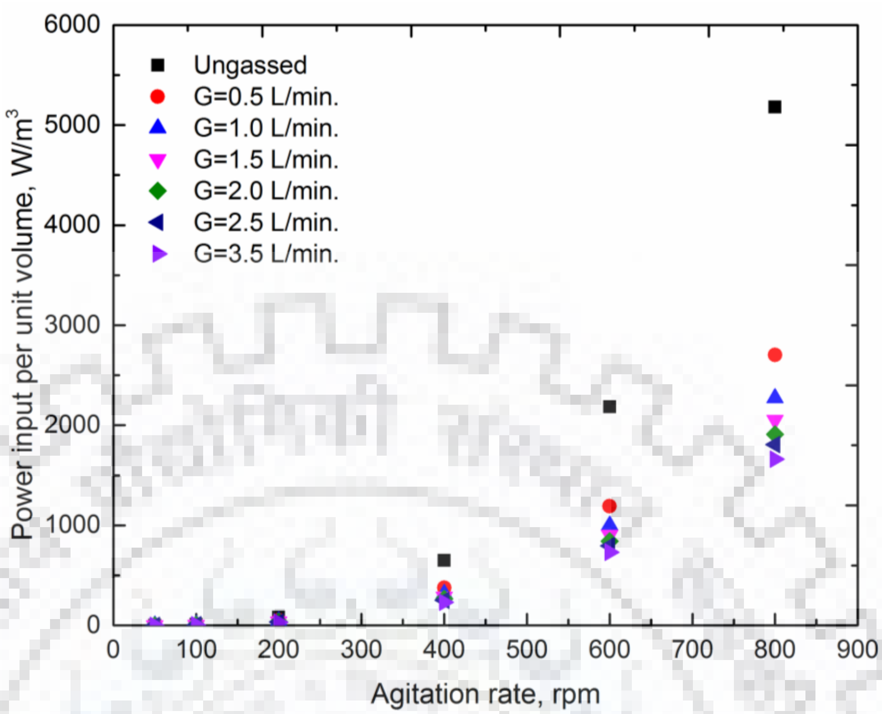


(a)

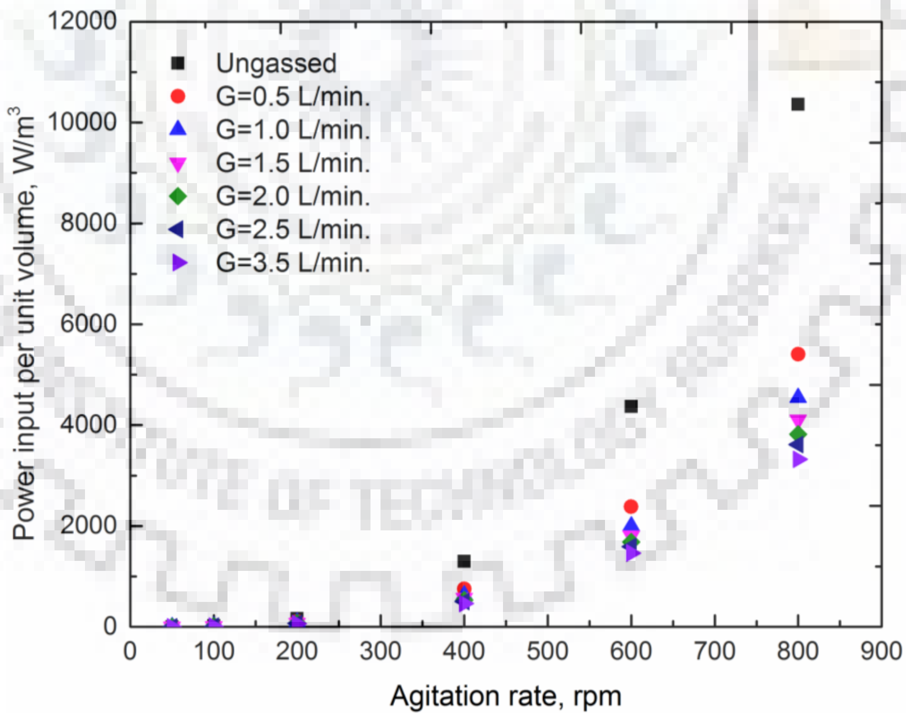


(b)

Figure 4.10. Effect of the agitation rate and aeration rate on $P/V_L$ for (a) single Rushton turbine and (b) dual Rushton turbine

## 4.3 DEVELOPMENT OF EMPIRICAL POWER-LAW CORRELATIONS

Several methods such as power-law, dimensionless correlations, etc. have been developed for theoretical estimation of the mass transfer coefficient in stirred tank bioreactors. Among the methods, power-law correlations have been most commonly used. In this study, power-law correlations have been developed for the single and dual Rushton turbines for all the three STBRs. Mass transfer rates in a stirred tank bioreactor mostly represented by the mass transfer coefficient, and $k_La$ is generally considered as a function of energy dissipation rates and superficial gas velocity and expressed in the form:

$$k_L a = \alpha\left(\frac{P_g}{V}\right)^{\beta}(v_{sg})^{\gamma} \tag{4.1}$$

where *α, β, γ* are the empirical constants, $P_g/V$ is the gassed power input per unit volume (W.m$^{-3}$) and $v_{sg}$ is the superficial gas velocity (m.s$^{-1}$), which means an increase in mass transfer rate would require an increase in specific power input and air flow rate. The experimental $k_La$ data for single and dual Rushton turbines for all the three STBRs have been used to develop correlations and then compared the experimental and predicted $k_La$ values. The power input per unit volume, i.e. $P_g/V$ for the Rushton turbines was calculated using the correlation by Hughmark (1980) as Eq. (4.3).

$$\frac{P_g}{P_{ug}} = 0.1\left[\frac{Q}{N_i V}\right]^{-0.25}\left[\frac{N_i^2 d_i^4}{gW_i V^{2/3}}\right]^{-0.2} \tag{4.2}$$

$$P_{ug} = N_P \rho N_i^3 d_i^5 \tag{4.3}$$

The superficial gas velocity was calculated using Equation (4.4) as follows:

$$v_{sg} = \frac{4Q}{\pi D_t^2} \tag{4.4}$$

where Q is the air flow rate (L/min.) entering the reactor and $D_t$ (m) is the reactor diameter. The empirical constants obtained for the power-law correlations for single and dual Rushton turbines for all the three STBRs have been presented in Table 4.1.

Table 4.1 Power-law coefficients in Equation 4.1

| Reactor Volume (L) | Impeller Type | α | β | γ |
|---|---|---|---|---|
| 7.5 | Single Rushton | 0.0003 | 0.43 | 0.58 |
| | Dual Rushton | 0.0004 | 0.34 | 0.69 |
| 5 | Single Rushton | 0.0007 | 0.36 | 0.50 |
| | Dual Rushton | 0.0006 | 0.27 | 0.72 |
| 1 | Single Rushton | 0.0028 | 0.28 | 0.33 |
| | Dual Rushton | 0.0017 | 0.34 | 0.39 |

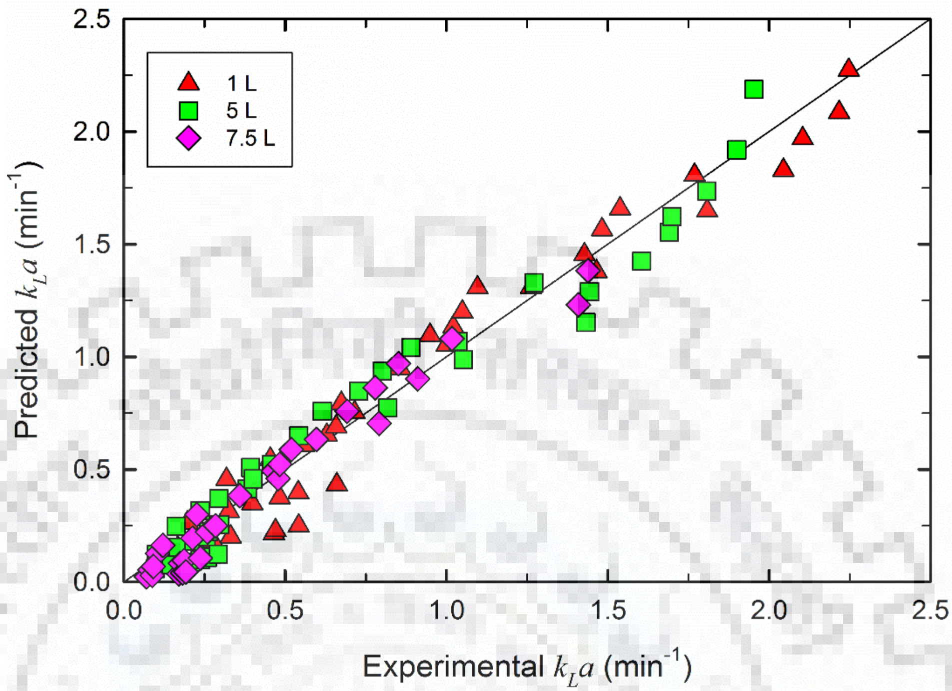


(a)

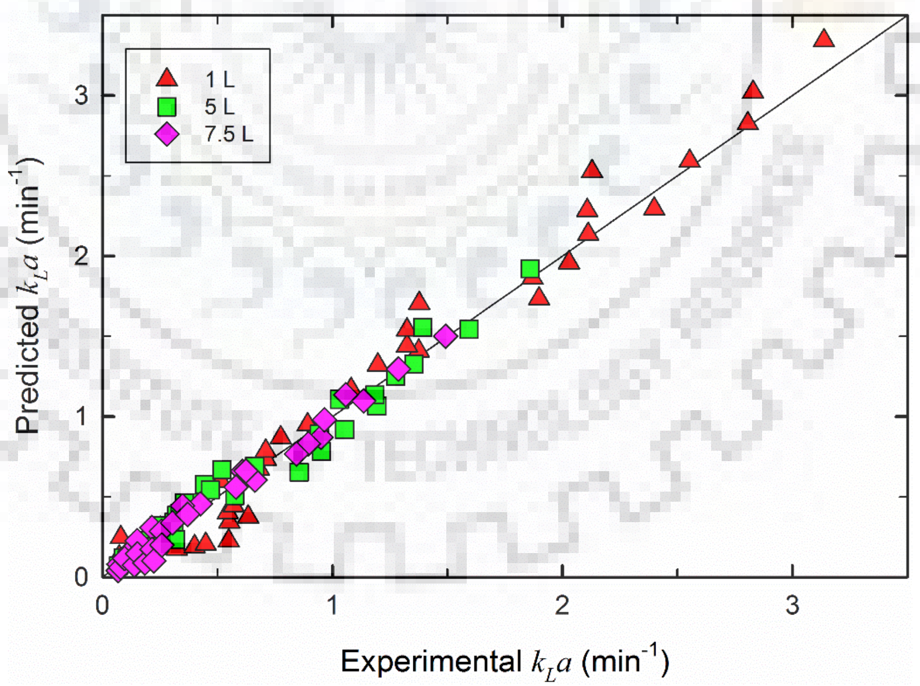


(b)

Figure 4.11. Parity plot between experimental and predicted $k_La$ for different volumes of stirred tank bioreactors for (a) single, and (b) dual Rushton turbines (N= 50-800 rpm, $Q_g$=0.5-3.5 L/min.)

The experimental $k_La$ values are shown as a parity plot with the predicted values in Figure 4.11 for single and dual Rushton turbines, for all the three STBRs. It can be observed that there is a close agreement between the experimental and predicted $k_La$. It can also be observed that stirred bioreactor of lowest volume i.e. 1 L has yielded higher $k_La$ than other two bioreactors of higher volumes under the same range of agitation rate and air flow rate. It may thus be inferred that as the bioreactor volume increases, there is a decrease in the volumetric mass transfer coefficient. During scale-up, this decrease in $k_La$ is one of the main challenges the stirred tank bioreactors are facing. This may be attributed to the fact that in larger size reactors, there may be poor mixing and thus there may be the formation of dead zones.

## 4.4 RSM-BBD MODELLING

A three level-three factor BBD was employed to correlate the volumetric mass transfer coefficient, $k_La$, and power input per unit volume, $P/V_L$ and the operating variables. The analysis of variance (ANOVA) was used to determine the accuracy of the developed models and identified the significant factors as well. Tables 4.2-4.9 show ANOVA results for different impellers investigated in this study. The ANOVA result is reported as an F-statistics and the associated degree of freedom (DF). The *F*-value always is used with the *P*-value to determine the significance of each term (e.g., $x_i$, $x_i^2$, or $x_ix_j$ in Equation 3.5 as mentioned in chapter 3) and higher *F*-value corresponds to lower *P*-value. The *P*-value less than 0.05 indicates that the effect of the corresponding term is significant (Tables 4.2-4.9). The significant terms have a dominant effect on the response, while the non-significant terms have a negligible response. Values of the square of the correlation coefficient, $R^2$, were determined from the developed models, as shown in Tables 4.2-4.9. In addition, adjusted $R^2$ (adj-$R^2$) and coefficient of variation (CV) were estimated to evaluate the model adequacy. The adj-$R^2$ was calculated by excluding the non-significant terms in the model. Therefore, the adj-$R^2$ is always lower than the $R^2$ due to reduced number of terms. The predicted $R^2$ indicates how well a regression model predicts response for new observations. Generally, a difference between predicted and adjusted $R^2$ values less than 0.2 indicates that the model has the sufficient capability to predict the response (Rai et al., 2016). As shown in Tables 4.2–4.9, the differences were calculated to be < 0.2 for all the cases, suggesting that the developed models by RSM are sufficient to predict the response. Generally, a low CV represents low variation in the mean value, suggesting that a satisfactory and adequate model is developed. Adequate precision (Adeq) measures the signal-to-noise ratio and a ratio greater than 4 is desirable (Sharma et al., 2013). For all the cases investigated, Adeq were determined to be greater than 18, indicating an adequate signal. In addition, the results show that “lack of fit” is not significant for all the cases.

Table 4.2 Analysis of variance for single Rushton turbine

| **Source** | **Sum of Squares** | **DF** | **Mean square** | **F-value** | **Prob>F** | **p-value** |
|---|---|---|---|---|---|---|
| Model | 4.660 | 9 | 0.520 | 61.62 | <0.0001 | <0.0001 |
| $x_1$ | 3.750 | 1 | 3.750 | 446.84 | <0.0001 | <0.0001 |
| $x_2$ | 0.310 | 1 | 0.310 | 36.72 | 0.0005 | 0.0037 |
| $x_3$ | 0.320 | 1 | 0.320 | 38.04 | 0.0005 | 0.0034 |
| $x_1^2$ | 0.120 | 1 | 0.120 | 14.72 | 0.0064 | 0.0297 |
| $x_2^2$ | 0.021 | 1 | 0.021 | 2.45 | 0.1617 | 0.2707 |
| $x_3^2$ | 0.007 | 1 | 0.007 | 0.81 | 0.3989 | 0.5135 |
| $x_1 x_2$ | 0.001 | 1 | 0.001 | 0.15 | 0.7139 | 0.7571 |
| $x_1 x_3$ | 0.130 | 1 | 0.130 | 15.17 | 0.0059 | 0.0223 |
| $x_2 x_3$ | 0.000 | 1 | 0.000 | 0.05 | 0.8294 | 0.8715 |
| Residual | 0.059 | 7 | 0.008 | …. | …. | |
| Pure error | 0 | 4 | 0 | …. | …. | |
| Cor total | 4.72 | 16 | …. | …. | …. | |
| Lack of fit | 0.059 | 3 | 0.020 | | | |

**Model statistics**

| | | | |
|---|---|---|---|
| $R^2$ | 0.9875 | Adeq precision | 28.981 |
| Adj-$R^2$ | 0.9715 | PRESS | 0.94 |
| Pre $R^2$ | 0.8006 | CV | 9.38 |
| Std. dev. | 0.092 | | |

Table 4.3 Analysis of variance for dual Rushton turbine

| **Source** | **Sum of Squares** | **DF** | **Mean square** | **F-value** | **Prob>F** | **p-value** |
|---|---|---|---|---|---|---|
| Model | 14.030 | 9 | 1.560 | 88.31 | <0.0001 | <0.0001 |
| $x_1$ | 10.500 | 1 | 10.500 | 594.68 | <0.0001 | <0.0001 |
| $x_2$ | 1.820 | 1 | 1.820 | 103.26 | <0.0001 | 0.0003 |
| $x_3$ | 0.810 | 1 | 0.810 | 45.97 | 0.0003 | 0.0018 |
| $x_1^2$ | 0.090 | 1 | 0.090 | 5.11 | 0.0600 | 0.0975 |
| $x_2^2$ | 0.130 | 1 | 0.130 | 7.31 | 0.0304 | 0.0861 |
| $x_3^2$ | 0.013 | 1 | 0.013 | 0.72 | 0.4248 | 0.5856 |
| $x_1 x_2$ | 0.480 | 1 | 0.480 | 27.32 | 0.0012 | 0.0056 |
| $x_1 x_3$ | 0.098 | 1 | 0.098 | 5.55 | 0.0507 | 0.0905 |
| $x_2 x_3$ | 0.091 | 1 | 0.091 | 5.17 | 0.0572 | 0.0990 |
| Residual | 0.120 | 7 | 0.018 | …. | …. | |
| Pure error | 0.036 | 4 | 0.010 | …. | …. | |
| Cor total | 14.16 | 16 | …. | …. | …. | |
| Lack of fit | 0.087 | 3 | 0.029 | 3.21 | …. | 0.1466 |

**Model statistics**

| | | | |
|---|---|---|---|
| $R^2$ | 0.9913 | Adeq precision | 31.857 |
| Adj-$R^2$ | 0.9800 | PRESS | 1.45 |
| Pre $R^2$ | 0.8973 | CV | 8.56 |
| Std. dev. | 0.13 | | |

Table 4.4 Analysis of variance for pitched blade turbine

| Source | Sum of Squares | DF | Mean square | F-value | Prob>F | p-value |
|---|---|---|---|---|---|---|
| Model | 11.160 | 9 | 1.240 | 61.88 | <0.0001 | <0.0001 |
| $x_1$ | 9.900 | 1 | 9.900 | 493.68 | <0.0001 | <0.0001 |
| $x_2$ | 0.770 | 1 | 0.770 | 38.47 | 0.0004 | 0.0033 |
| $x_3$ | 0.100 | 1 | 0.100 | 4.98 | 0.0608 | 0.0400 |
| $x_1^2$ | 0.100 | 1 | 0.100 | 5.22 | 0.0563 | 0.1894 |
| $x_2^2$ | 0.180 | 1 | 0.180 | 8.90 | 0.0204 | 0.0445 |
| $x_3^2$ | 0.031 | 1 | 0.031 | 1.54 | 0.2547 | 0.5121 |
| $x_1\ x_2$ | 0.087 | 1 | 0.087 | 4.34 | 0.0757 | 0.0450 |
| $x_1\ x_3$ | 0.010 | 1 | 0.010 | 0.51 | 0.4987 | 0.5709 |
| $x_2\ x_3$ | 0.000 | 1 | 0.000 | 0.02 | 0.9024 | 0.9182 |
| Residual | 0.14 | 7 | 0.020 | …. | …. | |
| Pure error | 0.008 | 4 | 0.002 | …. | …. | |
| Cor total | 11.30 | 16 | …. | …. | …. | |
| Lack of fit | 0.130 | 3 | 0.044 | 22.53 | …. | 0.0675 |
| **Model statistics** | | | | | | |
| $R^2$ | 0.9877 | | Adeq precision | 26.203 | | |
| Adj-$R^2$ | 0.9716 | | PRESS | 2.13 | | |
| Pre $R^2$ | 0.8114 | | CV | 9.99 | | |
| Std. dev. | 0.14 | | | | | |

Table 4.5 Analysis of variance for mixed turbine (Rushton + pitched blade turbine)

| Source | Sum of Squares | DF | Mean square | F-value | Prob>F | p-value |
|---|---|---|---|---|---|---|
| Model | 15.600 | 9 | 1.730 | 31.86 | <0.0001 | <0.0001 |
| $x_1$ | 8.000 | 1 | 8.000 | 147.02 | <0.0001 | 0.0001 |
| $x_2$ | 3.310 | 1 | 3.310 | 60.88 | 0.0001 | 0.0011 |
| $x_3$ | 0.990 | 1 | 0.990 | 18.22 | 0.0037 | 0.0143 |
| $x_1^2$ | 1.260 | 1 | 1.260 | 23.23 | 0.0019 | 0.0115 |
| $x_2^2$ | 0.320 | 1 | 0.320 | 5.85 | 0.0462 | 0.1097 |
| $x_3^2$ | 0.065 | 1 | 0.065 | 1.20 | 0.3096 | 0.4112 |
| $x_1\ x_2$ | 1.160 | 1 | 1.160 | 21.38 | 0.0024 | 0.0104 |
| $x_1\ x_3$ | 0.250 | 1 | 0.250 | 4.51 | 0.0713 | 0.1252 |
| $x_2\ x_3$ | 0.210 | 1 | 0.210 | 3.86 | 0.0901 | 0.1508 |
| Residual | 0.380 | 7 | 0.054 | …. | …. | |
| Pure error | 0.029 | 4 | 0.007 | …. | …. | |
| Cor total | 15.98 | 16 | …. | …. | …. | |
| Lack of fit | 0.350 | 3 | 0.12 | 16.37 | …. | 0.0704 |
| **Model statistics** | | | | | | |
| $R^2$ | 0.9767 | | Adeq precision | 18.372 | | |
| Adj-$R^2$ | 0.9455 | | PRESS | 5.68 | | |
| Pre $R^2$ | 0.7646 | | CV | 13.34 | | |
| Std. dev. | 0.23 | | | | | |

Table 4.6 Analysis of variance for Rushton-Rushton configuration for $k_La$

| Source | Sum of Squares | DF | Mean square | F-value | P-value |
|---|---|---|---|---|---|
| Model | 5.200 | 9 | 0.580 | 24.27 | 0.0013 |
| $x_1$ | 3.610 | 1 | 3.610 | 151.52 | <0.0001 |
| $x_2$ | 0.560 | 1 | 0.560 | 23.72 | 0.0046 |
| $x_3$ | 0.060 | 1 | 0.060 | 2.51 | 0.1742 |
| $x_1^2$ | 0.630 | 1 | 0.630 | 26.28 | 0.0037 |
| $x_2^2$ | 0.100 | 1 | 0.100 | 4.34 | 0.0918 |
| $x_3^2$ | 0.100 | 1 | 0.100 | 4.35 | 0.0913 |
| $x_1 x_2$ | 0.043 | 1 | 0.043 | 1.81 | 0.2359 |
| $x_1 x_3$ | 0.002 | 1 | 0.002 | 0.099 | 0.7652 |
| $x_2 x_3$ | 0.023 | 1 | 0.023 | 0.95 | 0.3754 |
| Residual | 0.120 | 5 | 0.024 | …. | 0.1617 |
| Pure error | 0 | 2 | 0 | …. | 0.2707 |
| Cor total | 5.320 | 14 | …. | …. | …. |
| Lack of fit | 0.110 | 3 | 0.038 | 11.83 | 0.0810 |
| **Model statistics** | | | | | |
| $R^2$ | 0.9776 | | Adeq precision | 14.878 | |
| Adj-$R^2$ | 0.9373 | | PRESS | 1.82 | |
| Pre $R^2$ | 0.7583 | | CV | 14.18 | |
| Std. dev. | 0.15 | | | | |

Table 4.7 Analysis of variance for Rushton-marine propeller configuration for $k_La$

| Source | Sum of Squares | DF | Mean square | F-value | P-value |
|---|---|---|---|---|---|
| Model | 3.930 | 9 | 0.440 | 12.96 | 0.0058 |
| $x_1$ | 2.680 | 1 | 2.680 | 79.40 | 0.0003 |
| $x_2$ | 0.780 | 1 | 0.780 | 23.05 | 0.0049 |
| $x_3$ | 0.130 | 1 | 0.130 | 3.99 | 0.1024 |
| $x_1^2$ | 0.086 | 1 | 0.086 | 2.57 | 0.1701 |
| $x_2^2$ | 0.008 | 1 | 0.008 | 0.24 | 0.6480 |
| $x_3^2$ | 0.037 | 1 | 0.037 | 1.11 | 0.3404 |
| $x_1 x_2$ | 0.120 | 1 | 0.120 | 3.56 | 0.1178 |
| $x_1 x_3$ | 0.076 | 1 | 0.076 | 2.24 | 0.1946 |
| $x_2 x_3$ | 0.006 | 1 | 0.006 | 0.17 | 0.6986 |
| Residual | 0.170 | 5 | 0.034 | …. | …. |
| Pure error | 0 | 2 | 0 | …. | …. |
| Cor total | 4.100 | 14 | …. | …. | …. |
| Lack of fit | 0.160 | 3 | 0.054 | 13.83 | 0.0719 |
| **Model statistics** | | | | | |
| $R^2$ | 0.9589 | | Adeq precision | 12.370 | |
| Adj-$R^2$ | 0.8849 | | PRESS | 2.62 | |
| Pre $R^2$ | 0.6959 | | CV | 16.09 | |
| Std. dev. | 0.18 | | | | |

Table 4.8 Analysis of variance for Rushton-Rushton configuration for $P/V_L$

| Source | Sum of Squares | DF | Mean square | F-value | P-value |
|---|---|---|---|---|---|
| Model | 8.060 | 9 | 0.900 | 91.59 | <0.0001 |
| $x_1$ | 7.510 | 1 | 7.510 | 767.64 | <0.0001 |
| $x_2$ | 0.026 | 1 | 0.026 | 2.70 | 0.1610 |
| $x_3$ | 0.042 | 1 | 0.042 | 4.33 | 0.0920 |
| $x_1^2$ | 0.36 | 1 | 0.36 | 36.61 | 0.0018 |
| $x_2^2$ | 0.001 | 1 | 0.001 | 0.01 | 0.7673 |
| $x_3^2$ | 0.003 | 1 | 0.003 | 0.35 | 0.5802 |
| $x_1 x_2$ | 0.042 | 1 | 0.042 | 4.26 | 0.0941 |
| $x_1 x_3$ | 0.077 | 1 | 0.077 | 7.85 | 0.0380 |
| $x_2 x_3$ | 0.002 | 1 | 0.002 | 0.24 | 0.6479 |
| Residual | 0.049 | 5 | 0.01 | …. | …. |
| Pure error | 0 | 2 | 0 | …. | …. |
| Cor total | 8.110 | 14 | …. | …. | …. |
| Lack of fit | 0.048 | 3 | 0.016 | 14.98 | 0.0604 |
| **Model statistics** | | | | | |
| $R^2$ | 0.9940 | | Adeq precision | 27.738 | |
| Adj-$R^2$ | 0.9831 | | PRESS | 0.77 | |
| Pre $R^2$ | 0.9051 | | CV | 8.58 | |
| Std. dev. | 0.099 | | | | |

Table 4.9 Analysis of variance for Rushton-Marine Propeller configuration for $P/V_L$

| Source | Sum of Squares | DF | Mean square | F-value | P-value |
|---|---|---|---|---|---|
| Model | 8.620 | 9 | 0.960 | 1589.23 | <0.0001 |
| $x_1$ | 8.230 | 1 | 8.230 | 13662.91 | <0.0001 |
| $x_2$ | 0.007 | 1 | 0.007 | 12.15 | 0.0175 |
| $x_3$ | 0.002 | 1 | 0.002 | 3.40 | 0.1245 |
| $x_1^2$ | 0.370 | 1 | 0.370 | 606.64 | <0.0001 |
| $x_2^2$ | 0.000 | 1 | 0.000 | 0.036 | 0.8574 |
| $x_3^2$ | 0.000 | 1 | 0.000 | 0.51 | 0.5088 |
| $x_1 x_2$ | 0.004 | 1 | 0.004 | 7.45 | 0.0413 |
| $x_1 x_3$ | 0.000 | 1 | 0.000 | 0.96 | 0.3730 |
| $x_2 x_3$ | 0.002 | 1 | 0.002 | 4.15 | 0.0972 |
| Residual | 0.003 | 5 | 0.000 | …. | …. |
| Pure error | 0.000 | 2 | 0 | …. | …. |
| Cor total | 8.620 | 14 | …. | …. | …. |
| Lack of fit | 0.003 | 3 | 0.01 | 14.7 | 0.0644 |
| **Model statistics** | | | | | |
| $R^2$ | 0.9997 | | Adeq precision | 104.572 | |
| Adj-$R^2$ | 0.9990 | | PRESS | 0.046 | |
| Pre $R^2$ | 0.9946 | | CV | 2.09 | |
| Std. dev. | 0.025 | | | | |

### 4.4.1 Single Rushton Turbine

Rushton turbines have flat blades which produce a unidirectional radial flow (see Figure 3.3a as shown in Chapter 3). Rushton-type impellers are commonly used in fermentation of non-shear-sensitive cells such as yeasts, bacteria, and some fungi (Mirro and Voll, 2009). Three-dimensional (3-D) response surface plots and their corresponding 2-D contour plots for the single Rushton turbine are shown in Figure 4.12, which provide visual insight into the rapport between $k_La$ and experimental variables at each level. The 3-D plots help to understand the overall profile of the response by showing the nature of the fitted surface as the maximum, minimum or saddle point, however, it is difficult to judge the levels of variables from the plots. For this reason, 2-D contour plots of $k_La$ are presented along with 3-D plots.

Figure 4.12 also shows the combined effect of two independent variables on the response keeping the other variable at middle level point. Figure 4.12a presents the effect of agitation rate and temperature on $k_La$ when air flow rate is set at 2 L/min. It was observed that the $k_La$ increases with increasing both agitation rate and temperature. Similar patterns can be found from Figures 4.12b and 4.12c that $k_La$ increases with an increase in the independent variables. Although each factor contributes to the change of $k_La$, the effect of agitation rate was determined to be more significant than those of other factors. The effects of the linear, quadratic and interaction terms can be found from p-values in Table 4.2. Based on the criterion of p-value (<0.05), effects of all the linear ($x_1$, $x_2$ and $x_3$), the quadratic of ($x_1^2$), agitation rate and the interaction between agitation rate and temperature ($x_1x_3$) appear to be significant on $k_La$.

### 4.4.2 Dual Rushton Turbine

The effect of operating variables on $k_La$ was investigated for dual Rushton turbines. 3-D response surface and 2-D contour plots of $k_La$ are shown in Figure 4.13 and the ANOVA results are presented in Table 4.3. The patterns of $k_La$ change for dual Rushton turbine were found to be similar to those for the single Rushton turbine. As shown in Figure 4.13, the $k_La$ increases with increasing independent variables. However, the effect of temperature on $k_La$ appears to be insignificant. As shown in Table 4.3, several factors (e.g. $x_1$, $x_2$, $x_3$, and $x_1x_2$) have p-values <0.05, indicating that these terms are significant, which is in good agreement with the observations from Figure 4.13.

### 4.4.3 Pitched Blade Turbine

Due to the angled flat blades (45° in this study), pitched blade impellers generate axial flow which provides better overall mixing and creates a higher oxygen transfer rate than Rushton type impellers. For this reason, pitched blade impellers are also widely used in fermentation processes particularly for highly viscous cells such as filamentous bacteria and fungi (Mirro and Voll, 2009).

Similar to the results observed from the single and dual Rushton turbines, the $k_La$ tends to increase with increasing independent variables, as shown in Figure 4.14. In addition, the $k_La$ was little influenced by temperature. These results agree with ANOVA predictions in Table 4.4 which clearly shows that effects of the linear ($x_1$, $x_2$ and $x_3$), the quadratic of ($x_2^2$), air flow rate and the interaction between agitation rate and air flow rate ($x_1x_2$) are significant.

### 4.4.4 Mixed Impeller (Rushton Turbine + Pitched Blade Turbine)

As compared to single configurations, the dual impeller configurations combined with different (radial and axial) flow impellers are expected to provide better mixing performance (Zhang et al., 2017). To generate radial and axial flows simultaneously, in the present work, a mixed impeller configured by Rushton and pitched blade turbines was investigated. As shown in Figure 4.15, among the independent variables, agitation rate plays a dominant role on $k_La$ while the effect of temperature is less significant than other variables. This result is evidenced by the p-values of individual variables in Table 4.5. The p-values of $x_1$, $x_2$ and $x_3$ for the mixed impeller were determined to be 0.0001, 0.0011, and 0.0143, respectively as shown in Table 4.5. Along with $x_1$, $x_2$ and $x_3$, it can be seen that $x_1x_2$ and $x_1^2$, are significant. Interestingly, any terms involved with temperature ($x_3$) were determined to be insignificant.

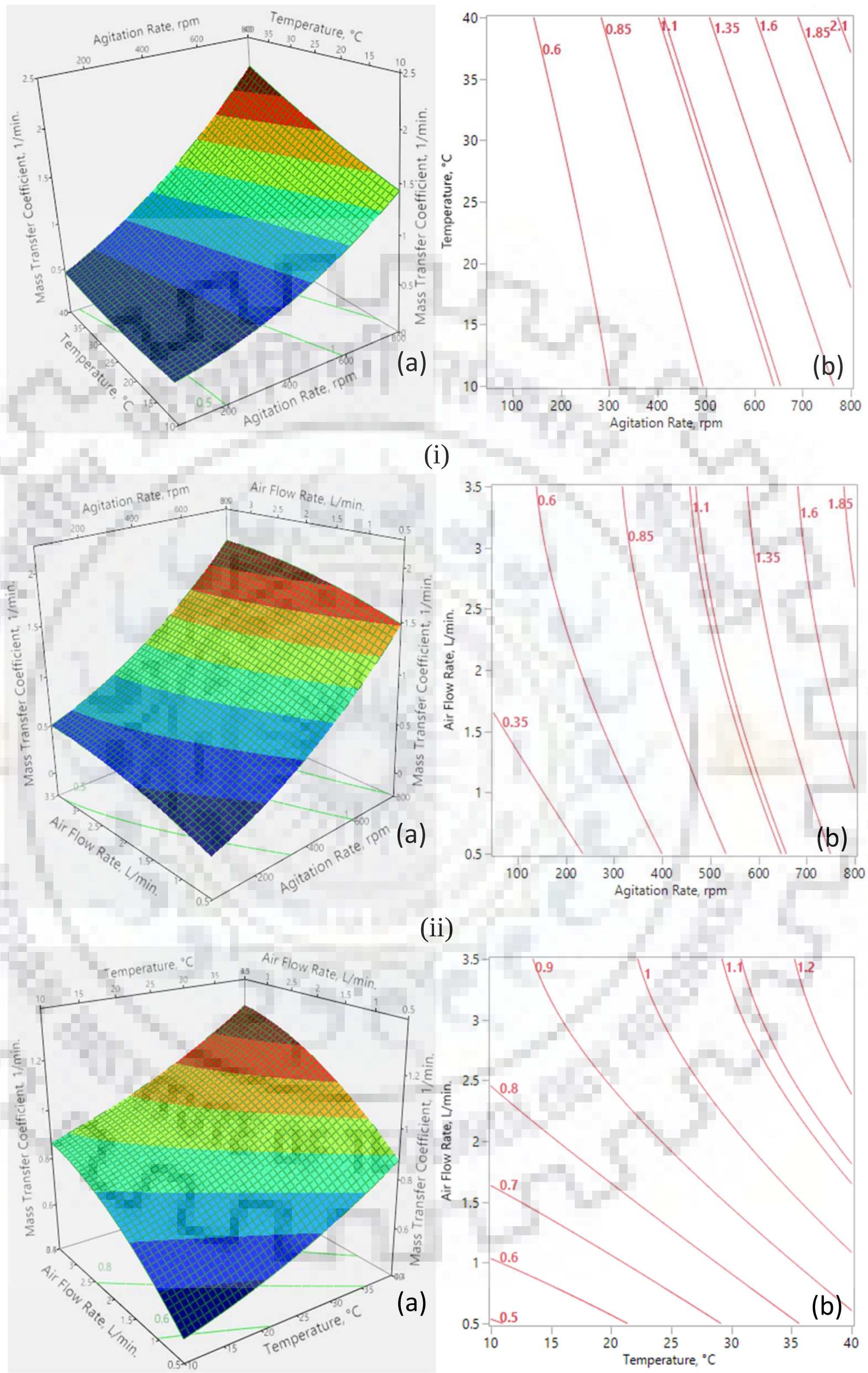


Figure 4.12. Effect of (i) agitation rate and temperature, (ii) agitation and air flow rate, and (iii) air flow rate and temperature on the $k_La$ for the single Rushton impeller: (a) 3-D response surface plot and (b) 2-D contour plot

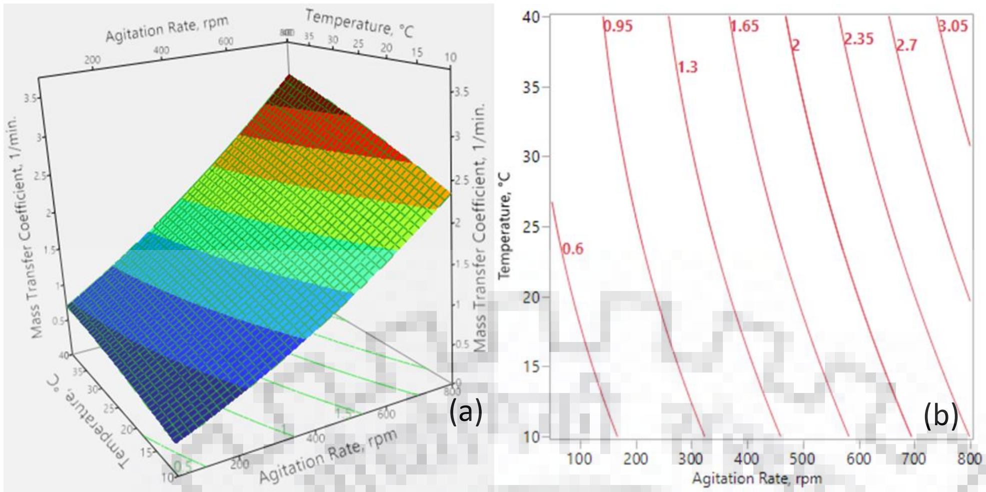


(i)

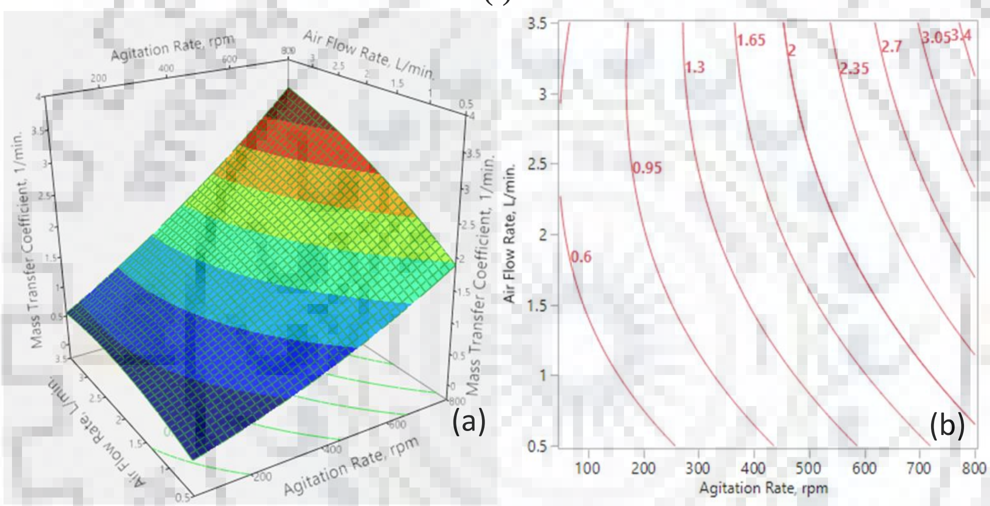


(ii)

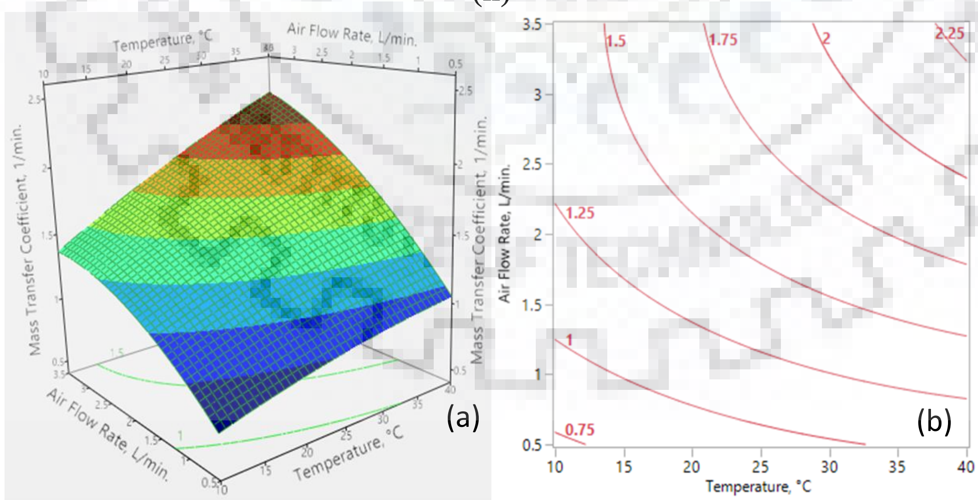


(iii)

Figure 4.13. Effect of (i) agitation rate and temperature, (ii) agitation and air flow rate, and (iii) air flow rate and temperature on the $k_La$ for the dual Rushton impeller: (a) 3-D response surface plot and (b) 2-D contour plot

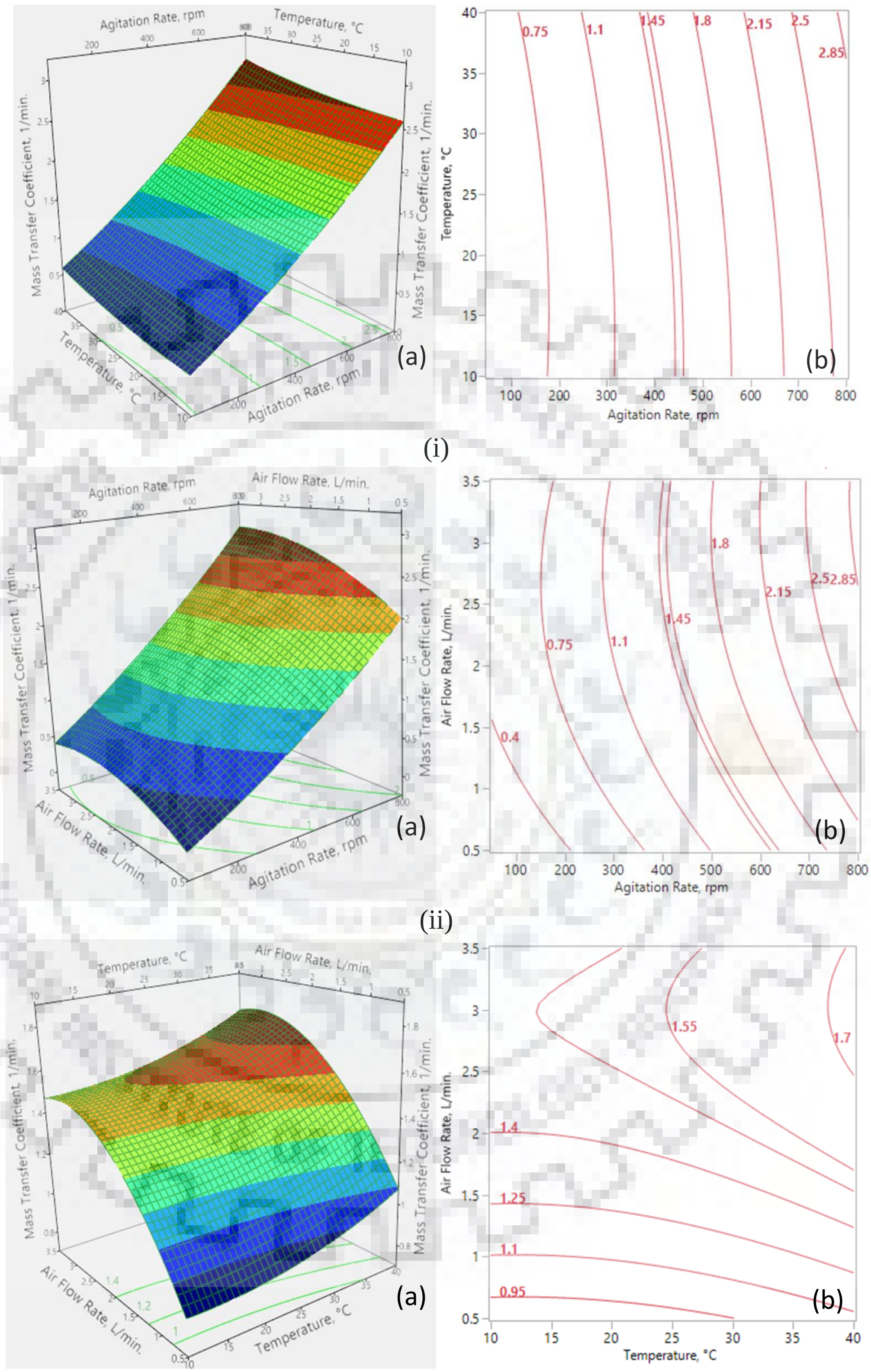


Figure 4.14. Effect of (i) agitation rate and temperature, (ii) agitation and air flow rate, and (iii) air flow rate and temperature on the $k_La$ for the pitched blade impeller: (a) 3-D response surface plot and (b) 2-D contour plot

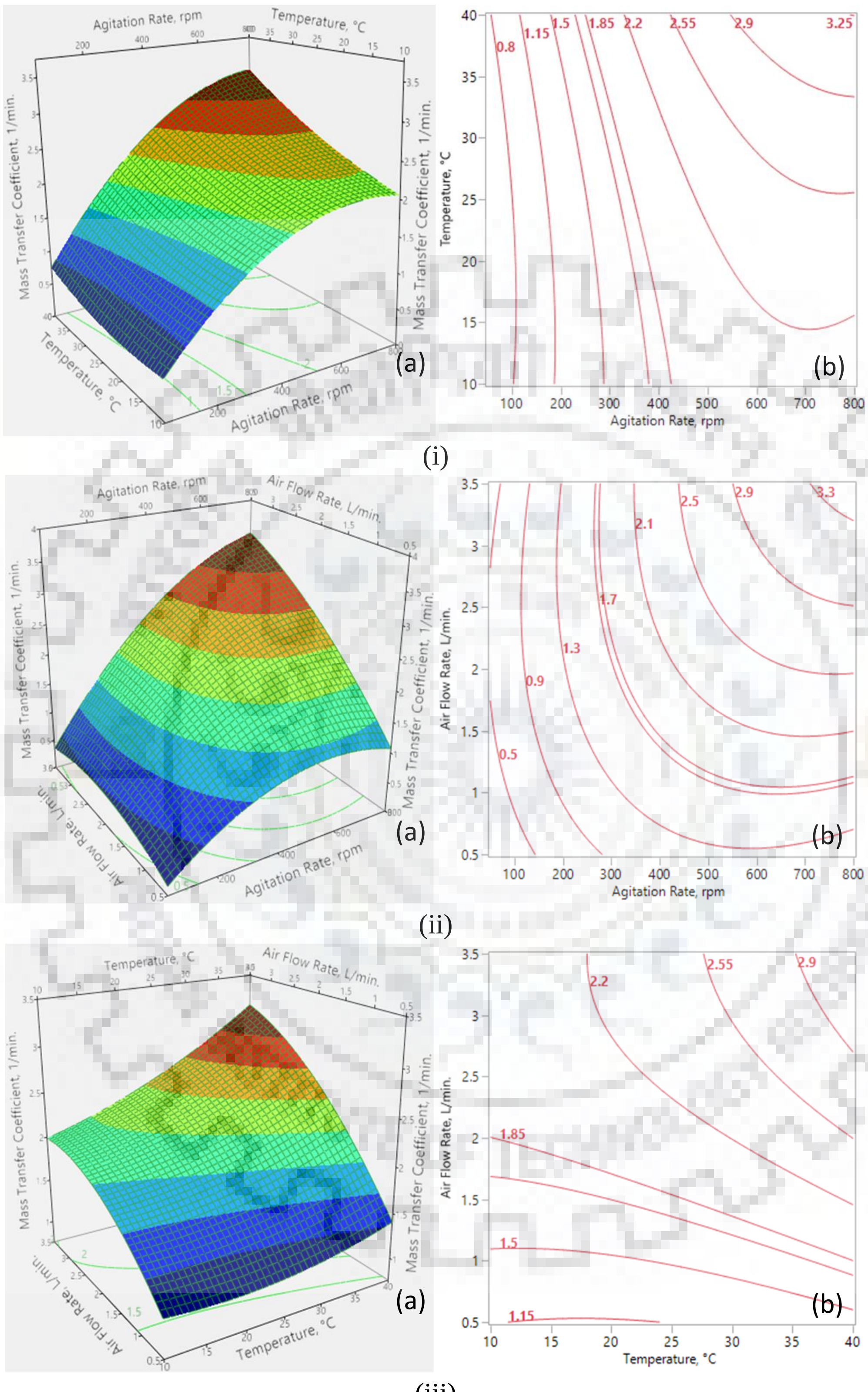


Figure 4.15. Effect of (i) agitation rate and temperature, (ii) agitation and air flow rate, and (iii) air flow rate and temperature on the $k_La$ for the mixed impeller: (a) 3-D response surface plot and (b) 2-D contour plot.

Using the RSM-BBD model, the values of coefficients in Eq. 3.5 as mentioned in Chapter 3 for each impeller configuration were determined and summarized in Table 4.10. In Table 4.10, bold values represent that corresponding variable terms are significant in influencing $k_La$.

Further, as shown in Tables 4.2-4.5, the $R^2$ values of the single Rushton, dual Rushton, pitched blade and mixed turbines were calculated to be 0.988, 0.991, 0.988, and 0.977, respectively. Thus, it may be seen that the regression model (Eq. 3.5 mentioned in Chapter 3) describes the experimental $k_La$ well. Figure 4.16 shows the goodness of fit in a parity plot between the experimental and predicted values of $k_La$. It was found that the significance of the linear, quadratic, and interaction terms effect on $k_La$ was different for impeller types investigated. The p-values in Tables 4.2-4.5 indicated that the effect of all the linear terms were found to be highly significant on $k_La$. In addition, most of the temperature-related effects in this study were relatively insignificant, as compared to others. This may be most likely because range of temperature examined in this study (10-40°C) was relatively narrower than others. Among the impeller configurations studied, under the same operating conditions, dual Rushton turbine configuration demonstrated the highest value of $k_La$, followed by the mixed and pitched blade, and single Rushton turbines (Figure 4.16). Particularly for cell cultivation, however, the power number of the impeller must be taken into account since high shear force can damage cells. Indeed, for shear-sensitive cells the axial impellers such as pitched blade type are more widely used due to relatively low power number, as compared to the radial impellers such as Rushton type (Ghotli et al., 2013). In this context, it is likely that the pitched blade impellers are most effective for cell culture applications.

Table 4.10 Estimated regression coefficients for $k_La$ at coded units

| Term | Single Rushton | Dual Rushton | Pitched blade | Mixed |
|---|---|---|---|---|
| $b_0$ | **0.911** | **1.592** | **1.399** | **2.077** |
| $b_1$ | **0.685** | **1.146** | **1.112** | **0.999** |
| $b_2$ | **0.196** | **0.477** | **0.311** | **0.644** |
| $b_3$ | **0.199** | **0.318** | **0.112** | **0.352** |
| $b_{12}$ | 0.018 | **0.347** | **0.147** | **0.539** |
| $b_{13}$ | **0.178** | 0.156 | 0.051 | 0.248 |
| $b_{23}$ | 0.010 | 0.151 | 0.009 | 0.229 |
| $b_{11}$ | **0.171** | 0.146 | 0.158 | **-0.548** |
| $b_{22}$ | -0.069 | -0.175 | **-0.206** | -0.275 |
| $b_{33}$ | 0.040 | -0.055 | 0.086 | 0.124 |

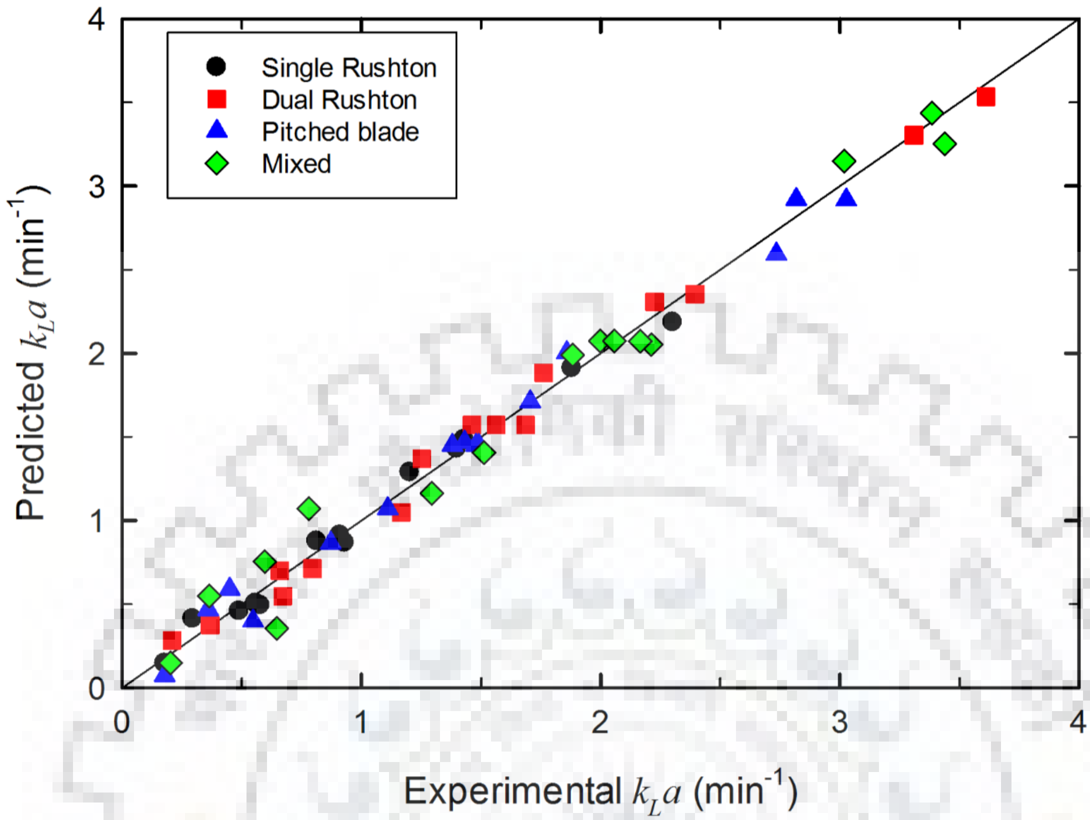


Figure 4.16. Parity plot between the experimental and predicted values of $k_La$ (N= 50-800 rpm, $Q_g$=0.5-3.5 L/min., T=10-40 °C)

## 4.5 SIMPLIFICATION OF MODEL DEVELOPED BY RSM

Using RSM, a correlation (Eq. 3.5 mentioned in Chapter 3) was obtained for each impeller case. High coefficients of correlation in the ANOVA analysis (Tables 4.2-4.5) suggest that the experimental $k_La$ was successfully correlated by the model using RSM. A fairly good agreement between experimental and predicted $k_La$ can also be seen in Figure 4.16. However, Eq. (3.5) with 10 coefficients (Table 4.10) is relatively lengthy as compared to traditional correlation equation. In addition, Eq. 3.5 fails to present direct correlation between $k_La$ and actual parameter values since coded units ($x_i$ = -1, 0, or 1) are used, instead. In this context, it is useful to develop a simplified correlation to determine $k_La$ from actual values of independent variables without any further encoding process.

Tables 4.2-4.5 show that several source terms (e.g. $x_i$, $x_ix_j$, $x_i^2$) have p-values >0.05, indicating that these terms are not significant for $k_La$. Therefore, Eq. (3.5) can be simplified by excluding these insignificant terms. In Table 4.2 (single Rushton turbine), e.g. the original equation (Eq. 3.5) is simplified by cancelling $x_1x_2$, $x_2x_3$, $x_2^2$, and $x_3^2$ terms. Instead of Eq. (3.5), the following equation is defined to correlate $k_La$ and actual operating variable values.

$$Y = B_0 + \sum_{i=1}^{n} B_i X_i + \sum_{i=1}^{n} B_{ii} X_i^{\,2} + \sum_{j>i}^{n} \sum_{i=1}^{n} B_{ij} X_i X_j \tag{4.6}$$

where $Y$ is $k_La$ (1/min), $X_1$ is agitation rate (rpm), $X_2$ is air flow rate (L/min), and $X_3$ is temperature (°C). After the simplification, the number of coefficients ($B_i$) were reduced from 10 to 5-6 and the coefficients values were re-estimated (Table 4.11). It is noteworthy that minor (or very small) deviation in $R^2$ values were observed even after the simplification process. This result suggests that the $k_La$ can be still correlated well by the simplified equations.

Table 4.11 Estimated regression coefficients for $k_La$ at actual units: before and after simplification

| Term | Single Rushton | | Dual Rushton | | Pitched blade | | Mixed | |
|---|---|---|---|---|---|---|---|---|
| | before | after | before | after | before | after | before | after |
| $B_0$ | 1.30E-01 | 8.15E-02 | 3.64E-02 | -4.03E-01 | -1.45E-01 | -5.13E-01 | 4.54E-01 | -4.61E-01 |
| $B_1$ | -6.67E-05 | -1.67E-05 | 1.81E-04 | 1.82E-03 | 1.42E-03 | 2.44E-03 | 2.95E-03 | 3.99E-03 |
| $B_2$ | 2.32E-01 | 1.31E-01 | 1.83E-01 | 5.68E-02 | 4.95E-01 | 5.30E-01 | 2.51E-01 | 2.02E-02 |
| $B_3$ | -9.84E-03 | -1.28E-04 | 6.19E-03 | 2.13E-02 | -1.06E-02 | 7.45E-03 | -4.38E-02 | 2.34E-02 |
| $B_{12}$ | 3.16E-05 | - | 6.16E-04 | 6.16E-04 | 2.62E-04 | 2.62E-04 | 9.61E-04 | 9.61E-04 |
| $B_{13}$ | 3.17E-05 | 3.17E-05 | 2.77E-05 | - | 8.98E-06 | - | 4.43E-05 | - |
| $B_{23}$ | 4.11E-04 | - | 6.67E-03 | - | 4.00E-04 | - | 1.02E-02 | - |
| $B_{11}$ | 1.22E-06 | 1.23E-06 | 1.12E-06 | - | 9.42E-07 | - | -3.89E-06 | -3.82E-06 |
| $B_{22}$ | -3.12E-02 | - | -7.33E-02 | - | -1.02E-01 | -1.09E-01 | -1.22E-01 | - |
| $B_{33}$ | 1.78E-04 | - | -2.00E-04 | - | 2.69E-04 | - | 5.61E-04 | - |
| **$R^2$** | **0.9875** | **0.9818** | **0.9913** | **0.9637** | **0.9877** | **0.9801** | **0.9767** | **0.9250** |

### 4.5.1 Comparison between Conventional and RSM Based Models

Various methods (e.g. power-law, dimensionless correlations, etc.) have been developed to estimate mass transfer coefficient in stirred tank bioreactors (Garcia-Ochoa and Gomez, 2009; Moucha et al., 2012; Labik et al., 2017). Among the methods, correlations in the form of power-law equations have been most commonly used (Karimi et al., 2013; Xie et al., 2014). To determine the accuracy of the models, in the present work, correlations by RSM (Eq. 4.6) were compared with the conventional power-law correlations in which power input per unit volume ($P_g/V$) and superficial gas velocity ($v_{sg}$) were used as main factors. The power input per unit volume for the Rushton turbines was determined by the correlation given by Hughmark (1980). The following power-law equation of $k_La$ was used (Eq. 4.7) and the corresponding coefficient values (α, β, and γ) determined at different temperatures are presented in Table 4.12.

$$k_L a = \alpha (\frac{P_g}{V})^{\beta} (v_{sg})^{\gamma} \tag{4.7}$$

where

$$\frac{P_g}{P_{ug}} = 0.1[\frac{Q}{N_i V}]^{-0.25}[\frac{N_i^2 d_i^4}{g W_i V^{2/3}}]^{-0.2} \tag{4.8}$$

$$P_{ug} = N_P \rho N_i^3 d_i^5 \tag{4.9}$$

The experimental $k_La$ is shown as a parity plot with the predicted values as shown in Figures 4.17 and 4.18, where the conventional and the RSM-based models are compared. It can be seen from that the values predicted by original and simplified equations by RSM were observed to be close to each other. However, RSM yield higher accuracy than those by the conventional method. These observations can be further confirmed by the $R^2$ values. The calculated $R^2$ values for the original, simplified RSM-based models and power-law models for the single Rushton turbine system were 0.988, 0.982 and 0.877, respectively. Those for the dual Rushton turbine system were determined to be 0.992, 0.964 and 0.899, respectively.

Table 4.12 Power-law coefficients in Equation 4.7

| **Impeller Type** | **T, °C** | **α** | **β** | **γ** |
|---|---|---|---|---|
| Single Rushton | 10 | 0.0021 | 0.28 | 0.38 |
| | 25 | 0.0026 | 0.28 | 0.33 |
| | 40 | 0.0046 | 0.24 | 0.43 |
| Dual Rushton | 10 | 0.0021 | 0.32 | 0.38 |
| | 25 | 0.0017 | 0.34 | 0.39 |
| | 40 | 0.0018 | 0.37 | 0.42 |

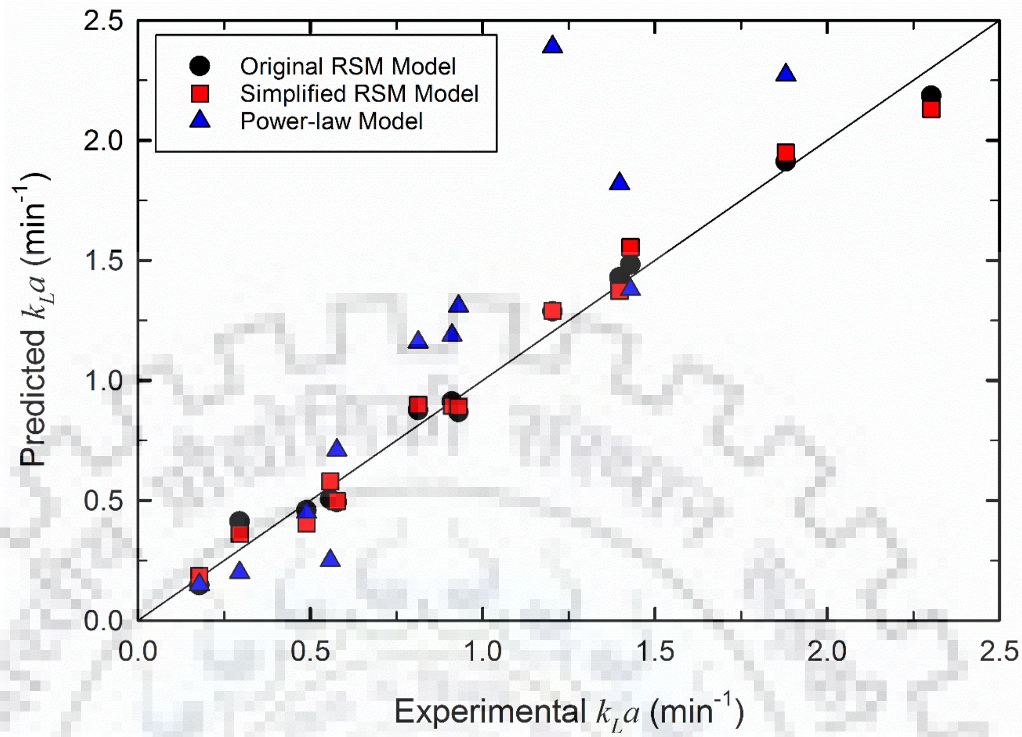


Figure 4.17. Parity plot for comparison between RSM-based and power-law models to predict $k_La$ in the single Rushton turbine system (N= 50-800 rpm, $Q_g$=0.5-3.5 L/min., T=10-40 °C)

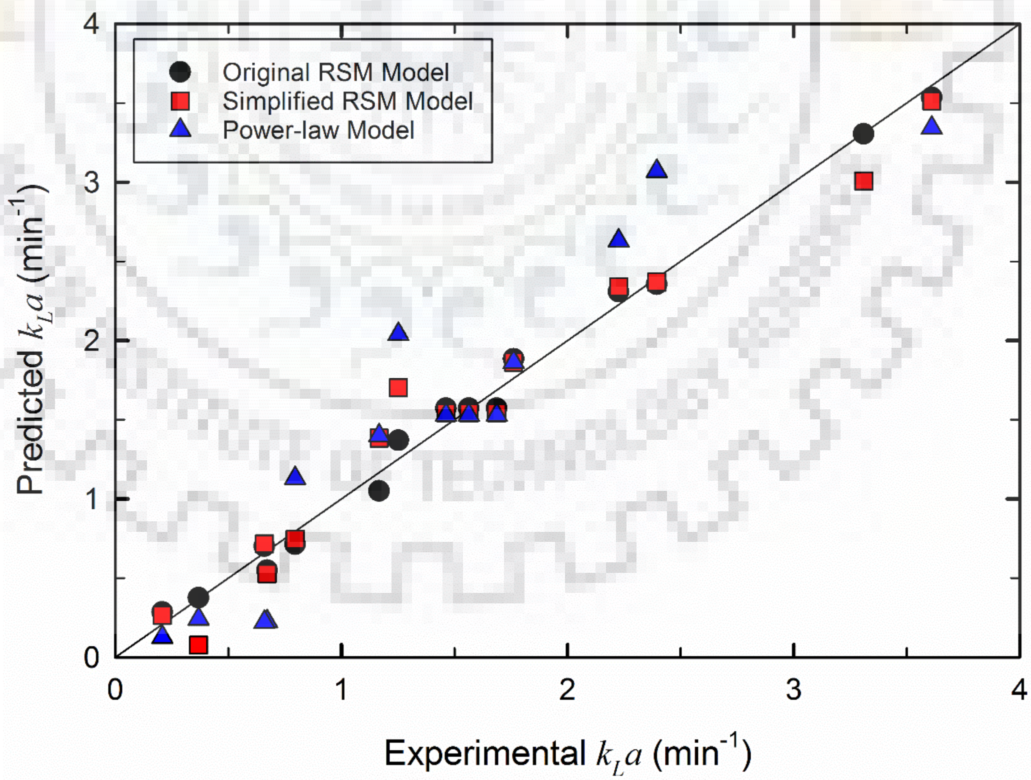


Figure 4.18. Parity plot for comparison between RSM-based and power-law models to predict $k_La$ in the dual Rushton turbine system ((N= 50-800 rpm, $Q_g$=0.5-3.5 L/min., T=10-40 °C)

### 4.5.2 Validation of Simplified Correlation by RSM

To validate the correlated equations by RSM, additional experiments were performed. The $k_La$ values were measured at the extreme combinations of the process factors (1, 1, 1), which are at the vertices of the experimental cubic space that are not included in their derivation (Table 4.13a). Additionally, to confirm the wide applicability of the equations, operating conditions which are within the range of each variable were chosen (Table 3.2 as mentioned in Chapter 3), but were not chosen from Table 3.4a as shown in Chapter 3 for design of experiments (Table 4.13b). The $k_La$ values can be determined directly from Eq. 4.6 along with the coefficient values in Table 4.11. As shown in Table 4.13, agreement between the experimental and the model predictions is satisfactory.

Table 4.13 Validation of simplified model by RSM

**(a) agitation rate = 800 rpm, air flow rate = 3.5 L/min, temperature = 40 °C**

| $k_La$ (min$^{-1}$) | Single Rushton | Dual Rushton | Pitched blade | Mixed turbine |
|---|---|---|---|---|
| Experimental | 2.395 | 4.307 | 3.420 | 4.621 |
| Predicted | 2.339 | 4.113 | 3.161 | 4.333 |
| Error (%) | 2.34 | 4.50 | 7.57 | 6.23 |

**(b) agitation rate = 600 rpm, air flow rate = 2.5 L/min, temperature = 30 °C**

| $k_La$ (min$^{-1}$) | Single Rushton | Dual Rushton | Pitched blade | Mixed turbine |
|---|---|---|---|---|
| Experimental | 1.4290 | 2.780 | 2.412 | 2.966 |
| Predicted | 1.4085 | 2.793 | 2.211 | 2.800 |
| Error (%) | 1.40 | 0.47 | 8.33 | 5.60 |

## 4.6 IMPELLER SPACING AND ITS EFFECT ON $K_LA$ AND $P/V_L$

It has been reported that mass transfer coefficient is affected by various parameters such as agitation rate, aeration rate, temperature, media properties (composition, viscosity, etc.) (Garcia-Ochoa et al., 2010). The spacing between impellers may also affect the flow patterns and thus oxygen transfer rate in stirred tank bioreactors. However, increase in the impeller spacing beyond certain level may create an ineffective agitation region between the adjacent impellers and thus may decrease the mass transfer (Dixit et al., 2015). On the other hand, the power input per unit volume ($P/V_L$) is a very important parameter for stirred tank reactors. It is an indispensable and one of the most used parameter for describing the hydrodynamics, mixing and mass transfer performance in stirred tank reactors. The power input per unit volume ($P/V_L$), also known as specific power input, is an important scaling-up parameter usually measured through the torque acting on the impeller shaft assembly under rotation. However, its experimental determination in small scale vessels is still a challenging task owing to frictional losses due to bearings and/or shaft seals. The specific power input is most commonly used as a scale-up criterion for stirred tank reactors as many engineering process parameters remain constant during scale-up (similar to mass transfer and shear stress conditions). This criterion has been proven for applications with cell culture and microorganisms. As a result, the measurement of the specific power input provides manufacturers and operators with valuable information in order to characterize the power capability of the stirred tank reactors.

In this study, an attempt has been made to study the effect of impeller spacing on $k_La$ and $P/V_L$ for dual Rushton and mixed impeller (Rushton-marine propeller) configurations in a stirred tank bioreactor. Although temperature also affects the mass transfer as studied previously using RSM, however, the present study has been carried out at 37 °C as it is most widely used for cell culture applications.

### 4.6.1 Rushton-Rushton Configuration

To study the effect of impeller spacing on $k_La$, an RSM-BBD study has been carried out considering three parameters viz. agitation and aeration rate and impeller spacing for Rushton-Rushton and Rushton-marine propeller configurations. The polynomial quadratic model based on ANOVA for Rushton-Rushton configuration in terms of actual factors is given by Eq. (4.10) as:

$$\begin{aligned} Y = &-1.4085 - 0.0011x_1 + 0.5283x_2 + 0.5183x_3 - 0.0004x_1x_2 \\ &- 4.86e-5x_1x_3 + 0.0341x_2x_3 + 6.58e-6x_1^2 - 0.1382x_2^2 - 0.0419x_3^2 \end{aligned} \tag{4.10}$$

where $x_1$, $x_2$ and $x_3$ are agitation rate, air flow rate and impeller spacing, respectively. The model has a probability value (p-value) of 0.0013, which is considered statistically significant if significance level is of the order of 0.05. The F-value of 11.83 indicated that the lack of fit is not significant. Three different response surface plots and their corresponding contour plots were generated using the developed model in order to understand the effects of interaction among the different variables on $k_La$. The response surface plots are generally used to predict the overall profile of the response by showing its nature as the fitted surface. However, it is difficult to find the levels of the variables with the help of response surface plots, and thus contour plots of $k_La$ were used to predict the response at each level.

Figure 4.19(i) shows the interaction between stirring and aeration rates at specific impeller spacing. It can be seen that at lower stirring rate, the $k_La$ value was small, and once the stirring rate was increased, $k_La$ value also enhanced. Conversely, in the case of aeration rate, $k_La$ was found to increase gradually with increasing aeration rate. Physically, it can be attributed to the breakage of the larger gas bubbles into smaller bubbles and thus gas-liquid interfacial area is increased for the mass transfer, resulting in an increase in the $k_La$ value. It can also be attributed to the higher gas hold-up and hence an increase in the $k_La$ values with increasing agitation rates. Similar observations can also be made from Figure 4.19(ii), which describes the dependence of $k_La$ on stirring rate and impeller spacing. It can be seen that $k_La$ increases with stirring rate, however, the effect of impeller spacing was not significant. Finally, Figure 4.19(iii) depicts the combined effect of air flow rate and impeller spacing on $k_La$ at specific stirring rate. As expected $k_La$ increases with an increase in the air flow rate, however, the effect of impeller spacing is insignificant. Other than the impeller spacing, the other two factors have been found to affect the $k_La$, however, the effect of stirring rate is more significant than air flow rate. The influence of linear, quadratic and interaction terms can be found from P-values as shown in Table 4.10. Considering the significance level of <0.05, effects of the linear ($x_1$, $x_2$), and the quadratic ($x_1^2$) term appears to be significant for $k_La$.

### 4.6.2 Rushton-Marine Propeller (Mixed Impeller) Configuration

When compared with single impeller configurations, it has been reported that the mixed impeller configurations producing radial and axial flow simultaneously deliver better mixing performance. In this work, a mixed impeller configured by Rushton turbine and marine propeller with Rushton turbine at the bottom and marine propeller at the top has been studied. The polynomial quadratic model based on the analysis of variance (ANOVA) for this configuration in terms of actual factors is given by Eq. (4.11) as:

$$\begin{aligned} Y = & -1.3195 + 0.0031x_1 + 0.7059x_2 + 0.3556x_3 - 0.0006x_1x_2 \\ & -0.0003x_1x_3 - 0.0171x_2x_3 + 2.44e-6x_1^2 - 0.0383x_2^2 - 0.0251x_3^2 \end{aligned} \tag{4.11}$$

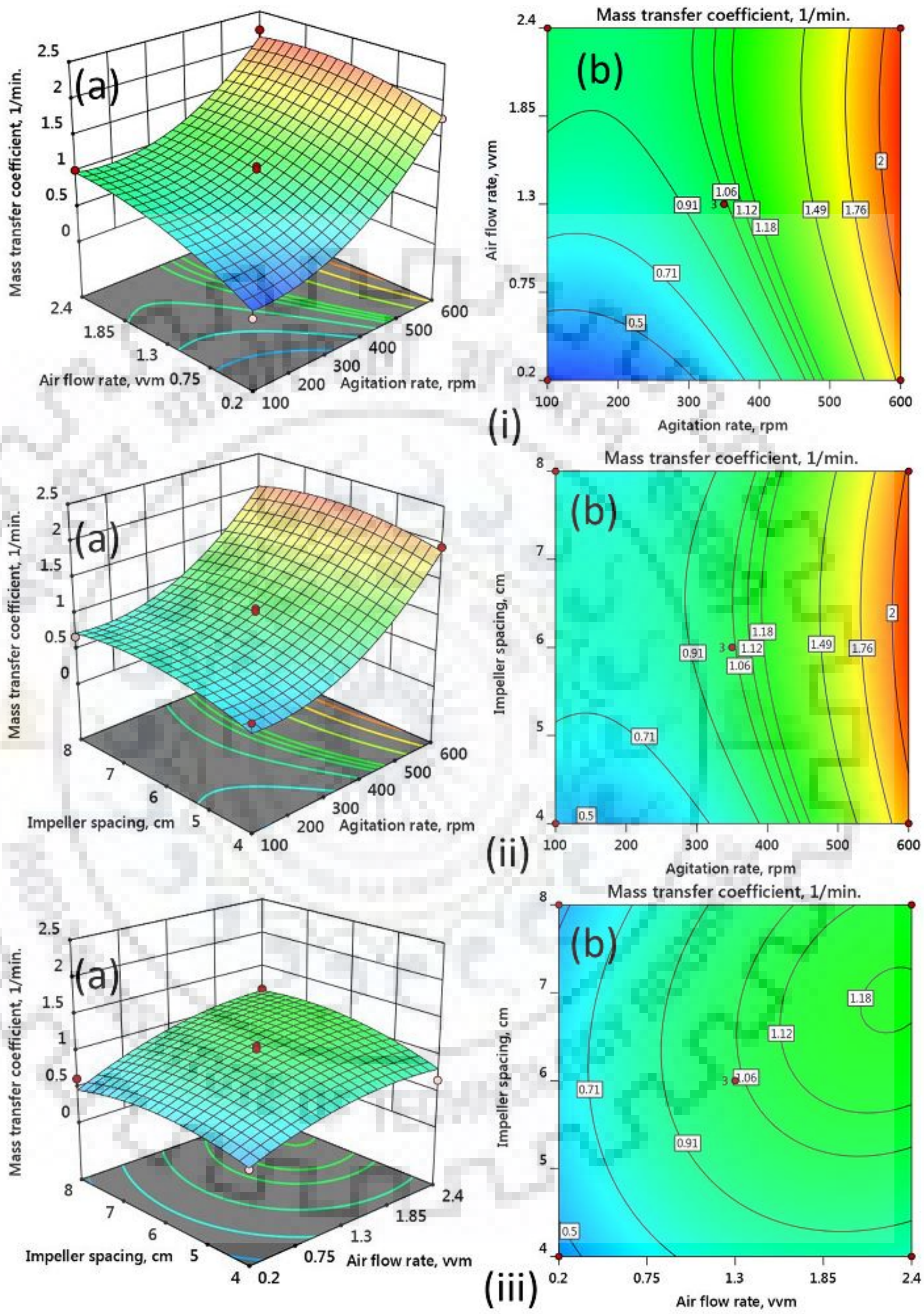


Figure 4.19. Influence of (i) stirring and air flow rates, (ii) stirring rate and impeller spacing and (iii) air flow rate and impeller spacing on $k_La$ for Rushton-Rushton configuration(a) 3D response surface plot; (b) 2D contour plot.

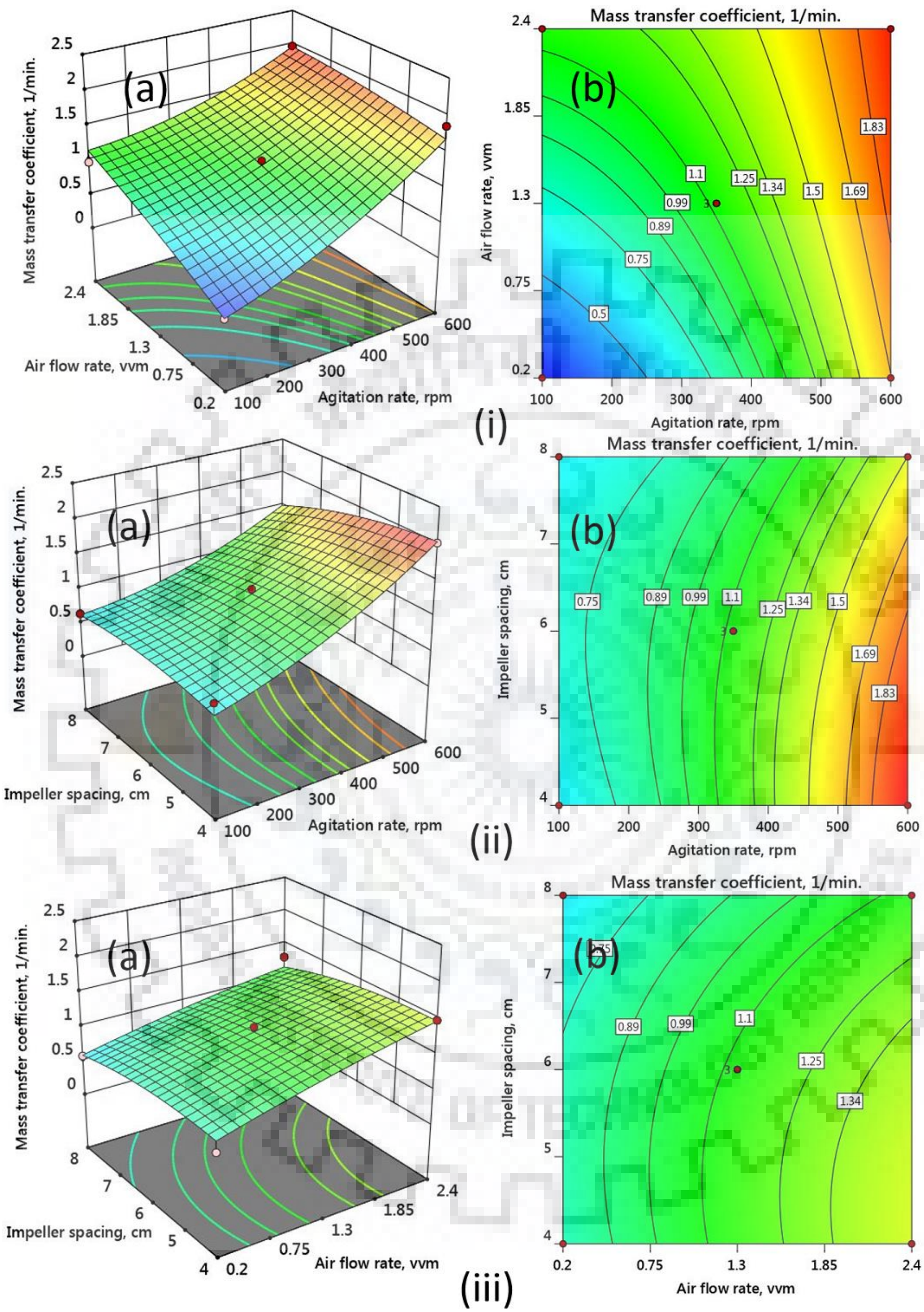


Figure 4.20. Influence of (i)stirring and air flow rates, (ii) stirring rate and impeller spacing and (iii) air flow rate and impeller spacing on $k_La$ for Rushton-marine propeller configuration(a) 3D response surface plot; (b) 2D contour plot.

The model has a p-value of 0.0058, which is statistically significant considering significance level of 0.05 (Table 4.11). Figure 4.20 shows the interactive effect of two independent variables on the response by keeping the third variable at middle level point from the surface and contour plots.

The influence of stirring and air flow rates can be observed from Figure 4.20(i). As can be seen from the surface and the corresponding contour plot, $k_La$ increases with increasing both the stirring and air flow rates. Physically, it can be attributed to the breakage of the larger gas bubbles into smaller bubbles and thus gas-liquid interfacial area is increased for the mass transfer, resulting in an increase in the $k_La$ value. It can also be attributed to the higher gas hold-up and hence an increase in the $k_La$ values with increasing agitation rates. Figure 4.20(ii) shows the effect of the stirring rate and impeller spacing on $k_La$ when air flow rate was maintained at 1.3 vvm. Again it was found that $k_La$ increases with increasing stirring rate, however, the effect of impeller spacing was not found that significant. The combined effect of air flow rate and impeller spacing on $k_La$ when stirring rate is kept at 350 rpm is shown in Figure 4.20(iii). It can be seen that $k_La$ increases with increasing the air flow rate, however, the effect of impeller spacing is again found insignificant. It was confirmed by the corresponding p-values (Table 4.11) of $x_1$, $x_2$ and $x_3$ for mixed-impeller configuration (0.0003, 0.0049, and 0.1024, respectively). Among the studied impeller configurations, Rushton-Rushton configuration demonstrated the highest $k_La$ value followed by mixed (Rushton-marine propeller) configuration. However, for the bioprocesses such as cell culture applications in stirred tank bioreactors, the power number of the impeller is an important parameter to be considered as high shear force can be detrimental for the cells.

Further, it has also been reported that, axial impellers such as marine propellers have been most widely used for shear-sensitive cells owing to their low power number as compared to the radial impellers such as Rushton type. Therefore, it is likely that mixed impellers may be most suitable for cell culture applications.

### 4.6.3 Simplification of the RSM Model for $k_La$

A model equation (Eq. 4.11) was developed using RSM, for both impeller configurations. High correlation coefficient suggests that the experimental $k_La$ has been successfully correlated by the model developed, as shown by the ANOVA analysis (Tables 4.10-4.11). However, Eqs. 4.10 and 4.11 with 10 coefficients are relatively complicated as compared to traditional empirical power-law correlations. Therefore, a simplified correlation need to be developed for predicting $k_La$ for different parameters (independent variables) considered. As can be observed from Tables 4.10-

4.11, several source terms (e.g. $x_i$, $x_ix_j$, $x_i^2$) have p-values >0.05, which implies that such terms are not significant for $k_La$ prediction. Therefore, the correlation model (Eq. 4.11) was simplified by omitting insignificant terms. For Ruston-Rushton configuration, the original equation (Eq. 4.11) was simplified by omitting the terms $x_1x_2$, $x_2x_3$, $x_1x_3$, $x_3$, $x_2^2$, and $x_3^2$ (Table 4.10). Similarly, for Rushton-marine propeller configuration (Table 4.11), the original equation is simplified by cancelling the insignificant terms such as $x_1x_2$, $x_2x_3$, $x_1x_3$, $x_3$, $x_1^2$, $x_2^2$, and $x_3^2$. After omitting the insignificant terms, there was significant reduction in number of coefficients from 10 to 2-3, and new coefficient values were predicted. It was observed that $R^2$ values changed slightly even after removing the insignificant terms. Figure 4.21 shows the experimental and predicted $k_La$ values for both configurations, which also include the predicted $k_La$ values obtained from the RSM based models with all coefficients. It was found that values predicted by original and simplified equations using RSM were fairly in good agreement, therefore suggesting that $k_La$ can also be correlated by the simplified model equations. The simplified equation for dual Rushton turbine and mixed impellers (Rushton-marine propeller) is given by Eq. 4.12 and 4.13, respectively.

$$Y = 0.455 - 2.19e-3 * x_1 + 0.241 * x_2 + 6.96e-6 * x_1^2 \tag{4.12}$$

$$Y = 0.037 + 2.31e-3 * x_1 + 0.283 * x_2 \tag{4.13}$$

### 4.6.4 Optimization of the Operating Parameters for $k_La$

The optimum value of each operating parameter that resulted in the maximum response (volumetric mass transfer coefficient) was estimated using the regressed polynomial equation obtained using RSM model. Figure 4.22 shows the optimum values of the operating parameters for the Rushton-Rushton and mixed impeller (Rushton-marine propeller) configurations. The optimum values for agitation rate, air flow rate and impeller spacing were found as 600 rpm, 1.91 vvm and 6.61 cm, respectively for the Rushton-Rushton, and 600 rpm, 1.67 vvm and 4.83 cm, respectively, for Rushton-marine propeller configurations.

### 4.6.5 Power Consumption for Rushton-Rushton Configuration

Power input per unit volume is a very important parameter in STBRs as it is an indispensable and one of the most used parameter for describing the hydrodynamics, mixing and mass transfer performance in STBRs. Thus, an attempt has been made to study the effect of key operating parameters such as agitation and aeration rate and impeller spacing on power input per unit volume

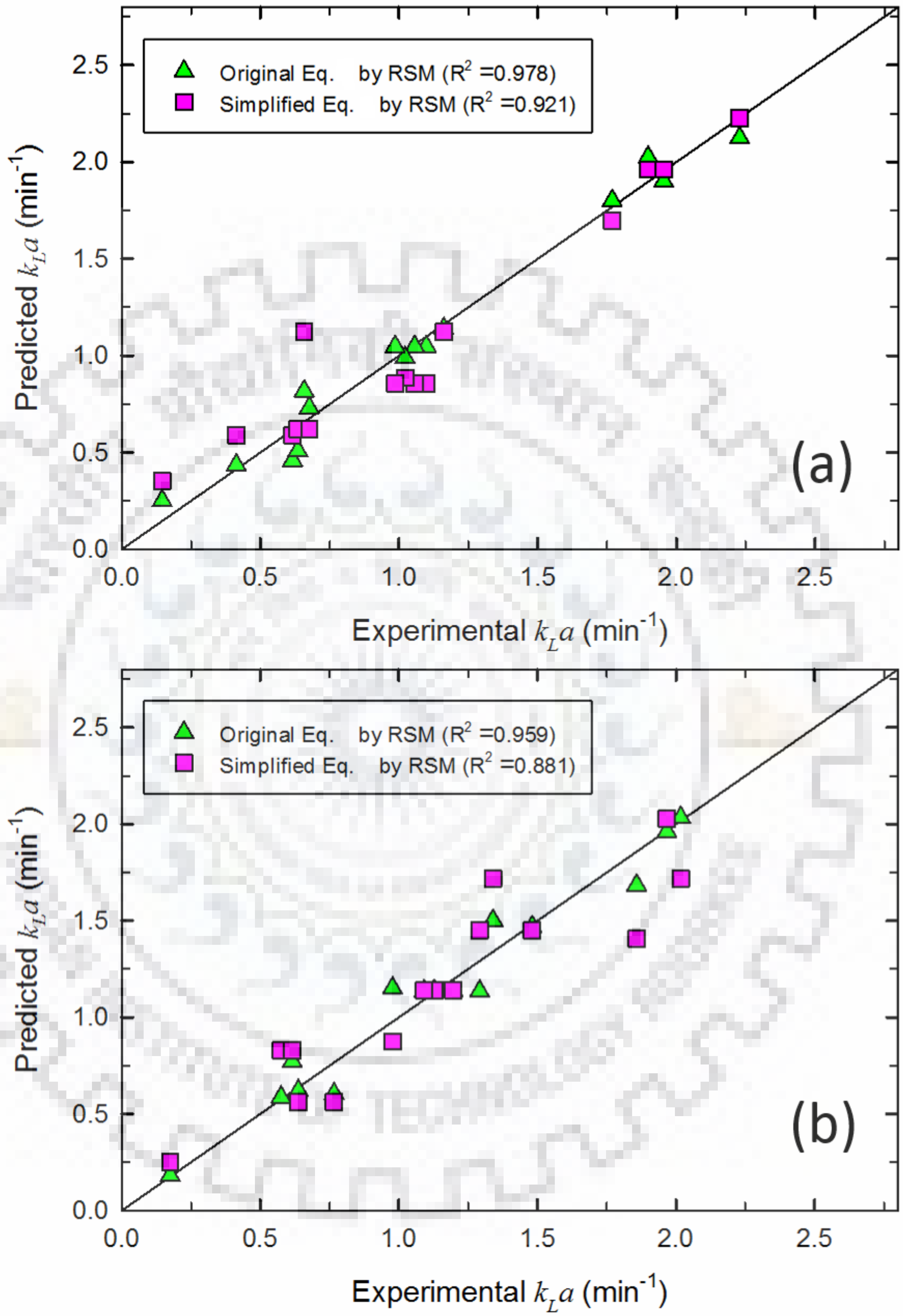


Figure 4.21. Experimental vs predicted $k_La$ comparison (i) Rushton-Rushton configuration, and (ii) Rushton-Marine propeller for RSM based models (N= 100-600 rpm, $Q_g$=1-12 L/min., T=37 °C)

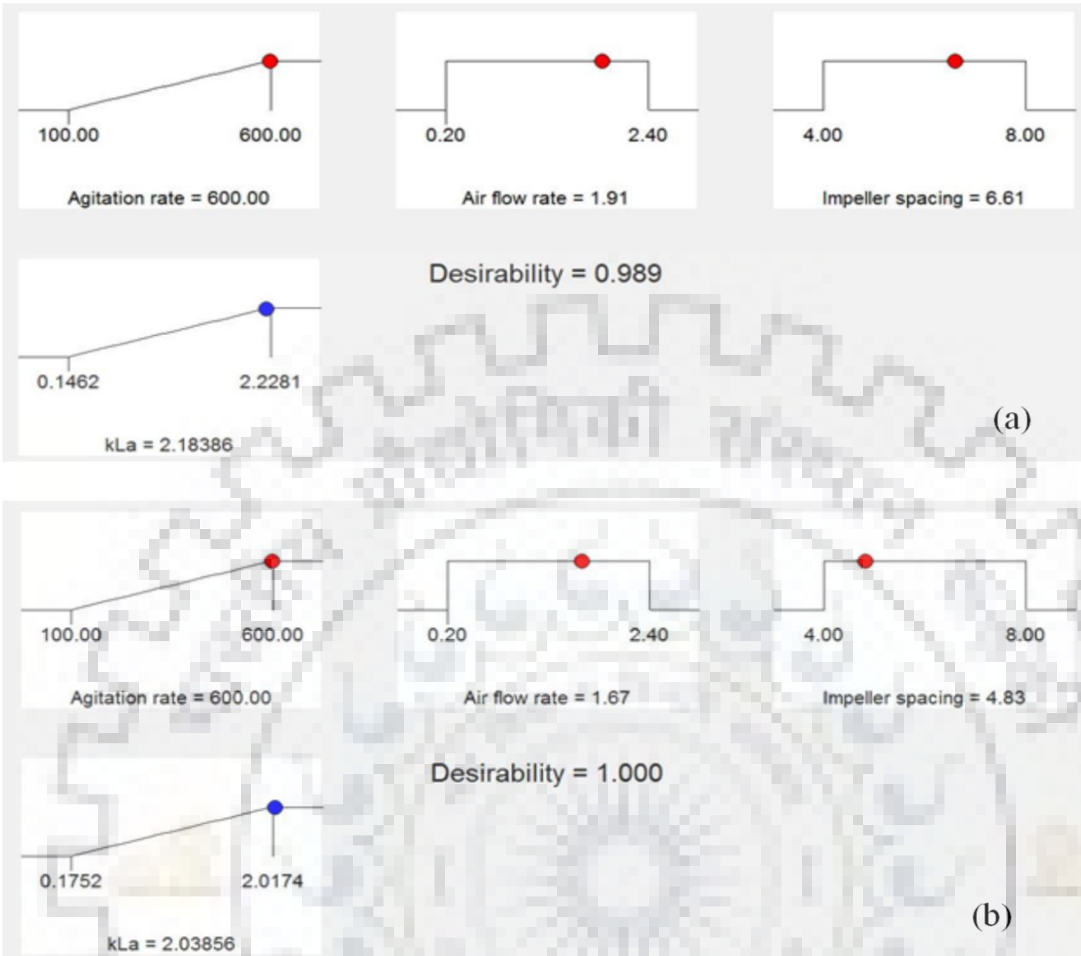


Figure 4.22. Optimum values of the operating parameters for (a) Rushton-Rushton, and (b) Rushton-marine propeller configurations

($P/V_L$) by using Box-Behnken design approach. The polynomial quadratic model based on ANOVA for Rushton-Rushton configuration in terms of actual factors is given by Eq. (4.14) as:

$$
\begin{aligned}
Y = {} & 0.341 - 3.67e-3x_1 + 0.2059x_2 - 0.041x_3 - 3.82e-4x_1x_2 \\
& + 2.77e-4x_1x_3 - 2.73e-3x_2x_3 + 6.76e-6x_1{}^2 - 0.038x_2{}^2 - 6.04e-4x_3{}^2
\end{aligned}
\tag{4.14}
$$

The response surface plots and their corresponding contour plots for the Rushton-Rushton configuration, which provide the variation of power input per unit volume with experimental variables at each level, are shown in Figure 4.23. Figure 4.23 also present the interactive effect of two independent variables on the response by maintaining the third variable at middle level point. The effect of stirring and air flow rates on power input per unit volume when impeller spacing is maintained at 6 cm can be seen from Figure 4.23(i). As expected, the power input per unit volume increased with an increase in the stirring rate, however, the effect of air flow rate was found to be insignificant. Similarly, Figure 4.23(ii) shows the effect of the stirring rate and impeller spacing on power input per unit volume when air flow rate was maintained at 1.3 vvm. Again it can be observed that power input per unit volume increases with increasing stirring rate, however, the effect of impeller spacing is insignificant. Finally, Figure 4.23(iii) depicts the combined effect of air flow rate and impeller spacing on $k_La$ when stirring rate is kept at 350 rpm. It can be observed that power input per unit volume decreases with increasing the air flow rate, however, it is found to gradually increase with an increase in the impeller spacing. Other than the air flow rate, other two factors have been found to affect the $k_La$, however, the effect of stirring rate is more significant than impeller spacing. The influence of linear, quadratic and interaction terms can be found from p-values, as shown in Table 4.8. Considering the significance level of <0.05, effects of the linear ($x_1$), the quadratic of stirring rate ($x_1^2$), the interaction effect of stirring rate and impeller spacing ($x_1x_3$) appear to be significant for power input per unit volume.

### 4.6.6 Power Consumption for Mixed Impeller Configuration

The polynomial quadratic model based on ANOVA for this configuration in terms of actual factors is given by Eq. (4.15) as:

$$\begin{aligned} Y = & -0.049 - 2.30e-3x_1 - 0.118x_2 + 0.0945x_3 - 1.31e-4x_1x_2 \\ & + 3.30e-5x_1x_3 + 0.0114x_2x_3 + 6.75e-6x_1^2 + 0.027x_2^2 - 9.06e-3x_3^2 \end{aligned} \tag{4.15}$$

Considering this case, it can be found that the stirring rate has the dominant effect on power input per unit volume (Figure 4.24). However, when considering the interactive effect of air flow rate and impeller spacing, it can be observed that power input per unit volume decreases with increasing air flow rate and at the same time increases very slightly with increasing impeller spacing (Figure 4.24(iii)). This decrease in the power input may be due to the fact that the aeration has the effect of lowering the liquid viscosity as compared to the ungassed systems. The decrease in the power consumption may be due to the formation of cavities behind the impeller blades and different density of fluid under gassed and ungassed conditions (Van't Riet and Smith, 1973). From the RSM analysis, it was observed that air flow rate is significant for mixed impeller configuration, which may be attributed to the fact that the mixed impeller provides both the radial and axial mixing inside the reactor thus leading to an overall improvement in mixing inside the reactor.

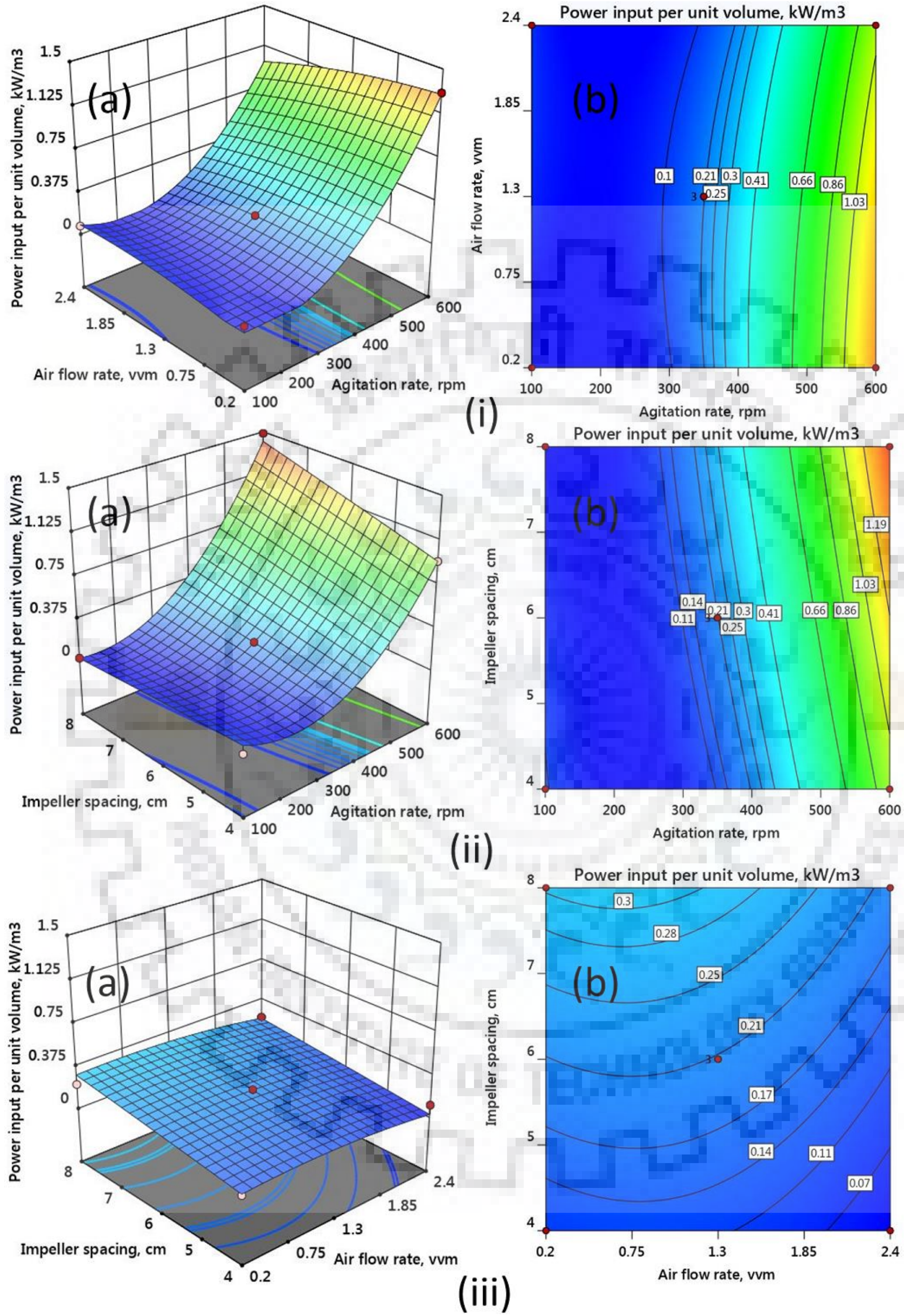


Figure 4.23. Influence of (i) stirring and air flow rate, (ii) stirring rate and impeller spacing, and (iii) air flow rate and impeller spacing on power input per unit volume for Rushton-Rushton configuration (a) 3D response surface plot; (b) 2D contour plot.

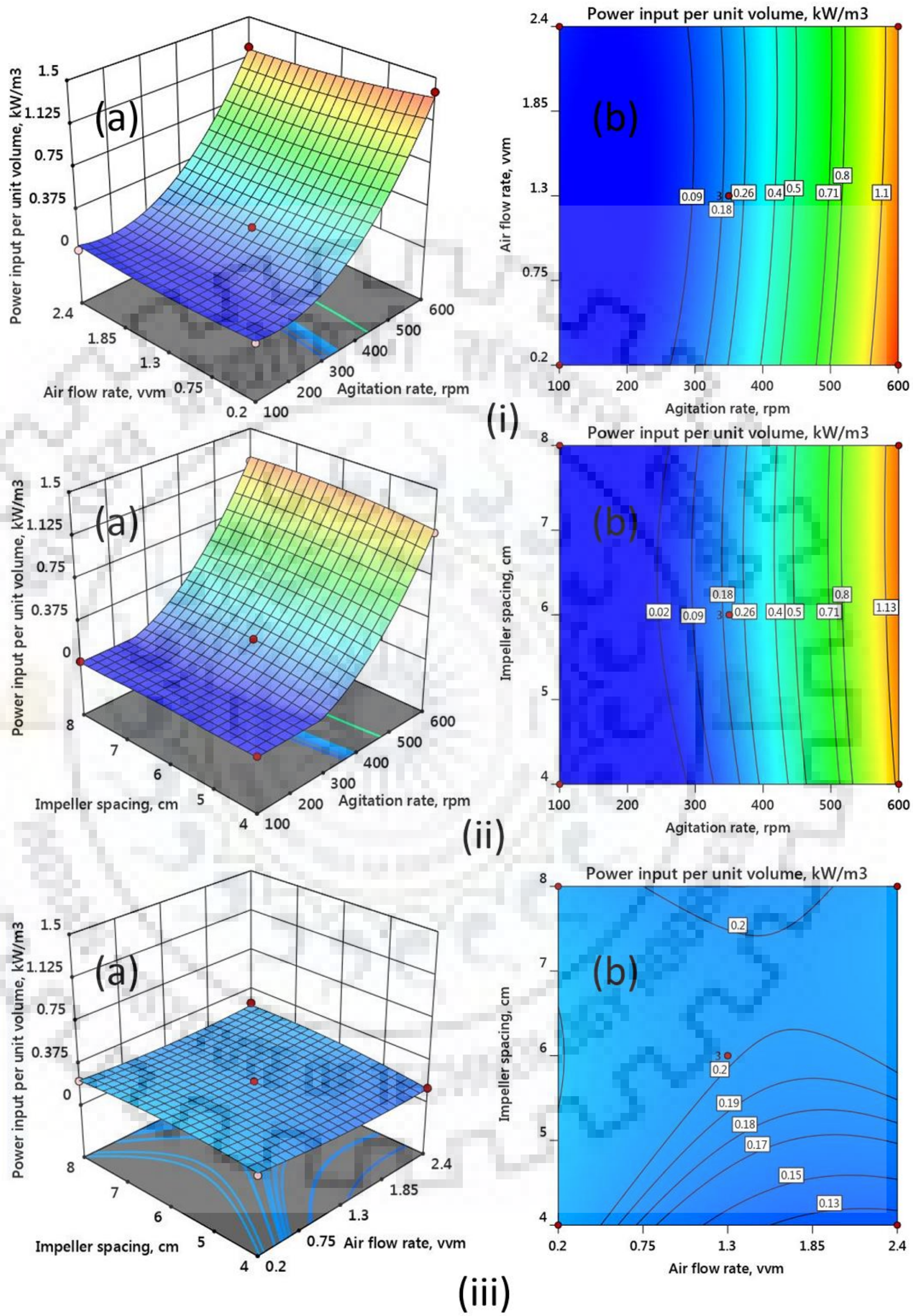


Figure 4.24. Influence of (i) stirring and air flow rate, (ii) stirring rate and impeller spacing, and (iii) air flow rate and impeller spacing on power input per unit volume for Rushton-marine propeller configuration (a) 3D response surface plot; (b) 2D contour plot.

### 4.6.7 Simplification of the RSM Model for $P/V_L$

A model equation (Eqs. 4.14 and 4.15) was developed for $P/V_L$ using RSM, for both the impeller configurations. High correlation coefficients were observed which implies that the experimental $P/V_L$ has been successfully correlated by the model developed, as shown by the ANOVA analysis (Tables 4.18-4.9). However, Eqs. 8 and 9 with 10 coefficients are relatively complicated as compared to traditional empirical correlations. Therefore, a simplified correlation need to be developed for predicting $P/V_L$ for different parameters (independent variables) considered. As can be observed from Tables 4.12-4.13 several source terms (e.g. $x_i$, $x_ix_j$, $x_i^2$) have p-values >0.05 which implies that such terms are not affecting the $P/V_L$ prediction. Therefore, the correlation model (Eq. 4.14 and 4.15) was simplified by omitting such terms. After omitting the insignificant terms, there was significant reduction in number of coefficients from 10 to 4-5, and predicted the new coefficient values. It was observed that the $R^2$ values changed very slightly even after removing the insignificant terms. The simplified equation for dual Rushton turbine and mixed impeller (Rushton-marine propeller) is given by Eqs. 4.14 and 4.15, respectively.

$$Y = 0.545 - 4.21e-3 * x_1 - 0.052 * x_3 + 2.77e-4 * x_1 * x_3 + 6.82e-6 * x_1^2 \tag{4.16}$$

$$Y = 0.1697 - 2.28e-3 * x_1 + 6.75e-6 * x_1^2 \tag{4.17}$$

Figure 4.25 shows the experimental and predicted $P/V_L$ values for both configurations, which also include the predicted $P/V_L$ values obtained from the RSM based models with all the coefficients. It can be seen that values predicted by original and simplified equations using RSM were fairly in very good agreement, therefore suggesting that $P/V_L$ can also be correlated by the simplified model equations. Further, a comparison has been made between RSM developed correlations (both original and simplified) for dual Rushton turbine configuration for calculating power input per unit volume with correlations available in the literature by Hughmark (1980) and Cui et al. (1996). Both original and simplified RSM developed correlations better predicted $P/V_L$ when compared with existing empirical correlations, as shown in Figure 4.25.

### 4.6.8 Power-law Correlations and a Comparison

Several methods such as power-law, dimensionless correlations, etc. have been developed to determine the mass transfer coefficient in stirred tank bioreactors (Labik et al., 2017; Garcia-Ochoa et al., 2009; Moucha et al., 2012). Among the methods, correlations in the form of power-law are mostly used since they are easy to develop and most widely used (Karimi et al., 2013; Xie

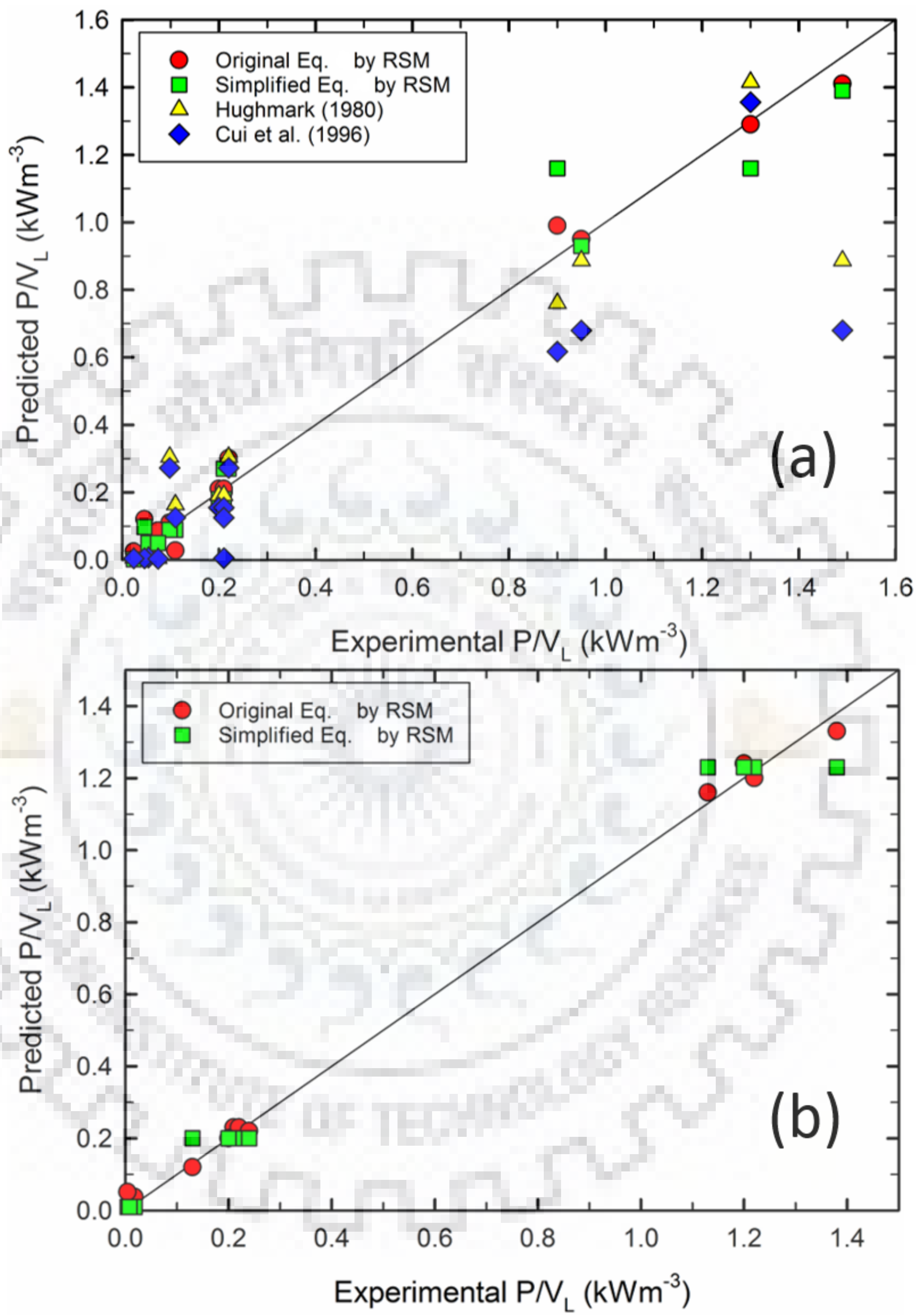


Figure 4.25 Experimental vs predicted $P/V_L$ comparison for (a) Rushton-Rushton, and (b) Rushton-marine propeller configurations (N= 100-600 rpm, $Q_g$=1-12 L/min.)

et al., 2014). From the RSM analysis, it was observed that impeller spacing has a negligible effect on the volumetric mass transfer coefficient and power-input per unit volume, thus the power-law correlation was developed by taking the power input per unit volume ($P/V_L$) and superficial gas velocity ($v_{sg}$) as the main factors. The superficial gas velocity was calculated using Eq. (4.18) (Xu et al., 2017), as follows:

$$v_{sg} = \frac{4Q}{\pi D_t^2} \tag{4.18}$$

where Q is the air flow rate (L/min.) entering the reactor and $D_t$ (m) is the reactor diameter. The power-law correlations for $k_La$ were developed for dual Rushton and mixed impeller configurations are given by Equations (4.19) and (4.20), respectively:

$$k_La = 0.006\left(\frac{P}{V_L}\right)^{0.39} (v_{sg})^{0.18} \tag{4.19}$$

$$k_La = 0.0001\left(\frac{P}{V_L}\right)^{0.56} (v_{sg})^{0.31} \tag{4.20}$$

The experimental $k_La$ is shown as a parity plot with the predicted values shown in Figure 4.26 and it can be observed that there is a close agreement between the experimental and predicted $k_La$ values. These results can be further confirmed by the $R^2$ values. The calculated $R^2$ values for dual Rushton and mixed impellers configuration were 0.91 and 0.95, respectively.

Power-law correlations were proposed for both dual Rushton turbine and the mixed impeller (Rushton + marine propeller) configurations and for dual Rushton turbine were compared with the correlations already available in the literature (Smith et al., 1977; Van't Riet, 1979; Hickman, 1988 Zhu et al., 2001) (Figure 4.27). For mixed impeller configuration there are no correlations available in the literature, hence developed first time. Different power-law correlations available literature for dual Rushton turbine with operating conditions are reported in Table 4.14. Except for few data points, the correlations are largely well able to predict the $k_La$, and it may be possibly due to the different size of the reactor system. It has also been observed that the power-law correlation by Van't Riet (1979) is better able to predict the $k_La$ for the present system and thus showing its wide applicability for $k_La$ estimation in stirred tank bioreactors. A previously developed response surface methodology (RSM) model, both original and simplified in this chapter has also been applied in this study and have been found to well predict the $k_La$. The RSM developed correlations have an advantage that it is directly in terms of the variables such as agitation rate, aeration rate, temperature and impeller spacing and hence there is no need for calculating the power input per unit volume ($P/V_L$) for the system. Overall, it can be concluded that the correlations are well able to predict the $k_La$ and $P/V_L$ in the present study.

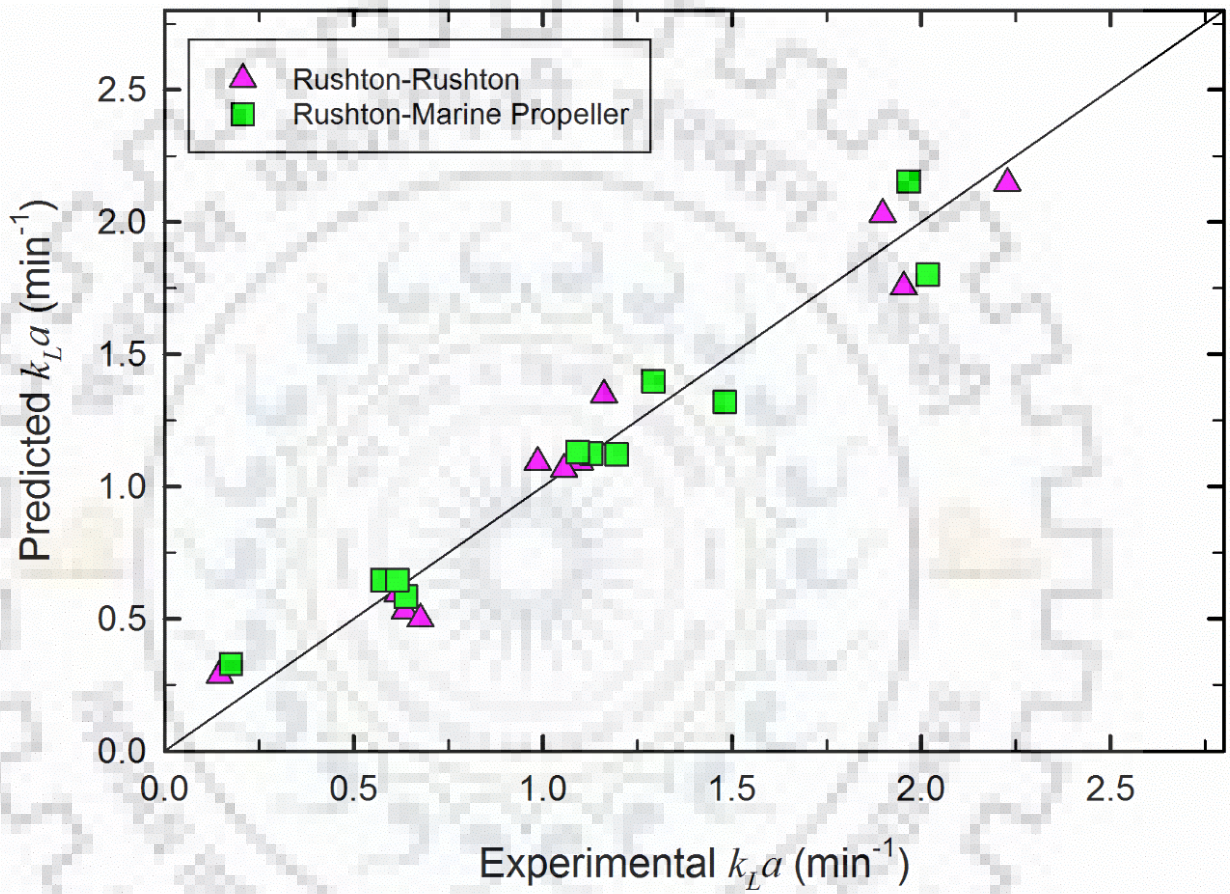


Figure 4.26 Experimental vs predicted $k_La$ for different impeller configurations using power-law correlations (N= 100-600 rpm, $Q_g$=1-12 L/min., T=37 °C)

Table 4.14 Various mass transfer coefficient correlations for stirred tank bioreactors

| **Impeller type** | **$k_La$ correlation** | **$D_t$, m** | **Sparger type** | **D, m** | **N, rev/s** | **$u_{sg}$, m/s** | **Authors** |
|---|---|---|---|---|---|---|---|
| 6DT | $k_La = 0.026\left(\frac{P_g}{V}\right)^{0.4}(u_{sg})^{0.5}$ | 0.50 | Orifice | 0.166 | -- | $5\times10^{-3}$-$4\times10^{-2}$ | Van't Riet (1979) |
| 6DT | $k_La = 0.031\left(\frac{P_g}{V}\right)^{0.4}(u_{sg})^{0.5}$ | 0.39 | Ring | 0.13 | -- | $1\times10^{-3}$-$7.5\times10^{-3}$ | Zhu et al. (2001) |
| 6DT | $k_La = 0.01\left(\frac{P_g}{V}\right)^{0.475}(u_{sg})^{0.4}$ | 0.61, 0.91 & 1.83 | Pipe | 0.20, 0.30, 0.67 and 0.91 | 0.9-8.5 | $4\times10^{-3}$-$4.6\times10^{-2}$ | Smith et al. (1977) |
| 6DT | $k_La = 0.043\left(\frac{P_g}{V}\right)^{0.4}(u_{sg})^{0.57}$<br>$k_La = 0.027\left(\frac{P_g}{V}\right)^{0.54}(u_{sg})^{0.68}$ | 0.60 & 2 | -- | 0.2 & 0.66 | -- | $2\times10^{-3}$-$1.7\times10^{-2}$ | Hickman et al. (1988) |
| 6DT (dual) | $k_La = 0.006\left(\frac{P_g}{V}\right)^{0.39}(u_{sg})^{0.18}$ | 0.18 | Ring | 0.06 | 0.833-13.33 | $1.06\times10^{-3}$-$7.42\times10^{-3}$ | Present study |

## 4.7 SUMMARY

The main objective of this chapter was to discuss the volumetric mass transfer coefficient for different impeller configurations in stirred tank bioreactors of different volumes (7.5 L, 5 L and 1 L). The effect of different parameters such as agitation rate, air flow rate, liquid volume inside the bioreactor, liquid viscosity, impeller diameter on the volumetric mass transfer coefficient was also reported. It was found that the volumetric mass transfer coefficient increases with increase in the agitation rate and air flow rate, and impeller diameter however the agitation rate impacts the mass transfer more than the air flow rate. It was also observed that with increase in volume and viscosity of the medium inside the bioreactor, $k_La$ was found to decrease. Further, the on $k_La$ values was reported different impeller configurations such as single and dual Rushton, pitched blade, marine propeller and mixed impeller considering different reactor volumes. Among the investigated impeller configurations, the dual Rushton turbine demonstrated the highest value of $k_La$. Empirical correlations have been developed for single and dual Rushton turbines for all the three bioreactors and it is observed that there is a good agreement between the experimental and predicted $k_La$. The volumetric mass transfer coefficient ($k_La$) of oxygen and power input per unit volume ($P/V_L$) were evaluated in a stirred tank bioreactor with an air-water system for the purpose of proposing new empirical correlation. The effects of various operating variables (e.g. agitation rate, air flow rate, temperature and impeller spacing) on $k_La$ and $P/V_L$ were investigated for different impeller configurations. The effect of impeller spacing on $k_La$ and $P/V_L$ was found to be insignificant. Taking account of both $k_La$ value and shear force generated by agitation, however, the pitched blade impeller and mixed impeller (Rushton + marine propeller) appears to be most effective for aerobic fermentation and cell culture applications. The lower values of $P/V_L$ for mixed impeller (Rushton + marine propeller) have also suggested its wide applicability in the bioprocess applications.

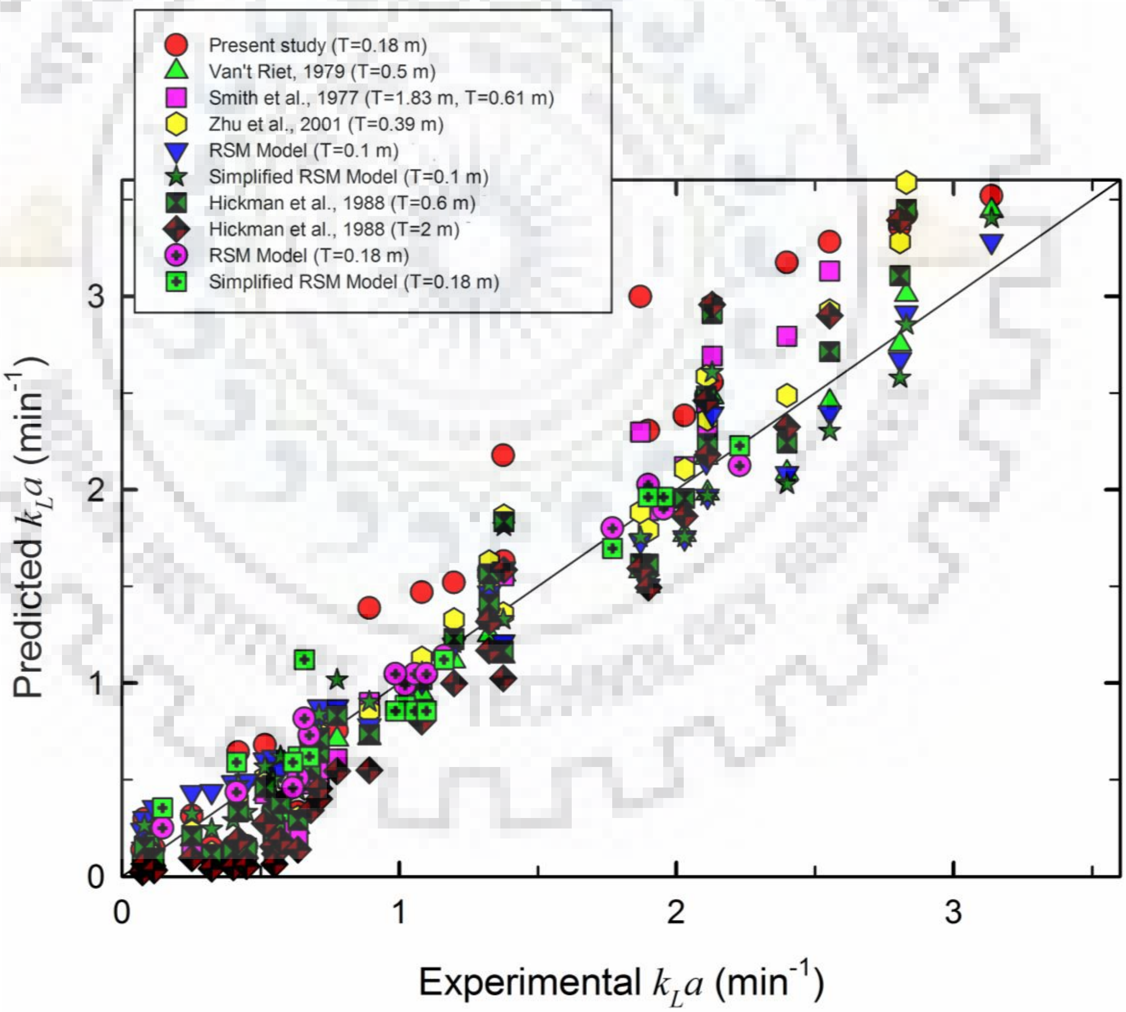


Figure 4.27 Comparison of experimental vs predicted $k_La$ for different stirred tank bioreactors (N= 50-800 rpm, $Q_g$=0.5-3.5 L/min., T=25 °C)

# CHAPTER 5

# MASS TRANSFER AND RHEOLOGY FOR *E. Coli* BL21

## 5.1 GENERAL

In this chapter, the effect of various key operating variables such as agitation (50–600 rpm) and aeration rates (0.5–2 L/min.), impeller diameter (0.04–0.05 m), and bioreactor working volume (0.25–0.75 L) for different impellers (Rushton turbine and pitched blade) and their different configurations on the volumetric mass transfer coefficient ($k_La$) have been investigated in a stirred tank bioreactor with cultivating *Escherichia coli*. All experiments, in the presence of cell culture were performed in the 1 L reactor. Finally, using dimensional analysis, the $k_La$ for different impeller configurations was correlated in the form of dimensionless groups, suggesting that this approach can be used for predicting $k_La$ in different scales of stirred tank bioreactors.

## 5.2 INTRODUCTION

The design of reactors is determined by various factors such as operating conditions, physical and chemical properties of components taking part in, mass and heat transfer, control and maintenance of processes, and safety. Among the reactor types, stirred tank bioreactors are one of the most commonly used reactors in the industry due to their simple design, effective mixing, and flexible operation (Naumann, 2008; Jossen et al., 2017). In the multiphase stirred tank bioreactors, design and configuration of impeller and baffle are important aspects to improve their mass transfer efficiency (Dhanasekharan et al., 2005; Kerdouss et al., 2008). Particularly in aerobic bioprocesses, the oxygen transfer is one of the fundamental characteristics to optimize the processes (Arrura et al., 1990; Garcia-Ochoa et al., 2000; Liu et al., 2006; Karimi et al., 2013). Mounsef et al. (2015) and Tervasmaki et al. (2016) studied the effect of agitation and aeration rates on $k_La$ for *Bacillus thuringiensis kurstaki* and *Pichia pastoris*, respectively. It was reported that $k_La$ increased with both agitation and aeration rates. It is noteworthy that oxygen transfer in the stirred tank reactor is also significantly influenced by the design and configuration of the impeller. In this context, it is important to understand the effect of impeller design and operating parameters on $k_La$ in the presence of cells.

Understanding the flow and mixing characteristics of particulate suspensions is essential in many industrial processes: food processing, polymer manufacturing, coating/deposition, and pharmaceutical processing (Apostolidis & Beris, 2016). When a molecule is suspended in a fluid, the viscosity of the fluid is influenced as a result of the hydrodynamic interactions (Einstein, 1906; Sklodowska et al., 2018). In bioprocesses with biological organisms, for instance, its proliferation influences the viscosity of the liquid medium. Cells in suspension may have viscous nature and thus affects the mass transport properties leading to poor oxygen transfer due to difficulty in mixing (Oolman et al., 1986; Olsvik & Kristiansen, 1994; Gibbs et al., 2000; Nevalainen et al., 2005). Therefore, rheological studies dealing with flow behaviors are vital for understanding mass transfer in cell cultivation applications because the cells in the medium may be sensitive to shear stress.

Once a process is demonstrated in the laboratory scale with cell culture, it must be translated into a larger scale. Scaling up from laboratory scale to a full production scale is challenging because the processes in both scales generally behave differently (Cybulski, 2001; Wood Black, 2014). In small laboratory equipment, almost perfect and uniform mixing is available in a relatively short time. In large reactors, however, stirrers are usually rotated slower than those in the laboratory because of a high cost of energy. Consequently, mixing conditions in production-scale reactors are usually worse than in laboratory-scale reactors. Unfortunately, there is no general procedure to translate directly from the laboratory to industrial production scales. Currently, scale-up is mostly based on geometric similarity, thumb rules, and empirical correlations (Nauha et al., 2015; Bashiri et al., 2016). Generally, the values of parameters in reactor systems are quantitatively defined based on concepts of physical phenomena (i.e., density, velocity, viscosity, flow rate, etc.) as time, length, mass, energy, temperature, and many other arbitrarily chosen entities. However, it is almost impossible to find correlations of all parameters and relationships between each of them. Such correlations are applicable only to respective systems and range of operating conditions (Sideman et al., 1966). For these reasons, effective and systematic approaches are required to define system dimensions for successful scale-up. Dimensional analysis is a method to reduce the number of experimental variables influencing a physical phenomenon by correlating them to form a set of dimensionless groups (Johnstone and Thring, 1957; Islam and Lye, 2009; Shen et al., 2014). By reducing complex physical problems to the simplest (more economical) form, it eventually presents a quantitative solution. The dimensional analysis offers several benefits: (1) reduction of the number of factors to be considered, (2) the analytical insights into the relations among variables generated, and (3) scalability of the results (Islam and Lye, 2009; Shen et al.,2014).

## 5.3 EFFECT of DIFFERENT PARAMETERS ON $k_La$

### 5.3.1 Effect of Agitation and Aeration Rates on $k_La$

It is well known that the $k_La$ values are influenced by various operating parameters and reactor properties. In the absence of cells, it was already observed that the $k_La$ increases with increasing agitation rate, air flow rate, and temperature in (Chapter 4). Among the operating parameters, impeller agitation and air flow rates are major factors influencing the $k_La$ values in a stirred tank reactor and thus dictating the overall power dissipation for the impeller. Figure 5.1 shows the effect of agitation and aeration rates on the $k_La$ for different impeller configurations in the presence of cells. As expected, $k_La$ increased with both agitation and aeration rates. With increasing agitation rate, it can be attributed to the breakage of the larger gas bubbles into smaller bubbles and thus the gas-liquid interfacial area is increased for the mass transfer, resulting in an increase in the $k_La$ values. As the air flow rate increases, gas hold-up inside the reactor increases and hence the interfacial area of the bubbles, which consequently leads to an increase in the $k_La$. The presence of gas bubbles also induces turbulence to the liquid medium and hence increases mass transfer rates.

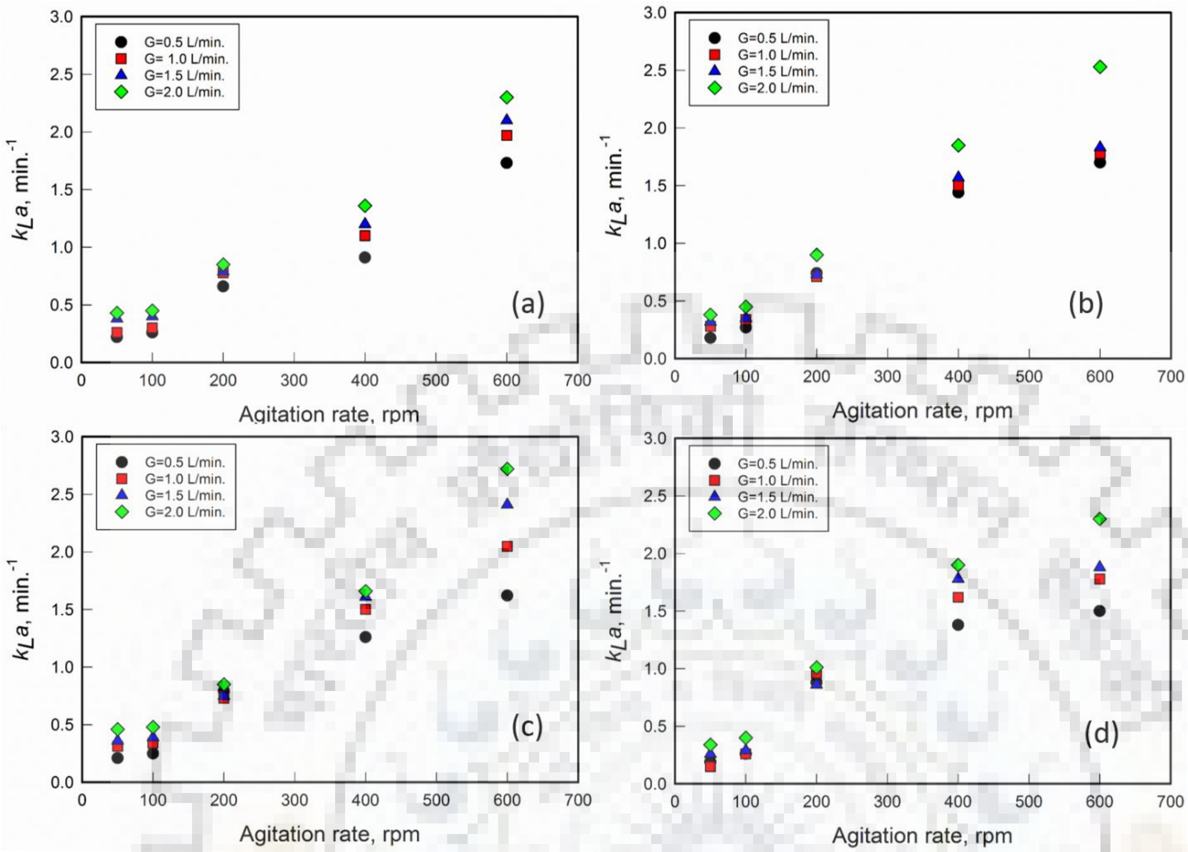


Figure 5.1. Effect of agitation and aeration rates on $k_La$ for (a) single Rushton turbine (b) dual Rushton turbine (c) pitched blade turbine, and (d) mixed turbine

### 5.3.2 Effect of Design of Rushton Turbine

Considering the fact that the standard Rushton turbine (SRT) is widely used impeller type in stirred bioreactors, however, several weaknesses such as low axial pumping capacity, large shear stress, low-pressure trailing vortices have been reported in this type of turbine, which results in power drop and low mass transfer (Ghotli et al., 2013; Gelves et al., 2014; Kadic and Heindel, 2014). To overcome these challenges, several efforts have been made for the modification of the SRT over the past few years. In this study, a dislocated Rushton turbine (DRT) has been investigated for its oxygen transfer performance and compared with that of the SRT. As shown in Figure 3.3 (Chapter 3), the DRT has the same dimensions as those of the SRT, except that the blades have been mounted above and below the impeller disc alternatively. It can be seen from Figure 5.2 that the dislocated Rushton turbine have better mass transfer performance, compared with standard Rushton turbine for *E. coli* BL21 cultivation. It is likely that dislocated Rushton turbine generates more chaotic flow, which provides more uniform mixing and generates smaller bubbles than the SRT. Furthermore, the power consumption and power drop after gassing are also lower than SRT

(Yang et al., 2015). Therefore, DRT can be considered for such applications where higher $k_La$ values are needed.

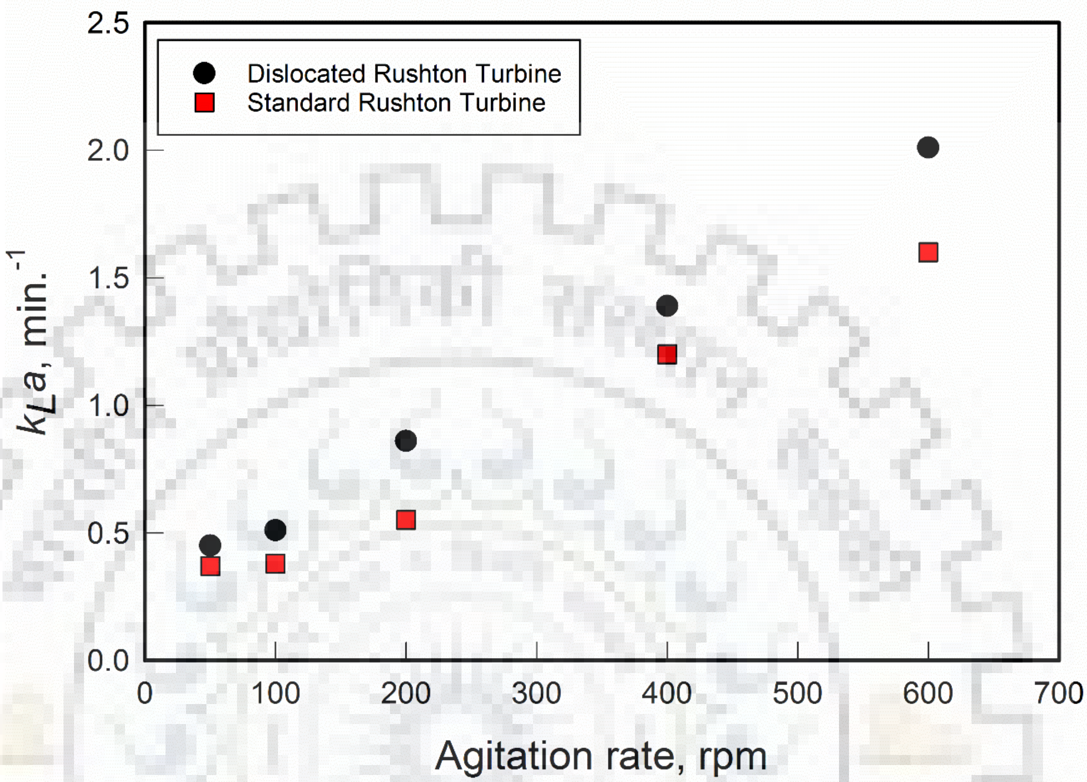


Figure 5.2. Effect of the designs of Rushton turbine on $k_La$

### 5.3.3 Effect of the Reactor Working Volume and the Impeller Diameter

Along with the effects of operating conditions described in section 5.3.1, the effect of reactor working volume and the impeller diameter was also investigated using a single Rushton turbine. Although there may exist slight differences, the same tendencies are expected to be observed in the various impeller types examined earlier. For this reason, only a single Rushton turbine was tested to understand those effects in the present study. Figure 5.3(a) shows the effect of the reactor working volume (0.25 L and 0.75 L) on the $k_La$ with varying agitation rates. Bolic et al. (2016) also studied the influence of bioreactor working volume on the oxygen transfer and reported that there was no significant effect of the reactor working volume at the milliliter scale. As reported by Bolic et al. (2016) the effect of reactor working volume on $k_La$ was not significant at lower agitation rate (50 rpm) in the present study. With increasing agitation rate further, however, it was observed that $k_La$ decreases with an increase in the working volume. Reducing the reactor working volume increases the ratio of surface to volume, which likely led to an increase in oxygen transfer.

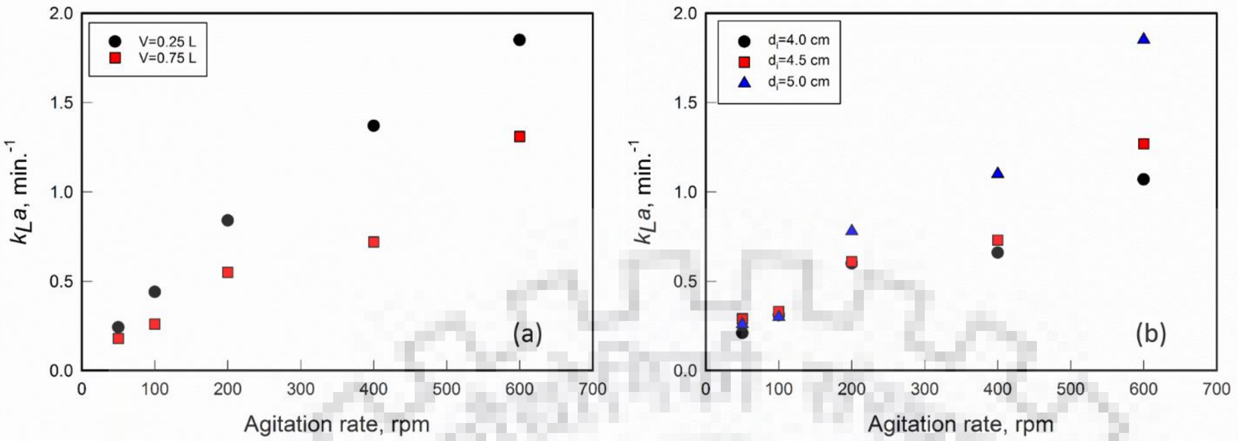


Figure 5.3. Effect of (a) reactor working volume and (b) impeller diameter on $k_La$

It is widely known that impeller diameter is one of the important parameters in STBRs, which affects the power input per unit volume in a stirred tank bioreactor, which in turn influences $k_La$ (Hsu et al., 1997; Hsu and Huang, 1997; Bao et al., 2015). Particularly for the shear-rate sensitive cell cultures, the impeller diameter was considered a highly important factor (Cherry and Papoutsakis, 1986; Joshi et al., 1996; Zhou and Kresta, 1996; Hu et al., 2011). Amer et al. (2019) found that the larger impeller diameter produced higher $k_La$ values. As seen in Figure 5.3(b), an increase in the impeller diameter does not significantly affect the $k_La$ at the smaller agitation rate (≤100 rpm). However, it is clearly observed in this figure that the effect of impeller diameter on $k_La$ is significant as the agitation rate increases, which is in an agreement with the results reported by Amer et al. (2019). Increase in $k_La$ may be attributed to enhanced gas-liquid mixing due to efficient gas distribution with increasing impeller diameter (Amer et al., 2019).

### 5.3.4 Effect of Cell Cultivation on $k_La$

The effect of the presence of cells on oxygen transfer rates has been investigated in various bioreactors (Mounsef et al., 2015; Tervasmaki et al., 2016; Bolic et al., 2016; Amani, 2018). Oxygen transfer in cell cultivation can be interpreted by several mechanisms (Ju and Sundararajan, 1995), e.g. the physical and chemical properties of the culture medium are changed by cell metabolism. In addition, the cell can be present as solid particles, which leads to a change in viscosity of the culture medium. Finally, oxygen may transfer from the gas bubble to respiring cells accumulated at the gas-liquid interface.

Figure 5.4 shows the $k_La$ values evaluated in the absence and presence of cells for different impellers with varying agitation rate. For the case of the absence of cells, only water without cells was used as a liquid medium while *E. coli* in the liquid LB medium was taken for the presence of cells. As observed earlier, the $k_La$ increased with agitation rate for both cases. At lower agitation rate, the effect of cells on the $k_La$ values is not significant for all the impellers tested in this study. At higher agitation rate, however, higher $k_La$ values were observed in the presence of the cell. It was also found that the effect of cells on oxygen transfer was strong at higher agitation rate. It seems to be attributed to the higher gas-liquid interfacial respiring cells accumulated with smaller bubbles under the conditions studied. Furthermore, with increasing agitation rate, the impeller can disperse gas more efficiently, thereby increasing the mass transfer coefficient. Ju and Sundararajan (1995) also found that an enhancement due to cell respiration was found stronger at higher agitation speed and lower aeration rates employed (Ju and Sundararajan, 1995). It is noteworthy that oxygen transfer in bioprocess is severely reduced by non-Newtonian behavior. However, in the present study, it was observed that the liquid culture medium used behaves as a Newtonian liquid, which will be discussed further in the next section.

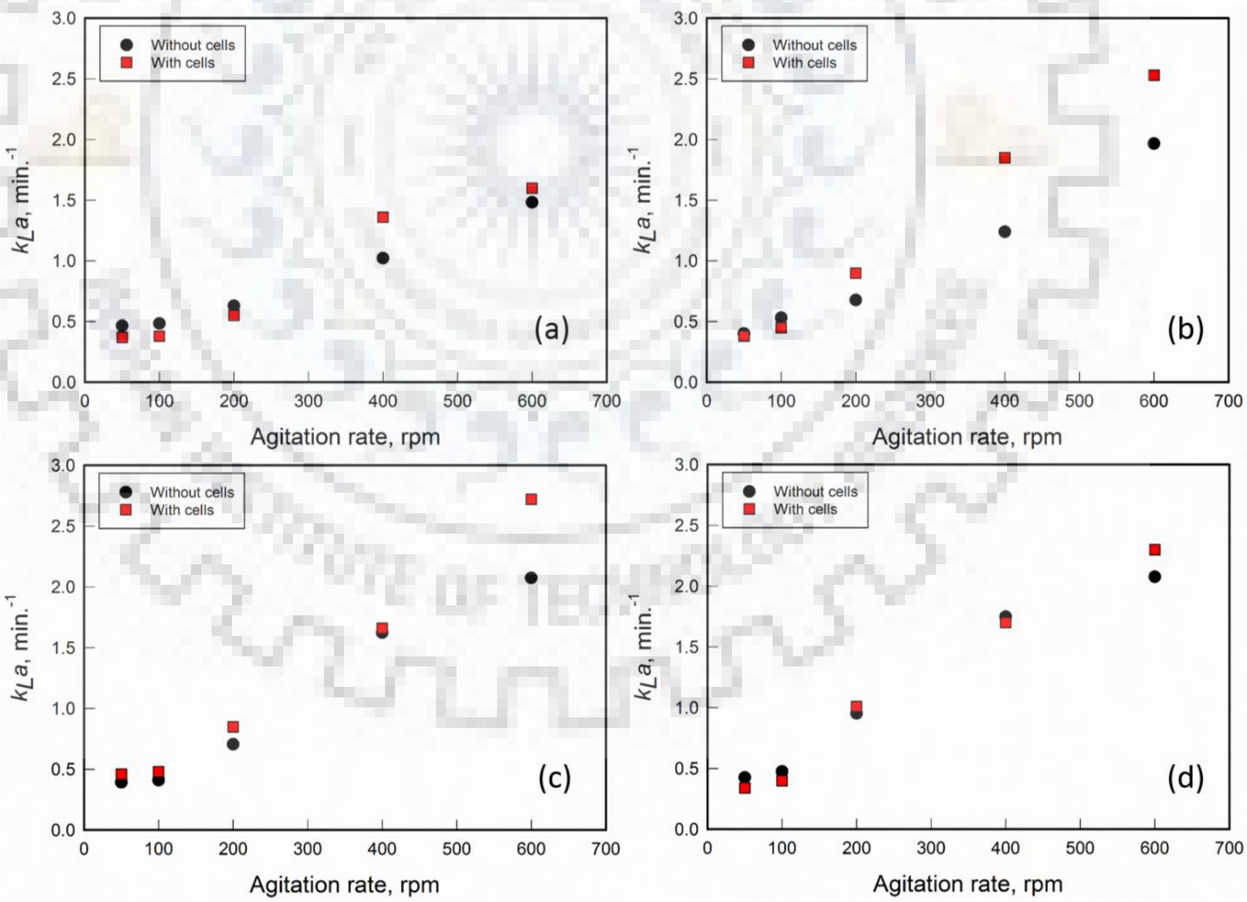


Figure 5.4. Effect of agitation rate on $k_La$ in the absence and the presence of cells for a) single Rushton turbine, b) dual Rushton turbine, c) pitched blade turbine, and d) mixed turbine

## 5.4 RHEOLOGICAL CHARACTERIZATION OF *E. COLI* BL21

While growing cells in the bioreactor, there is always a concern about the viscosity of the medium. This is because the cells in suspension form can have viscous nature and behave in a non-Newtonian manner (Shi et al., 1993; Gabelle et al., 2012; Newton et al., 2017). In the fermentation process for producing extracellular biopolymers, e.g., the broth becomes highly viscous due to the accumulation of the produced biopolymer, which leads to severe reduction of oxygen transfer (Whitcomb and Macosko, 1978; Galindo et al., 1989). In this context, a proper understanding of rheological properties such as viscosity, shear stress, and shear rate are crucial in stirred bioreactors for cell cultivation applications. To understand rheological properties of the culture medium, in the present work, samples of the liquid medium with a dual Rushton turbine were collected at specific time intervals, and their viscosity was evaluated using a rheometer. Figures 5.5 and 5.6 show viscosity and shear stress profiles with time as a function of shear rate for two different agitation rates (i.e., 100 and 350 rpm). Figure 5.5(a) shows that the viscosity at 100 rpm is independent on shear rate, indicating that the liquid medium used in this study behaves as a Newtonian liquid like water. At higher agitation rate of 350 rpm also the viscosity remains almost constant as the shear rate increases, which is commonly observed for Newtonian liquids (Figure 5.5(b)). It can be also found from Figure 5.5(b) that at higher shear rates, the viscosity is almost independent on shear rate, suggesting that the liquid medium behaves as a Newtonian liquid at higher agitation rate.

To further investigate the properties of the liquid medium, the shear rate versus shear stress behavior was also studied, as shown in Figure 5.6. It was observed that the shear stress linearly increases with the shear rate for both agitation rates, which indicates that the liquid medium can be classified as a Newtonian liquid. This result is in good agreement with the observation from the section 5.3.4 that the liquid culture medium used in this study behaves as a Newtonian liquid.

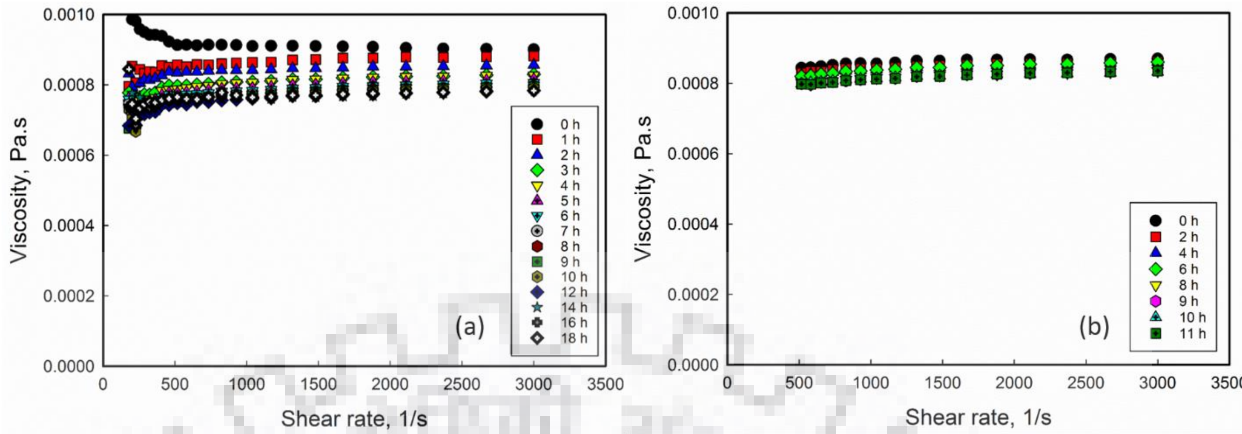


Figure 5.5. Variation of viscosity with shear rate for *E. coli* BL21 at 1 L/min and (a) 100 rpm and (b) 350 rpm.

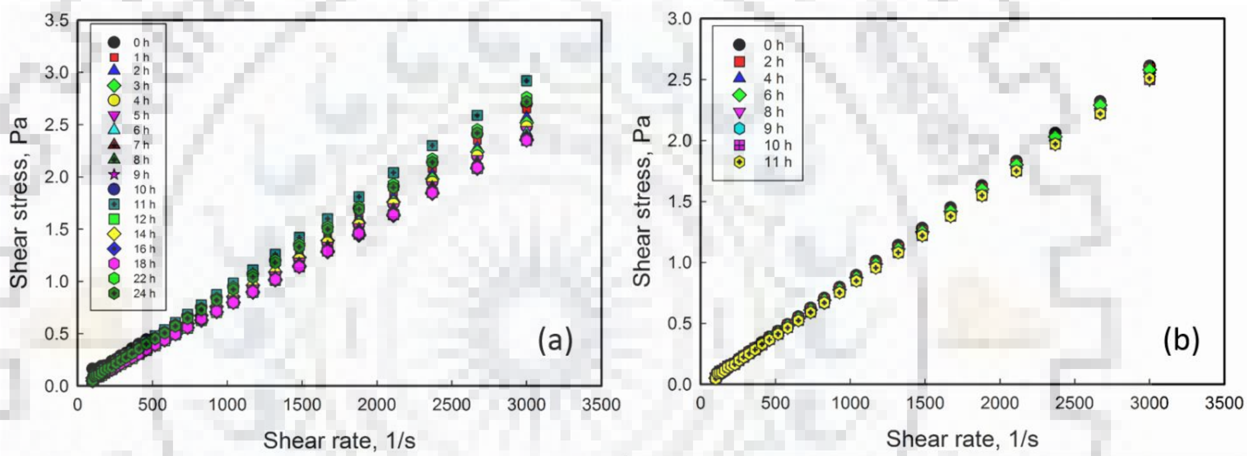


Figure 5.6 Variation of shear stress with shear rate for *E. coli* BL21 at 1 L/min and (a) 100 rpm and (b) 350 rpm.

## 5.5 DIMENSIONAL ANALYSIS FOR CORRELATION OF $k_La$

The scale-up of a bioprocess involves transferring the process developed at the laboratory scale to the production scale. This procedure is not simple due to hydrodynamic complexity and transport characteristics (Nauha et al., 2015; Bashiri et al., 2016; He et al., 2019). Consequently, it has become a challenging task for process engineers to develop substantial rules for scale-up from the laboratory scale. Particularly for quantitative estimation of the oxygenation capacity in stirred tank bioreactor systems, the volumetric mass transfer coefficient is frequently used as one of the important parameters.

Various correlation methods have been developed to estimate $k_La$ in stirred tank bioreactors (Garcia-Ochoa and Gomez, 2009; Moucha et al., 2012; Labik et al., 2017). Among the methods, power-law correlations have been most commonly used. However, Sideman et al. (1966) reviewed the available correlations in the literature on mass transfer in gas-liquid systems and found that such correlations apply only to the particular systems and operating ranges and are thus scale-dependent. In this study, the dimensionless analysis was employed to correlate $k_La$ for scale-up of stirred tank bioreactors. Dimensional analysis is a method for developing functional relationships that describe any given process in a dimensionless form to facilitate modeling and scale-up or down (Maa et al., 1996; Zolkarnik, 1998; Zolkarnik, 2012). Indeed, the correlations in the form of dimensionless numbers are independent on the process scales because they can be used for both scale -up and -down. In general, the oxygen transfer in the stirred tank bioreactor depends on several factors that may be classified as follows:

(1) Geometric or design parameters: tank diameter ($D_t$), impeller diameter ($d_i$), and liquid height inside the tank ($H_L$)

(2) Material parameters: density of liquid ($\rho_L$), viscosity of liquid ($\mu_L$), and diffusivity of oxygen in water ( $D_{o_2}$ )

(3) Process parameters: air flow rate ($Q$), agitation rate ($N_i$), and gravitational acceleration ($g$)

Thus, the performance parameter, $k_La$, can be written as the function of these factors such as following functional relationship:

$$k_L a = f_1(D_t, H_L, N_i, d_i, \rho_L, \mu_L, Q, g, D_{o_2}) \tag{5.1}$$

In the present work, however, $D_t$ and $H_L$ were constant, and hence, were not treated as variables. Using dimensional analysis, this relationship of seven variables can be expressed by only four dimensionless groups (Eqs. 5.2–5.5) as follows:

Reynolds Number
$$Re = \frac{\rho_L N_i {d_i}^2}{\mu_L} \tag{5.2}$$

Flow Number
$$Fl_g = \frac{Q}{N_i {d_i}^3} \tag{5.3}$$

Froude Number
$$Fr = \frac{{N_i}^2 d_i}{g} \tag{5.4}$$

Oxygenation Capacity $$k_L a^* = k_L a \left(\frac{\mu_L}{\rho_L g^2}\right)^{1/3} \left(\frac{\mu_L}{\rho_L D_{o_2}}\right) \tag{5.5}$$

Finally, the original equation for the performance parameter (Eq. 4) can be written in the following generalized form as:

$$k_L a^* = f_2(Re, Fl_g, Fr) \tag{5.6}$$

The left-hand side of the generalized equation represents the performance parameter, $k_L a$, characterizing oxygenation capacity of the system while the right-hand side involves dimensionless groups such as Reynolds, Froude, and Flow numbers.

Upon applying the similarity principle in scale-up, it is desirable to identify the regime of the process of the dimensionless group, which dominates the performance parameter (Holland and Chapman, 1966; Hyman, 1962). In practice, however, especially in complex systems, it is not simple to determine which variable or variable groups should be the basis of similarity at different scales of operation (Jordan, 1955; Jhonstone and Thring, 1957; Hyman, 1962; Holland and Chapman, 1966). Therefore, it is necessary to develop a relationship between performance parameter and variables. For the scale-up purpose, it is preferred to derive such relationship in terms of dimensionless groups, which can be best established using data generated experimentally. By applying this approach, Eq. 5.6 can be finally reduced to Eq. 5.7, where the dimensionless groups (Eqs. 5.2–5.5) are expressed in the form of power-law with corresponding coefficients ($\alpha$, $\beta$, $\gamma$, and $\delta$):

$$k_L a = \alpha (Re)^{\beta} (Fl_g)^{\gamma} (Fr)^{\delta} \tag{5.7}$$

The experimental $k_L a$ was correlated using Eq. 5.7, and the corresponding coefficient values determined for different impeller configurations are presented in Table 5.1. Note that the above dimensionless correlation can be applicable for ($H_L/D_t$=1) and ($d_i/D_t$>1/3). Table 2 also shows the $R^2$ value for each impeller type. The $R^2$ values of the single Rushton, dual Rushton, pitched blade, and mixed turbines were determined to be 0.964, 0.972, 0.985, and 0.951, respectively. The $k_L a$ values calculated by Eq. 10 are plotted with experimental data in Figure 5.7, indicating a good fit. This successful correlation suggests that the correlation by dimensional analysis can be employed as a promising tool for scaling the stirred tank bioreactors.

Table 5.1 Dimensionless correlation coefficients in Equation 5.7

| **Impeller Type** | $\alpha$ | $\beta$ | $\gamma$ | $\delta$ | $R^2$ |
|---|---|---|---|---|---|
| Single Rushton | 0.028 | 0.185 | 0.197 | 0.473 | 0.964 |
| Dual Rushton | 0.023 | 0.103 | 0.068 | 0.393 | 0.972 |
| Pitched Blade | 0.005 | 0.407 | 0.282 | 0.391 | 0.985 |
| Mixed Turbine | 0.003 | 0.439 | 0.253 | 0.298 | 0.951 |

## 5.6 SUMMARY

The effect of various operating parameters and different impeller types on the $k_La$ in a stirred tank bioreactor for *E. coli* BL21 cultivation have been investigated. It was found that the $k_La$ increased with agitation and aeration rates, and impeller diameter while decreased with bioreactor working volume. A pitched blade turbine appears to be most effective for *E. coli* cultivation because the highest $k_La$ was demonstrated among the tested impeller configurations. Higher $k_La$ values were found for dislocated Rushton turbine than the conventional Rushton turbine. The rheological analysis showed that the viscosity of the liquid medium used in this study is independent on the shear rate, indicating that it behaves as a Newtonian liquid. The $k_La$ values for different impeller types were correlated in the form of dimensionless groups including Reynolds, Flow, and Froude numbers using dimensional analysis, which provided an effective tool for the scale-up of the stirred tank bioreactors for cell cultivation applications.

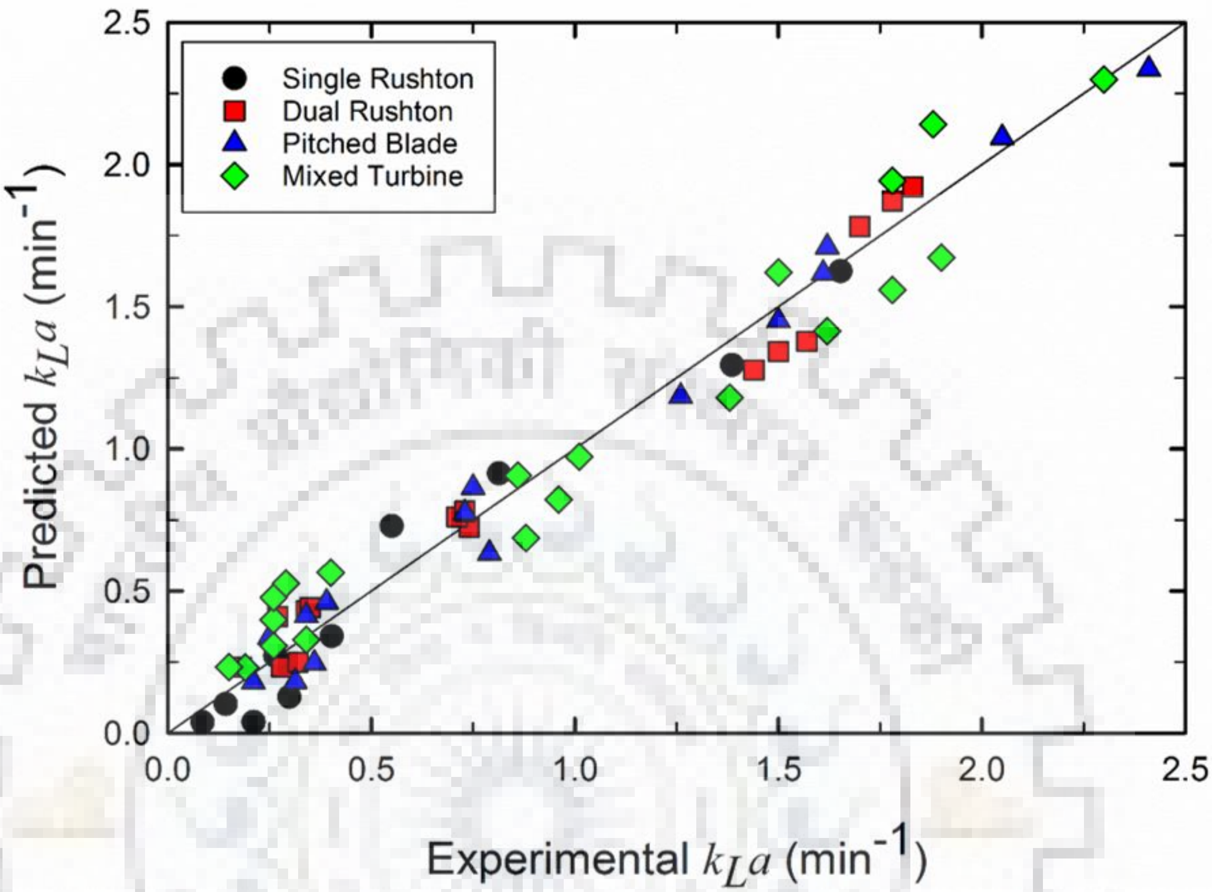


Figure 5.7. Parity plot between the experimental and predicted $k_La$ values using the dimensionless correlations (N= 50-600 rpm, $Q_g$=0.5-2 L/min., T=37 °C)

# CHAPTER 6

# CONCLUSIONS AND RECOMMENDATIONS

## 6.1 CONCLUSIONS

Based on the work carried out in this thesis for characterizing the performance of Rushton, pitched blade, marine propeller and their different combinations on the volumetric mass transfer coefficient, $k_La$ in the presence as well as absence of cell culture in stirred tank bioreactors, the following inferences were made:

### 6.1.1 $k_La$ Characterization in Absence of Cell Culture

The volumetric mass transfer coefficient, $k_La$ was characterized using different impeller types such as Rushton turbine, pitched blade turbine, marine propeller and their different combinations both in the presence as well as absence of cell culture. Firstly, $k_La$ was characterized in stirred tank bioreactors of different volumes i.e. 7.5 L, 5 L and 1 L using a simple air/water system. The effect of various key operating variables on $k_La$ such as agitation rate (50-800 rpm), aeration rate (0.5-3.5 L/min.), impeller diameter (4-5 cm), liquid volume (0.35-0.90 L), liquid medium viscosity (0.001-0.3 Pa.s). The findings of this work can be summarized as follows:

- The mass transfer coefficient, $k_La$ increases with an increase in agitation rate and aeration rate for all the STBRs, however, the impact of agitation rate is more as compared to the aeration rate.
- As the scale of the bioreactor increases from 1 L to 7.5 L, $k_La$ was found to decrease irrespective of the impeller configuration used. This decrease in the $k_La$ with an increase in the volume of the bioreactor is one of the key concerns as far as the scale-up of the stirred tank bioreactors is concerned.
- Different impeller diameters have been tested to study their influence on the $k_La$, however, keeping the impeller to reactor diameter ratio between 0.33-0.5, $k_La$ was found to increase with an increase in the impeller diameter.
- Different liquid working volumes were tested inside the reactor to study their effect on the $k_La$. As the liquid volume was increased inside the bioreactor, the $k_La$ decreased.

- The liquid medium viscosity was varied by using different amounts of glycerol to check for the effect of viscosity on $k_La$. As the liquid viscosity was increased inside the bioreactor, the $k_La$ would decrease suggesting that the rheology of the liquid medium is an important parameter to be studied while carrying out the cell cultivation study inside the bioreactor.
- A new impeller type, i.e. dislocated blade Rushton turbine has also been investigated having the same diameter as that of the standard Rushton turbine. It was found to give superior mass transfer performance ($k_La$ for SRT= 1.8 min$^{-1}$ and $k_La$ for DRT= 2.0 min$^{-1}$ at 800 rpm) as compared to the standard Rushton turbine.
- Effect of the aeration rate on power input per unit volume in the STBR has been investigated in this study. The calculated power consumption for single and dual Rushton turbines increases exponentially with agitation rate. Further, the gassed power consumption was found to be lower than the ungassed power consumption. The difference between gassed and ungassed power inputs was more pronounced at higher agitation rates (400-800 rpm).
- Empirical correlations based on power input per unit volume ($P_g/V_L$) and superficial gas velocity ($v_{sg}$) were developed for single and dual Rushton turbine configurations and further have been compared with the already available correlations in the literature. Good agreement between the experimental and predicted $k_La$ was observed.

### 6.1.2 Statistical Analysis of $k_La$

Design of experiments (DOE) has been utilized for studying the effect of several important operational variables such as agitation rate (50-800 rpm), aeration rate (0.5-3.5 L/min.) and temperature (10-40°C) on $k_La$. Response surface methodology (RSM) has been employed for developing the models for $k_La$ for several impeller configurations such as single and dual Rushton, pitched blade and mixed turbines. Most widely used response surface method, i.e. Box-Behnken Design (RSM-BBD) was used in this study and the following conclusions were made:

- A rotatable Box-Behnken design (RSM-BBD) has been implemented to design 15 experiments and generate 15 experimental data for each impeller configuration. Model equations provided the parametric interactions of the operating variables on response variable, $k_La$.
- Surface and corresponding contour plots suggested that the operating variable, i.e. agitation rate influenced most effectively the $k_La$. However, aeration rate and temperature have less

significant effect on $k_La$ as compared to the agitation rate. The p-values in ANOVA has also suggested the similar observations.

- 3-D response surface and corresponding contour plots suggested that the interaction between agitation and air flow rates was significant for single and dual Rushton, and mixed turbines.
- The p-values indicated that the effect of all the linear terms was significant for $k_La$ with agitation rate as highly significant followed by air flow rate and temperature. In addition, most of the temperature related effects in this study were relatively insignificant as compared to others. This may be because of the range of the temperature (10-40 °C) examined in the present work was relatively narrower than others.
- Among the different impeller configurations investigated, under the same operational conditions, dual Rushton turbine demonstrated the highest $k_La$ followed by the mixed (Rushton + pitched blade), pitched blade and single Rushton turbine.
- Empirical correlation model using RSM was developed for each impeller configuration. High coefficients of correlation have suggested that the experimental $k_La$ was successfully correlated by the RSM model.
- AVOVA analysis indicated that several terms in the original model were insignificant and thus can be omitted and a new simplified model was developed for each impeller configuration. After simplification, the number of terms were reduced from 10 to (5-6). It was noteworthy to found that even after the simplification $R^2$ values changed slightly suggesting that $k_La$ can still be well correlated by using the simplified model.
- Percentage error between the experimental and predicted $k_La$ was approximately in the range ~ ± 10% thus showing the importance of RSM-BBD model.
- The RSM developed models were also further validated under other operating conditions other than those used in developing the models.
- Compared with existing power-law models, the RSM approach enables a more efficient correlation procedure and formulates simplified models with comparably high accuracy suggesting that RSM is promising for evaluation of oxygen transfer in stirred tank bioreactors.

### 6.1.3 Effect of Impeller Spacing on $k_La$ and $P/V_L$

To study the effect of impeller spacing on $k_La$ and $P/V_L$, experiments were performed on 7.5 L stirred tank reactor considering three important variables i.e. agitation rate (100-600 rpm), aeration rate (0.2-2.4 vvm) and impeller spacing (4-8 cm) using Rushton-Rushton and Rushton-marine propeller configurations. The experiments were designed according to RSM-BBD modeling technique and the following conclusions were made:

- Surface and corresponding contour plots suggested that agitation rate mostly affects $k_La$ and power input per unit volume ($P/V_L$) and the interaction between agitation and air flow rates is also important for both the impeller configurations
- The impeller spacing does not have any significant effect on $k_La$ and $P/V_L$ for both the impeller configurations.
- The RSM developed correlations for dual Rushton turbine have better predictability than correlations available in the literature.
- A power-law correlation proposed for dual Rushton turbine has been found to well predict $k_La$ and a comparison has also been made with several available correlations in the literature.
- Further, a new power-law correlation is proposed for mixed (Rushton-marine propeller) configuration.

### 6.1.4 $k_La$ Characterization in Presence of Cell Culture

The volumetric mass transfer coefficient, $k_La$, was also characterized using different impeller types such as single and dual Rushton turbine, pitched blade turbine, mixed turbine (Rushton + pitched blade) in the presence of cell culture in a 1 L stirred tank bioreactor. *E. coli* BL21 was used in this study owing to its wide industrial importance for protein expression and purification, the transfer of oxygen from gas to liquid becomes crucial for its production. The effect of various key operating variables such as agitation rate (50-800 rpm), aeration rate (0.5-2.0 L/min.), impeller diameter (4-5 cm), bioreactor working volume (0.25-0.75 L). The findings of this work can be summarized as follows:

- The volumetric mass transfer coefficient, $k_La$ increases with an increase in agitation rate and aeration rate for *E. coli* BL21 cultivation. However, the effect of agitation is more pronounced than aeration rate. It was also observed at lower agitation rates such as 50 and 100 rpm, the $k_La$ values were almost same.

- Different impeller diameters have been used in this study to test their effect on $k_La$, however keeping the impeller to reactor diameter ratio between 0.33-0.50. It was observed that at lower agitation rates such as 50 and 100 rpm, the effect of the impeller diameter was not significant. As the agitation rate was increased, the effect of the impeller diameter was appreciable.
- It was observed that at lowest agitation rate employed, i.e. 50 rpm, the effect of the bioreactor working volume on $k_La$ was insignificant. However, as the agitation rate was increased, the effect of the bioreactor working volume was found to be significant.
- Among the examined impeller configurations, pitched blade turbine showed the highest $k_La$ (2.72 $min^{-1}$), thus suggesting that it is promising for the successful production of *E. coli* BL21 as it also generates relatively less shear force owing to its low power number.
- A new impeller type, i.e. dislocated blade Rushton turbine, was also investigated having the same diameter as that of standard Rushton turbine and it was found to give superior mass transfer ($k_La$ for SRT= 1.6 $min^{-1}$ and $k_La$ for DRT= 2.0 $min^{-1}$ at 600 rpm) performance and thus can be used in applications requiring higher oxygen transfer.
- A scale-up correlation employing dimensionless groups such as Reynolds, Froude and Flow numbers has been developed for different impeller configurations. A good agreement between the experimental and predicted $k_La$ has been found.

### 6.1.5 Rheological Behavior of *E. coli* BL21

The rheological behavior of *E. coli* BL21 was also investigated at 25°C and shear rate range of 100 to 3000 $s^{-1}$. The samples were collected for two different experimental conditions, i.e. agitation rates of 100 rpm and 350 rpm and aeration rate of 1 L/min and samples were collected initially after every hour and then after two hours. The following inferences were made:

- All the samples collected using the two sets of experimental conditions were checked and showed Newtonian behavior at a shear rate range of 100-3000 $s^{-1}$.
- The viscosity of *E. coli* BL21 after growing for several hours was almost close to that of water showing that there would not be mass transfer limitations during *E. coli* BL21 culturing.

## 6.2 RECOMMENDATIONS FOR FUTURE WORK

On the basis of the present study, the following recommendations can be made for the future study:

- It is further needed to develop more robust and reliable method for determining the $k_La$ in STBRs. Especially the emphasis is needed on decoupling of $k_L$ and $a$ to further understanding the behavior of individual parameters. Further, more data need to be generated to develop more accurate empirical correlations for $k_La$.
- Design of new impeller types to deliver better mixing, consume less energy and also produce less hydrodynamic shear to be used in cell culture and other similar applications based on hydrodynamic studies with both experimental and computational studies.
- Experimentation with different reactor geometries for their application as stirred tank reactors at larger volumes.
- Scale-up of stirred tank reactors remains a key challenge, thus new methods needed to be devised for their scale-up, which are applicable over a large scale of reactors.

## REFERENCES


Abdella, A., Mazeed, T.E.S., El-Baz, A.F., Yang, S.T. 2016. Production of β-glucosidase from wheat bran and glycerol by *Aspergillus niger* in stirred tank and rotating fibrous bed bioreactors. *Process Biochemistry* 51, 1331–1337.

Adzamic, Z., Adzamic, T., Muzic, M., Sertic-Biond, K. 2013. Optimization of the n-hexane isomerization process using response surface methodology. *Chemical Engineering Research and Design*. 91, 100–105.

Aghbolaghy, M. & Karimi, A. 2014. Simulation and optimization of enzymatic hydrogen peroxide production in a continuous stirred reactor using CFD-RSM combined method. *Journal of Taiwan Institute of Chemical Engineers* 45, 101-107.

Ahamed, A. and Vermette, P. 2010. Effect of mechanical agitation on the production of cellulases by Trichoderma reesei RUT-C30 in a draft-tube airlift bioreactor. *Biochemical Engineering Journal*. 49, 379–387.

Akita, K. and Yoshida, F. 1974. Bubble size, interfacial area and liquid phase mass transfer coefficient in bubble columns. *Ind Eng Chem Process Des Dev*. 13, 84–91.

Albal, R.S., Shah, Y.T., Shumpe, A., Carr, N.L. 1983. Mass transfer in multiphase agitated contactors. *Chemical Engineering Journal* 27, 61–80.

Amani, H. 2018. Application of a Dynamic Method for the Volumetric Mass Transfer Coefficient Determination in the Scale-Up of Rhamnolipid Biosurfactant Production. *Journal of Surfactants and Detergents* 21, 827-833.

Amanullah, A., Buckland, B.C., Nienow, A.W. 2004. Mixing in the Fermentation and Cell Culture Industries. In *Handbook of Industrial Mixing*. Hoboken, New Jersey, John Wiley and Sons.

Amer, M., Feng, Y., Ramsey, J.D. 2019. Using CFD simulations and statistical analysis to correlate oxygen mass transfer coefficient to both geometrical parameters and operating conditions in a stirred-tank bioreactor. *Biotechnology Progress* 35(3), e2785.

Apostolidis, A. J., and Beris, A. N. 2016. The effect of cholesterol and triglycerides on the steady state shear rheology of blood. *Rheologica Acta* 55, 497–509.

Arrura, L.A., McCoy, B.J., Smith, J.M. 1990. Gas-liquid mass transfer in stirred tanks. *AIChE Journal* 36 1768–1772.

Ascanio, G. 2015. Mixing time in stirred vessels: A review of experimental techniques. *Chinese Journal of Chemical Engineering* 23, 1065–1076.

Ashley, K.I., Hall, K.J., Mavinic, D.S. 1991. Factors influencing oxygen transfer in fine pore diffused aeration. *Water Research* 25, 1479–1486.

Azargoshasb, H., Mousavi, S.M., Amani, T., Jafari, A., Nosrati, M. 2015. Three-phase CFD simulation coupled with population balance equations of anaerobic syntrophic acidogenesis and methanogenesis reactions in a continuous stirred bioreactor. *Journal of Industrial and Engineering Chemistry* 27, 207–217.

Azargoshasb, H., Mousavi, S.M., Jamialahmadi, O., Shojaosadati, S.A., Mousavi, S.B. 2016. Experiments and a three-phase computational fluid dynamics (CFD) simulation coupled with population balance equations of a stirred tank bioreactor for high cell density cultivation. *The Canadian Journal of Chemical Engineering* 94, 20–32.

Bach, C., Yang, J.F., Larsson, H., Stocks, S.M., Gernaey, K.V., Albaek, M.O., Kruhne, U. 2017. Evaluation of mixing and mass transfer in a stirred pilot scale bioreactor utilizing CFD. *Chemical Engineering Science* 171, 19–26.

Baird, M.H.I., Rama, N.V., Shen, Z.J. 1993. Oxygen absorption in a baffled tank agitated by delta paddle impeller. *Canadian Journal of Chemical Engineering*. 71, 195–201.

Bandaiphet, C. & Prasertsan, P. 2006. Effect of aeration and agitation rates and scale-up on oxygen transfer coefficient, kLa in exopolysaccharide production from Enterobacter cloacae WD7. *Carbohydrate Polymers* 66(2), pp.216–228.

Bao, Y., Wang, B., Lin, M., Gao, Z., Yang, J. 2015. Influence of impeller diameter on overall gas dispersion properties in a sparged multi-impeller stirred tank. *Chinese Journal of Chemical Engineering* 23, 890–896.

Bashiri, H., Bertrand, F., Chaouki, J. 2016. Development of a multiscale model for the design and scale-up of gas/liquid stirred tank reactors. *Chemical Engineering Journal* 297, 277–294.

Bawadi, A. 2011. *PhD Thesis, The Performance of a Gas-inducing Stirred Tank Reactor for Fischer- Tropsch synthesis: Electrical Process Tomography Analysis and Computational Fluid Dynamics Studies*. The University of New South Wales, Australia.

Bezerra, M.A., Santelli, R.E., Oliveira, E.P., Villar, L.S., Escaleira, L.A., 2008. Response surface methodology (RSM) as a tool for optimization in analytical chemistry. *Talanta* 76, 965-977.

Bolic, A., Larsson, H., Hugelier, S., Lantz, A.E., Krühne, U., Gernaey, K.V. 2016. A flexible well-mixed milliliter-scale reactor with high oxygen transfer rate for microbial cultivations. *Chemical Engineering Journal* 303, 655–666.

Bombac, A., Zun, I., Filipic, B. 1997. Gas-filled cavity structures and local void fraction distribution in aerated stirred vessel. *AIChE Journal* 43, 2921-2931.

Bonvillani, P., Ferrari, M.P., Ducros, E.M., Orejas, J.A.  2006. Theoretical and experimental study of the effects of scale-up on mixing time for a stirred-tank bioreactor. *Brazilian Journal of Chemical Engineering* 23, 1–7.

Bouaifi, M. & Roustan, M. 2001. Power consumption, mixing time and homogenisation energy in dual-impeller agitated gas-liquid reactors. *Chemical Engineering and Processing* 40, 87–95.

Bouaifi, M., Hebrad, G., Bastoul, D., Roustan, M. 2001. A comparative study of gas hold-up, bubble size, interfacial area and mass transfer coefficients in stirred gas-liquid reactors and bubble columns. *Chemical Engineering Processing*. 40, 97–111.

Box, G.E.P. & Behnken, D.W. 1960. Some new three level designs for the study of quantitative variables. *Thermometrics* 2, 455–475.

Branyik, T.A.A., Vicente, P.D.A.T. 2005. Continuous beer fermentation using immobilized yeast cell bioreactor systems. *Biotechnology Progress* 21, 653–663.

Brumano, L.P., Antunes, F.A.F., Souto, S.G., Santos, J.C., Venus, J., Schneider, R., Silva, S.S. 2017. Biosurfactant production by Aureobasidium pullulans in stirred tank bioreactor : New approach to understand the influence of important variables in the process. *Bioresource Technology* 243, 264–272.

Brumano, L.P., Antunes, F.A.F., Souto, S.G., Santos, J.C., Venus, J., Schneider, R., Silva, S.S. 2017. Biosurfactant production by *Aureobasidium pullulans* in stirred tank bioreactor : New approach to understand the influence of important variables in the process. *Bioresource Technology* 243, 264–272.

Butcher, M. & Eagles, W. 2002. Fluid Mixing Re-engineered. in TCE, The Chemical Engineer 28-29.

Cherry, R.S. and Papoutsakis, E.T. 1986. Hydrodynamic effects on cells in agitated tissue culture reactors. *Bioprocess Engineering* 1, 29–41.

Clarke, K.G., Williams, P.C, Smit, M.S., Harrison, S.T.L. 2006. Enhancement and repression of the volumetric oxygen transfer coefficient through hydrocarbon addition and its influence on oxygen transfer rate in stirred tank bioreactors. *Biochemical Engineering Journal*. 28, 237–242.

Costa, E., Lucas, A., Aguado, J., Avila, J.A. 1982. Transfer of matter in agitated tanks: gas bubbling in Newtonian and non-Newtonian liquids.I. Turbines with 6 vanes and flat diffuser. *An Quim* 78, 387–392.

Couper, J.R., Penny, W.R., Fair, J.R., Walas, S.M., 2005. Mixing and Agitation *In Chemical Process Equipment*. 2nd Edition., Burlington, Gulf Professional Publishing.

Cui, Y.Q, van der Lans R.G.J.M., Ch, K., Luyben, A.M. 1996. Local power uptake in gas–liquid systems with single and multiple Rushton turbines. *Chemical Engineering Science*. 51, 2631–2636.

Cybulski, A., Sharma, M.M., Sheldon, R.A., Moulijn, J.A. 2001. *Fine Chemicals Manufacture: Technology and Engineering.* Gulf Professional Publishing.

Deglon, D.A. & Meyer, C.J. 2006. CFD modelling of stirred tanks: Numerical considerations. *Minerals Engineering* 19, 1059–1068.

Delafosse, A., Collignon, M.L., Calvo, S., Delvigne, F., Crine, M., Thonart, P., Toye, D. 2014. CFD-based compartment model for description of mixing in bioreactors. *Chemical Engineering Science* 106, 76–85.

Dhanasekharan, K.M., Sanyal, J., Jain, A., Haidari, A. 2005. A generalized approach to model oxygen transfer in bioreactors using population balances and computational fluid dynamics. *Chemical Engineering Science* 60, 213-218.

Dixit, P., Mehta, A., Gahlawat, G., Prasad S., Choudhury A.R. 2015. Understanding the effect of interaction among aeration, agitation and impeller positions on mass transfer during pullulan fermentation by Aureobasidium pullulans. *RSC Advances*. 5, 38984–38994.

Djelal, H., Larher, F., Martin, G., Amrane, A. 2006. Effect of the dissolved oxygen on the bio production of glycerol and ethanol by Hansenula anomala growing under salt stress conditions. *Journal of Biotechnology*. 125, 95-103.

Dudukovic, M. 2007. Relevance of Multiphase Reaction Engineering to Modern Technological Challenges. *Industrial and Engineering Chemistry Research* 46, 8674–8686.

Dumont, E., Andr, Y., Le Cloirec, P. 2006. Effect of organic solvents on oxygen mass transfer in multiphase systems : Application to bioreactors in environmental protection. *Biochemical Engineering Journal* 30, 245–252.

Einstein, A. 1906. Eine neue bestimmung der moleküldimensionen. *Annalen der Physik* 324, 289–306.

Elqotbi, M., Vlaev, S.D., Motastruc, L., Nikov, I. 2013. CFD modelling of two-phase stirred bioreaction systems by segregated solution of the Euler-Euler model. *Computers and Chemical Engineering* 48, 113–120.

Eppinger, T., Wehinger, G., Kraume, M. 2014. Parameter optimization for the oxidative coupling of methane in a fixed bed reactor by combination of response surface methodology and computational fluid dynamics. *Chemical Engineering Research and Design*. 92, 1693–1703.

Euzen, J.P., Trambouze, P., Wauquier, J.P. 1993. Scale-up Methodology for Chemical Processes. Technip, Paris.

Fan, L.S., Bavarian, F., Gorowara, R.L., Kreischer, B.E. 1987. Hydrodynamics of gas-liquid-solid fluidization under high gas hold-up conditions. *Powder Technology*. 53, 285–293.

Ferreira, S.C., Bruns, R.E., Ferreira, H.S, Matos, G.D, David, J.M., Brandao, G.C., Silva, E.G., Portugal, L.A., Reis, P.S, Souza, A.S., Santos, W.N. 2007. Box-Behnken design: an alternative for the optimization of analytical methods. *Analytica Chimica Acta* 597, 179-186.

Gabelle, J.C., Jourdier, E., Licht, R.B., Chaabane, F.B., Henaut, I., Morchain, J., Augier, F. 2012. Impact of rheology on the mass transfer coefficient during the growth phase of *Trichoderma reesei* in stirred bioreactors. *Chemical Engineering Science* 75, 408–417.

Galindo, E., Torrestiana, B., Garcia-Rejon, A. 1989. Rheological characterization of xanthan fermentation broths and their reconstituted solutions. *Bioprocess Engineering* 4, 113–117.

Garcia-Ochoa, F. & Gomez, E. 1998. Mass transfer coefficient in stirrer tank reactors for xanthan solutions. *Biochemical Engineering Journal* 1, 1–10.

Garcia-Ochoa, F. and Gomez, E. 2009. Bioreactor scale-up and oxygen transfer rate in microbial processes: An overview. *Biotechnology Advances* 27, 153–176.

Garcia-Ochoa, F., Castro, E.G. 2001. Estimation of oxygen mass transfer coefficient in stirred tank reactors using artificial neural networks. *Enzyme and Microbial Technology* 28, 560–569.

Garcia-Ochoa, F., Castro, E.G., Santos, V.E. 2000. Oxygen transfer and uptake rates during xanthan gum production. *Enzyme and Microbial Technology* 27, 680–690.

Garcia-Ochoa, F., Castro, E.G., Santos, V.E., Merchuk, J.C. 2010. Oxygen uptake rate microbial processes: An overview. *Biochemical Engineering Journal* 49, 289-307.

Gelves, R., Dietrich, A., Takors, R. 2014. Modeling of gas-liquid mass transfer in a stirred tank bioreactor agitated by a Rushton turbine or a new pitched blade impeller. *Bioprocess and Biosystems Engineering* 37, 365–375.

Ghotli, R.A., Abdul Aziz, A.R., Ibrahim, S., Baroutian, S., Arami-Niya, A. 2013. Study of various curved-blade impeller geometries on power consumption in stirred vessel using response surface methodology. *Journal of the Taiwan Institute of Chemical Engineers* 44, 192–201.

Gibbs, P.A., Seviour, R.J., and Schmid, F. 2000. Growth of filamentous fungi in submerged culture: Problems and possible solutions. *Critical Reviews in Biotechnology* 20, 17–48.

Gill, N.K., Appleton, M., Baganz, F., Lye, G.J. 2008a. Quantification of power consumption and oxygen transfer characteristics of a stirred miniature bioreactor for predictive fermentation scale-up. *Biotechnology and Bioengineering* 100, 1144–1155.

Gill, N.K., Appleton, M., Baganz, F., Lye, G.J. 2008b. Design and characterisation of a miniature stirred bioreactor system for parallel microbial fermentations. *Biochemical Engineering Journal* 39, 164–176.

Gimbun, J., Rielly, C.D., Nagy, Z.K. 2009. Modelling of mass transfer in gas-liquid stirred tanks agitated by Rushton turbine and CD-6 impeller: A scale-up study. *Chemical Engineering Research and Design* 87, 437–451.

Gogate, P.R., Beenackers, A.A.C.M., Pandit, A.B. 2000. Multiple-impeller systems with a special emphasis on bioreactors: a critical review. Biochemical Engineering Journal 6, 109–144.

Greaves, M. and Barigou, M. 1990. Estimation of Gas Hold up and Impeller Power in a Stirred Vessel Reactor in "Fluid Mixing III", *Institution of Chemical Engineering*, Symposium Series No: 108, 235–255.

Hadjiev, D., Sabiri, N.E., Zanati, A. 2006. Mixing time in bioreactors under aerated conditions. *Biochemical Engineering Journal* 27, 323–330.

He, C., Ye, P., Wang, H., Liu, X., and Li, F. 2019. A systematic mass-transfer modeling approach for mammalian cell culture bioreactor scale-up. *Biochemical Engineering Journal* 141, 173–181.

Hickman A.D. 1988. Gas–Liquid Oxygen Transfer and Scale-up. A Novel Experimental Technique with Results for Mass Transfer in Aerated Agitated Vessels. in Proceedings of 6th European Conference on Mixing. 369–374.

Hocker, H., Langer, G., Werner, U. 1981. Mass transfer in aerated Newtonian and non- Newtonian liquids in stirred reactors. *German Chemical Engineering* 4, 51–62.

Hoffmann, R.A., Garcia, M.L., Veskivar, M., Karim, K., A1-Dahhan, M.H., Angenent, L.T. 2008. Effect of shear on performance and microbial ecology of continuously stirred anaerobic digesters treating animal manure. *Biotechnology and Bioengineering*, 100, 38–48.

Holland, F.A. and Chapman, F.S. 1966. *Liquid Mixing and Processing in Stirred Tanks*. Reinhold Publishing, New York.

Hsu, Y.C., and Huang, K.F. 1997. Effects of Geometrical Factors on Liquid Mixing in a Gas-Induced Agitated Tank. *Journal of Chemical Technology and Biotechnology* 68, 222–228.

Hsu, Y.C., Peng, R.Y., Huang, C.J. 1997. Onset of gas induction , power consumption , gas holdup and mass transfer in a new gas-induced reactor. *Chemical Engineering Science* 52, 3883–3891.

Hu, W., Berdugo, C., Chalmers, J.J. 2011. The potential of hydrodynamic damage to animal cells of industrial relevance : current understanding. *Cytotechnology* 63, 445–460.

Hughmark, G. A. 1980. Power Requirements and Interfacial Area in Gas-Liquid Turbine Agitated Systems. *Industrial & Engineering Chemistry Process Design & Development* 19, 638-641.

Hyman, D. 1962. Mixing and Agitation in *Advances in Chemical Engineering*, Academic Press, London.

Isailovic, B., Kradolfer, M., Rees, B. 2015. Fluid Dynamics of a Single-Use, Stirred- Tank Bioreactor for Mammalian Cell Culture. *BioProcess International* 13, 60–66.

Islam, M. and Lye, L.M. 2009. Combined Use of Dimensional Analysis and Statistical Design of Experiment Methodologies in Hydrodynamics Experiments. *Ocean Engineering* 36, 237–247.

Jesus, S.S., Neto, J.M., Filho, R.M. 2017. Hydrodynamics and mass transfer in bubble column, conventional airlift, stirred airlift and stirred tank bioreactors, using viscous fluid : A comparative study. *Biochemical Engineering Journal* 118, 70–81.

Jiang, P., Lin, T.J., Luo, X., Fan, L.S. 1995. Flow visualization of high pressure (21 MPa) bubble column: Bubble characteristics. *Chemical Engineering Research and Design*. 73, 269–274.

Johnstone, R.E. and Thring, M.W. 1957. *Pilot Plants, Models and Scale-up Methods in Chemical Engineering*. McGraw Hill, New York.

Jordan, D.G. *Chemical Pilot Plant Practice*. Interscience Publishers, New York, 1955.

Joshi, J.B., Elias, C.B., Patole, M.S. 1996. Role of hydrodynamic shear in the cultivation of animal, plant and microbial cells. *Biochemical Engineering Journal* 62, 121–141.

Jossen, V., Eibl, R., Portner, R., Kraume, M., Eibl, D. 2017. Stirred Bioreactors Current State and Developments, With Special Emphasis on Biopharmaceutical Production Processes. In *Current Developments in Biotechnology and Bioengineering*. pp. 179–215. doi: 10.1016/B9780444636638000070.

Ju, L.K. and Sundararajan, A. 1995. The effects of cells on oxygen transfer in bioreactors. *Bioprocess Engineering* 13, 271–278.

Kadic, E. & Heindel, T.J. 2014. *An Introduction to Bioreactor Hydrodynamics and Gas-Liquid Mass Transfer*, John Wiley & Sons, New Jersey.

Kaiser, S C., Werner, S., Jossen, V., Blaschczok, K., Eibl, D. 2018. Power Input Measurements in

Stirred Bioreactors at Laboratory Scale. *Journal of Visualized Experiments*. 135:e56078. doi: 10.3791/56078.

Kantarci, N., Borak, F., Ulgen, K.O. 2005. Bubble column reactors. *Process Biochemistry* 40, 2263–2283.

Kapic, A. & Heindel, T.J. 2006. Correlating gas-liquid mass transfer in a stirred tank reactor. *Chemical Engineering Research and Design* 84, 239–245.

Karimi, A., Golbabaei, F., Mehrnia, M.R., Neghab, M., Mohammad, K., Nikpey, A., Pourmand, M.R. 2013. Oxygen mass transfer in a stirred tank bioreactor using different impeller configurations for environmental purposes. *Iranian Journal of Environmental Health Sciences & Engineering* 10, 1-9. doi: 10.1186/1735-2746-10-6.

Kerdouss, F., Bannari, A. & Proulx, P. 2006. CFD modeling of gas dispersion and bubble size in a double turbine stirred tank. *Chemical Engineering Science* 61, 3313–3322.

Kerdouss, F., Bannari, A., Proulx, P., Bannari, R., Skrga, M., Labrecque, Y. 2008. Two-phase mass transfer coefficient prediction in stirred vessel with a CFD model. *Computers and Chemical Engineering* 32, 1943–1955.

Kumar, A., Prasad, B., Mishra, I.M. 2007. Process parametric study for ethane carboxylic acid removal onto powder activated carbon using Box-Behnken design. *Chemical Engineering & Technology*. 30, 932–937.

Kumar, A., Prasad, B., Mishra, I.M. 2008. Optimization of process parameters for acrylonitrile removal by low-cost adsorbent using Box-Behnken design. *Journal of Hazardous Materials*. 150, 174–182.

Kundu, P., Paul, V., Kumar, V., Mishra, I.M. 2015. Formulation development, modeling and optimization of emulsification process using evolving RSM coupled hybrid ANN-GA framework. *Chemical Engineering Research and Design*. 104, 773–790.

Laakkonen, M., Moilanen, M., Miettinen, T., Saari, K., Honkanen, M., Saarenrinne, P., Aittamaa, J. 2005. Local Bubble Size Distribution in Agitated Vessel: Comparison of Three Experimental Techniques. *Chemical Engineering Research and Design* 83, 50–58.

Labik, L., Moucha, T., Petricek, R., Rejl, J.F., Valenz, L., and Haidl, J. 2017. Volumetric mass transfer coefficient in viscous liquid in mechanically agitated fermenters. Measurement and correlation. *Chemical Engineering Science* 170, 451–463.

Lamotte, A., Delafosse, A., Calvo, S., Toye, D. 2018. Analysis of PIV measurements using modal decomposition techniques, POD and DMD, to study flow structures and their dynamics within a stirred-tank reactor. *Chemical Engineering Science* 178, 348–366.

Lee, B.W. & Dudukovic, M.P. 2014. Determination of flow regime and gas holdup in gas-liquid stirred tanks. *Chemical Engineering Science* 109, 264–275.

Lejeune, R. and Baron, G.V. 1995. Effect of agitation on growth and enzyme production of Trichoderma reesei in batch fermentation. *Applied Microbiology and Biotechnology*. 43, 249–258.

Li, G., Li, H., Wei, G., He, X., Xu, S., Chen, K., Ouyang, P., Ji, X. 2018. Hydrodynamics, mass transfer and cell growth characteristics in a novel microbubble stirred bioreactor employing sintered porous metal plate impeller as gas sparger. *Chemical Engineering Science* 192, 665–677.

Linek, V., Kordac, M., Fujasova, M., Moucha, T. 2004. Gas-liquid mass transfer coefficient in stirred tanks interpreted through models of idealized eddy structure of turbulence in the bubble vicinity. *Chemical Engineering and Processing* 43, 1511–1517.

Liu, H., Zhao, S., Jin, Y., Yue, X., Deng, L., Wang, F., Tan, T. 2017. Production of fumaric acid by immobilized Rhizopus arrhizus RH 7-13-9# on loofah fiber in a stirred-tank reactor. *Bioresource Technology* 244, 929–933.

Liu, M. 2011. Quantitative characterization of mixing in stirred tank reactors with mean age distribution. *The Canadian Journal of Chemical Engineering* 89, 2011-2022.

Liu, Y., Wu, J., Ho, K. 2006. Characterization of oxygen transfer conditions and their effects on Phaffia rhodozyma growth and carotenoid production in shake-flask cultures. *Biochemical Engineering Journal* 27, 331–335.

Luo, X., Lee, D.J., Lau, R., Yang, G., Fan, L. 1999. Maximum stable bubble size and gas hold-up in high-pressure slurry bubble columns. *AIChE Journal*. 45, 665–685.

Luong, H.T., Volesky, B. 1979. Mechanical power requirements of gas-liquid agitated systems. *AIChE Journal* 25, 893–895.

Maa, Y.F. and Hsu, C. 1996. Microencapsulation reactor scale-up by dimensional analysis. *Journal of Microencapsulation* 13, 53–66.

Magelli, F., Montante, G., Pinelli, D., Paglianti, A. 2013. Mixing time in high aspect ratio vessels stirred with multiple impellers. *Chemical Engineering Science* 101, 712–720.

Mavros, P. 2001. Flow Visualization In Stirred Vessels: A Review of Experimental Techniques. *Trans IChemE* 79, 113–127.

McClure, D.D., Kavanagh, J.M., Fletcher, D.F., Barton, G.W. 2015. Oxygen transfer in bubble columns at industrially relevant superficial velocities: Experimental work and CFD modelling. *Chemical Engineering Journal* 280, 138–146.

Mcclure, D.D., Kavanagh, J.M., Fletcher, D.F., Barton, G.W. 2016. Characterizing bubble column bioreactor performance using computational fluid dynamics. *Chemical Engineering Science* 144, 58–74.

Mirro, R. & Voll, K. 2009. Which Impeller is Right for Your Cell Line? *Bioprocess International* 7, 52-58.

Montante, G. & Paglianti, A. 2015. Gas hold-up distribution and mixing time in gas-liquid stirred tanks. *Chemical Engineering Journal* 279, 648–658.

Montante, G., Magelli, F., Paglianti, A. 2013. Fluid-dynamics characteristics of a vortex-ingesting stirred tank for biohydrogen production. *Chemical Engineering Research and Design* 91, 2198–2208.

Montes, F.J., Catalan, J., Galan, M.A. 1999. Prediction of $k_La$ in yeast broths. *Process Biochemistry* 34, 549–555.

Moucha, T., Linek, V., Prokopova, E. 2003. Gas hold-up , mixing time and gas–liquid volumetric mass transfer coefficient of various multiple-impeller configurations :Rushton turbine, pitched blade and techmix impeller and their combinations. *Chemical Engineering Science* 58, 1839–1846.

Moucha, T., Rejl, J.F., Kordac, M., Labik, L. 2012. Mass transfer characteristics of multiple-impeller fermenters for their design and scale-up. *Biochemical Engineering Journal* 69, 17–27.

Mounsef, J.R., Salameh, D., Louka, N., Brandam, C., Lteif, R. 2015. The effect of aeration conditions, characterized by the volumetric mass transfer coefficient $k_La$, on the fermentation kinetics of *Bacillus thuringiensis* kurstaki. *Journal of Biotechnology* 210, 100–106.

Mujtaba, A., Ali, M., Kohli, K. 2014. Statistical optimization and characterization of pH-independent extended-release drug delivery of cefpodoxime proxetil using Box–Behnken design. *Chemical Engineering Research and Design*. 92, 156–165.

Myers, R.H., Montgomery, D.C., Anderson-Cook, C.M. 2009. *Response Surface Methodology: Process and Product Optimization Using Designed Experiments*. 3rd Edition, Hoboken, New Jersey, John Wiley & Sons.

Nauha, E.K., Visuri, O., Vermasvuori, R., Alopaeus, V. 2015. A new simple approach for the scale-up of aerated stirred tanks. *Chemical Engineering Research and Design* 95, 150–161.

Nauman, E.B. 2008. *Chemical Reactor Design, Optimization and Scale-up*. John Wiley & Sons, New York.

Nevalainen, K.M.H., Teo, V.S.J., Bergquist, P.L. 2005. "Heterologous protein expression in filamentous fungi," *Trends in Biotechnology* 23, 468–474.

Newton, J.M., Vlahopoulou, J., Zhou, Y. 2017. Investigating and modelling the effects of cell lysis on the rheological properties of fermentation broths. *Biochemical Engineering Journal* 121, 38–48.

Nienow, A. 1996. Gas-liquid mixing studies: A comparison of Rushton turbines with some modern impellers. *Chemical Engineering Research and Design* 74, 417–423.

Nienow, A.W, Wisdom, D.J, Middleton, J. 1977. Effect of scale and geometry on flooding, recirculation and power in stirred vessels. In *Proceedings of the 2nd European Conference on Mixing*. Cambridge, United Kingdom.

Nienow, A.W. 2014. Stirring and Stirred-Tank Reactors. *Chemie Ingenieur Technik* 86, 2063–2074.

Nishikawa, M., Nakamura, M., Yagi, H., Hashimoto, K. 1981. Gas absorption in aerated mixing vessels. *Journal of Chemical Engineering of Japan* 14, 219–226.

Olsvik, E. and Kristiansen, B. 1994. Rheology of filamentous fermentations. *Biotechnology Advances* 12, 1–39.

Oolman, T., Blanch, H.W., and Erickson, L.E. 1986. Non-Newtonian fermentation systems. *Critical Reviews in Biotechnology* 4, 133–184.

Oosterhuis, N.M.G., Kossen N.W.F. 1985. *Biotechnology*, Vol. 2. Berlin, Germany.

Oosterhuis, N.M.G., Kossen, N.W.F. 1981. Power Input Measurements in a Production Scale Bioreactor. *Biotechnology Letters* 3, 645–650.

Ozbek, B., Gayik, S. 2001. The studies on the oxygen mass transfer coefficient in a bioreactor. *Process Biochemistry* 36, 729–741.

Ozcan-Taskin, G. & Wei, H. 2003. The effect of impeller to tank diameter ratio on draw down of solids. *Chemical Engineering Science* 53, 3109-3118.

Patel, N. and Thibault, J. 2009. Enhanced in situ dynamic method for measuring $k_La$ in fermentation media. *Biochemical Engineering Journal*. 47, 48–54.

Pedersen, A.G., Bundgaard-Nielsen, M., Nielsen, J., Villadsen, J. 1994. Characterization of Mixing in Stirred Tank Bioreactors Equipped With Rushton Turbines. *Biotechnology and*

*Bioengineering* 44, 1013–1017.

Perez, J.F. & Sandall, O.C. 1974. Gas absorption by non-Newtonian fluids in agitated vessels. *AIChE Journal* 20, 770–775.

Petitti, M., Vanni, M., Marchisio, D.L., Buffo, A., Podenzani, F. 2013. Simulation of coalescence, break-up and mass transfer in a gas-liquid stirred tank with CQMOM. *Chemical Engineering Journal* 228, 1182–1194.

Puthli, M.S., Rathod, V.K., Pandit, A.B. 2005. Gas-liquid mass transfer studies with triple impeller system on a laboratory scale bioreactor. *Biochemical Engineering Journal* 23(1), 25–30.

Rai, A., Mohanty, B., Bhargava, R. 2016. Supercritical extraction of sunflower oil: A central composite design for extraction variables. *Food Chemistry* 192, 647-659.

Ranade, V.V., Deshpande, V.R. 1999. Gas-liquid flow in stirred reactors: Trailing vortices and gas accumulation behind impeller blades. *Chemical Engineering Science*. 54, 2305-2315.

Ranade, V.V., Van den & Akker, H.E.A. 1994. A computational snapshot of gas-liquid flow in baffled stirred reactors. *Chemical Engineering Science*. 49, 5175-5192.

Ranganathan, P. & Sivaraman, S. 2011. Investigations on hydrodynamics and mass transfer in gas-liquid stirred reactor using computational fluid dynamics. *Chemical Engineering Science* 66, 3108–3124.

Rewatkar, V.B., Deshpande, A.J., Pandit, A.B., Joshi, J.B. 1993. Gas Hold-up Behavior of Mechanically Agitated Gas–Liquid Reactors using Pitched Blade Downflow Turbines. *Canadian Journal of Chemical Engineering*. 71, 226–237.

Rushton, J. & Bmbinet, J. 1968. Holdup and flooding in air liquid mixing. *The Canadian Journal of Chemical Engineering* 46, 16–21.

Rushton, J., Costich, E., Everett, H. 1950. Power characteristics of mixing impellers. *Chemical Engineering Progress* 46, 395–476.

Sanchez, A., Garcia, F., Contreras, A., Molina, E., Chisti, Y. 2000. Bubble-column and airlift photobioreactors for algal culture. *AIChE Journal* 46, 1872–1887.

Sangal, V.K., Kumar, V., Mishra, I.M. 2012. Optimization of structural and operational variables for the energy efficiency of a divided wall distillation column. *Computers and Chemical Engineering*. 40, 33–40.

Sarkar, J., Shekhawat, L. K., Loomba, V., Rathore, A. S. 2016. CFD of Mixing of Multi-Phase Flow in a Bioreactor Using Population Balance Model. *Biotechnology Progress* 32, 613-628.

Scargiali, F., Busciglio, A., Grisafi, F., Brucato, A. 2014. Mass transfer and hydrodynamic characteristics of unbaffled stirred bio-reactors: Influence of impeller design. *Biochemical Engineering Journal* 82, 41–47.

Schaepe, S., Kuprijanov, A., Sieblist, C., Jenzsch, M., Simutis, R., Lubbert, A. 2013. $k_La$ of stirred tank bioreactors revisited. *Journal of Biotechnology* 168, 576-583.

Schluter, V. & Deckwer, W.D. 1992. Gas-Liquid Mass Transfer in Stirred Vessels. *Chemical Engineering Science* 47, 2357–2362.

Sharma, K. K., Shrivastava, B., Sastry, V.R.B., Sehgal, N., Kuhad, R. C. 2013. Middle-redox potential laccase from *Ganoderma sp.*: its application in improvement of feed for monogastric animals. *Scientific Reports*. doi: 10.1038/srep01299.

Shen, W., Lin, D.T., Nachtsheim, C.J. 2014. Dimensional Analysis and Its Applications in Statistics. *Journal of Quality Technology* 46, 185–198.

Shi, Y., Ryu, D.D.Y., Ballica, R. 1993. Rheological properties of mammalian cell culture suspensions: Hybridoma and HeLa cell lines. *Biotechnology and Bioengineering* 41, 745–754.

Shukla, V.B., Veera, U.P., Kulkarni, P.R., Pandit, A.B. 2001. Scale-up of biotransformation process in stirred tank reactor using dual impeller bioreactor. *Biochemical Engineering Journal* 8, 19–29.

Sideman, S., Hortacsu, O., Fulton, J.W. 1966. Mass Transfer in Gas-Liquid Contacting Systems. *Industrial and Engineering Chemistry Research* 58, 32–47.

Siedenberg, D., Gerlach, S.R., Weigel, B., Schugerl, K., Giuseppin, M.L.F., Hunik, J. 1997. Production of xylanase by Aspergillus awamori on synthetic medium in stirred tank and airlift tower loop reactors : the influence of stirrer speed and phosphate concentration. *Journal of Biotechnology* 56, 103–114.

Sklodowska, K., Debski, P.R., Michalski, J.A., Korczyk, P.M., Dolata, M., Zajac, M., Jakiela, S. 2018. Simultaneous Measurement of Viscosity and Optical Density of Bacterial Growth and Death in a Microdroplet. *Micromachines* 9, 251. doi:10.3390/mi9050251

Smith, J.M., Van't Riet, K., Middleton, J.C. 1977. Scale-up of Agitated Gas-Liquid Reactors for Mass Transfer. In *Proceedings of 2nd European Conference on Mixing*. Cambridge, United Kingdom.

Wernersson, S.E. and Tragardh, C. 1999. Scale-up of Rushton turbine-agitated tanks. *Chemical Engineering Science* 54, 4245–4256.

Stenberg, O & Andersson, B. 1988. Gas-Liquid Mass Transfer in Agitated Vessels-II. Modelling of Gas-Liquid Mass Transfer. *Chemical Engineering Science* 43, 725–730.

Suresh, S., Srivastava, V.C., Mishra, I.M. 2009. Techniques for oxygen transfer measurement in bioreactors: a review. *Journal of Chemical Technology and Biotechnology*. 84, 1091-1103.

Taghavi, M., Zadghaffari, R., Moghaddas, J., Moghaddas, Y. 2011. Experimental and CFD investigation of power consumption in a dual Rushton turbine stirred tank. *Chemical Engineering Research and Design* 89, 280–290.

Tatterson, G.B. 1991. *Fluid Mixing and Gas Dispersion in Agitated Tanks*. McGraw-Hill, New York.

Tervasmaki, P., Latva-Kokko, M., Taskila, S., Tanskanen, J. 2016. Mass transfer, gas hold-up and cell cultivation studies in a bottom agitated draft tube reactor and multiple impeller Rushton turbine configuration. *Chemical Engineering Science* 155, 83–98.

Van't Riet, K. 1979. Review of measuring methods and nonviscous gas–liquid mass transfer in stirred vessels. *Industrial and Engineering Chemistry Process Design and Development* 18, 357–364.

Van't Riet, K. and Smith, J.M. 1973. "The behaviour of gas-liquid mixtures near Rushton turbine blades," *Chemical Engineering Science*. 28, 1031–1037.

Veera, U.P., Patwardhan, A.W., Joshi, J.B. 2001. Measurement Of Gas Hold-Up Profiles In Stirred Tank Reactors By Gamma Ray Attenuation Technique. *Trans IChemE* 79, 684–688.

Vilaca, P.R., Badino, A.C., Facciotti, M.C.R., Schmidell, W. 2000. Determination of power consumption and volumetric oxygen transfer coefficient in bioreactors. *Bioprocess Engineering* 22, 261–265.

Wang, H., Jia, X., Wang, X., Zhou, Z., Wen, J., Zhang, J. 2014. CFD modeling of hydrodynamic characteristics of a gas-liquid two-phase stirred tank. *Applied Mathematical Modelling* 38, 63–92.

Warmoeskerken, M.M.C.G. & Smith, J. 1981. Surface contamination effects in stirred tank reactors. In *Proceedings of 8$^{th}$ Conference of Mixing*. Cambridge, United Kingdom.

Wernersson, E.S., & Tragardh, C. 1999. Scale-up of Rushton turbine-agitated tanks. *Chemical Engineering Science* 54, 4245–4256.

Whitcomb, P.J., and Macosko, C.W., 1978. Rheology of Xanthan Gum. *Journal of Rheology* 22, 493–505.

Williams, J. 2002. Keys to Bioreactor Selections. *Chemical Engineering Progress* 98, 34–41.

Wood-Black, F. 2014. Considerations for Scale-Up –Moving from the Bench to the Pilot Plant to

Full Production. in *Academia and Industrial Pilot Plant Operations and Safety*, American Chemical Society. 10.1021/bk-2014-1163.ch003

Wutz, J., Lapin, A., Siebler, F., Schafer, J.F., Wucherpfenning, T., Berger, M., Takors, R., 2016. Predictability of $k_La$ in stirred tank reactors under multiple operating conditions using an Euler–Lagrange approach. *Engineering in Life Sciences* 16, 633–642.

Xie, M. H., Xia, J.Y., Zhou, Z., Zhou, G. Z., Chu, J., Zhuang, Y. P., Zhang, S. L., Noorman, H. 2014. Power consumption, local and average volumetric mass transfer in multiple-impeller stirred bioreactors for xanthan gum solutions. *Chemical Engineering Science* 106, 144-156.

Xu, S., Hoshan, L., Jiang, R., Gupta, B., Brodean, E., O'Neill, K., Seamans, T.C., Bowers, J., Chen, H., 2017. A Practical Approach in Bioreactor Scale-up and Process Transfer Using a Combination of Constant P/V and vvm as the Criterion. *Biotechnology Progress* 33, 1146–1159.

Yagi, H., & Yoshida, F., 1975. Gas absorption by Newtonian and non-Newtonian fluids in sparged agitated vessels. *Industrial and Engineering Chemistry Process Design and Development* 14, 488–493.

Yang, F., Zhou, S., An, X., 2015. Gas-liquid hydrodynamics in a vessel stirred by dual dislocated-blade Rushton impellers. *Chinese Journal of Chemical Engineering* 23, 1746–1754.

Yawalkar, A.A., Pangarkar, V.G., Beenackers, A.A.C.M. 2002. Gas Hold-up in Stirred Tank Reactors. *Canadian Journal of Chemical Engineering*. 80, 158–166.

Yawalkar, A.A., Heesink, A.B.M., Versteeg, G.F., Pangarkar, V.G. 2002. Gas–Liquid Mass Transfer Coefficient in Stirred Tank Reactors. *The Canadian Journal of Chemical Engineering*. 80, 840–848.

Youssef, A.A., Hamed, M.E., Al-Dahhan, M.H., Dudukovic, M.P., 2014. A new approach for scale-up of bubble column reactors. *Chemical Engineering Research and Design* 92, 1637–1646.

Zadghaffari, R., Moghaddas, J.S., Revstedt, J., 2009. A mixing study in a double-Rushton stirred tank. *Computers and Chemical Engineering* 33, 1240–1246.

Zhan, T., Wang, T., Wang, J. 2006. Analysis and measurement of mass transfer in airlift loop reactors. *Chinese Journal of Chemical Engineering*. 14, 604–610.

Zhang, J., Gao, Z., Cai, Y., Cao, H., Cai, Z., Bao, Y. 2017. Power consumption and mass transfer in a gas-liquid-solid stirred tank reactor with various impeller combinations. *Chemical Engineering Science* 170, 464-475.

Zhou, G. and Kresta, S.M. 1996. Impact of tank geometry on the maximum turbulence energy dissipation rate for impellers. *AIChE Journal* 42, 2476–2490.

Zhu, Y., Bandopadhayay, P.C., Wu, J. 2001. Measurement of Gas-Liquid Mass Transfer in an Agitated Vessel-A Comparison between Different Impellers. *Journal of Chemical Engineering of Japan* 34, 579–584.

Zlokarnik, M. 1998. Problems in the application of dimensional analysis and scale-up of mixing operations. *Chemical Engineering Science* 53, 3023–3030.

Zolkarnik, M. 1991. *Dimensional Analysis and Scale-up in Chemical Engineering*. Ist Edition, Springer-Verlag Berlin Heidelberg Berlin, Germany. 10.1007/978-3-642-76673-2

# CURRICULUM VITAE

| | |
|---|---|
| **Name** | **Sohail Rasool Lone** |
| **Date of Birth** | March 21, 1986 |
| **Place of Birth** | Sopore, Kashmir |
| **Degrees** | B.Tech., Chemical Engineering, July 2009 (NIT Srinagar, J&K) |
| | M.Tech., Chemical Engineering, December 2012 (AMU, Aligarh) |
| **Professional Societies** | American Institute of Chemical Engineers (AIChE), United States |
| | Institution of Chemical Engineers (IChemE), United Kingdom |
| **Email Address** | lonesohail92@gmail.com; slone@ch.iitr.ac.in |

## Research Publications from The Thesis

1. **Lone, S.R.,** Kumar, V., Seay, J.R., Englert, D.L., Hwang, H.T., 2018. Evaluation of Volumetric Mass Transfer Coefficient in a Stirred Tank Bioreactor Using Response Surface Methodology. Environmental Progress & Sustainable Energy. 38(2), 387-401.
2. **Lone, S.R.,** Rajput, S.S., Ghosh, S., Kumar, V., 2019. Mass Transfer Coefficient and Power Consumption in a Mixed Impeller Configuration Stirred Tank Bioreactor. (To be Communicated)
3. **Lone, S.R.,** Kumar, V., Englert, D.L, Seay, J.R., Hwang, H.T., 2020. Mass Transfer and Rheological Characteristics in a Stirred Tank Bioreactor for *Escherichia coli* BL21 Cultivation. (Under Review in Biotechnology and Bioprocess Engineering)
4. **Lone, S. R.,** Kumar, V. Mass Transfer Characteristics in Stirred Tank Reactors: A Review (Under Preparation)

## International Conferences

1. **Lone, S.R.,** Kumar, V., Seay, J., Englert, D., Hwang, H.T., 2017. Hydrodynamic Study to Determine Volumetric Mass Transfer Coefficient for Cell Culture Applications. **2017 AIChE Annual Meeting**, Minneapolis, Minnesota, United States of America, October 29-November 03, 2017.
2. **Lone, S.R.,** Rajput, S.S., Ghosh, S., Kumar, V., 2018. Rheological Study of *E. coli* BL21 in a Stirred Tank Bioreactor. **CHEMCON-2018**, National Institute of Technology Jalandhar, Punjab, India, December 27-30, 2018.

3. **Lone, S.R.,** Khichi, S.S., Ghosh, S., Kumar, V., 2019. Scale-up Criterion for Stirred Tank Reactors based on Volumetric Mass Transfer Coefficient. **14th International Conference on Gas-Liquid & Gas-Liquid-Solid Reactor Engineering (GLS-14)**, Guilin, China, May 30-June 03, 2019.

## Workshops

1. Workshop on "Using Web of Science for Research" held on February 27, 2015 organized by Mahatma Gandhi Central Library, IIT Roorkee.
2. Hands-on Training Workshop on "Basic Cell Culture Technology" at the National Centre for Cell Science (NCCS), Pune, May16-19, 2016.
3. Workshop on "Modeling, Optimization and Simulation of Stochastic Systems" at Department of Mathematics, IIT Roorkee, November 26, 2016.
4. Workshop on "Basics of Intellectual Property Rights" conducted by the IPR Chair, Department of Management Studies, IIT Roorkee on January 20, 2018.
5. Workshop on Research Fundamentals: Innovation and Entrepreneurship organized by Sponsored Research and Industrial Consultancy (SRIC), IIT Roorkee, October 13-14, 2018.
6. Indo-US Workshop on Soft Matter (IUWSM) at Department of Chemical Engineering, IIT Roorkee, December 9-11, 2018.